NASA
Technical
Paper
3325

May 1993

Robust Controller Design for Flexible Structures Using Normalized Coprime Factor Plant Descriptions

Ernest S. Armstrong

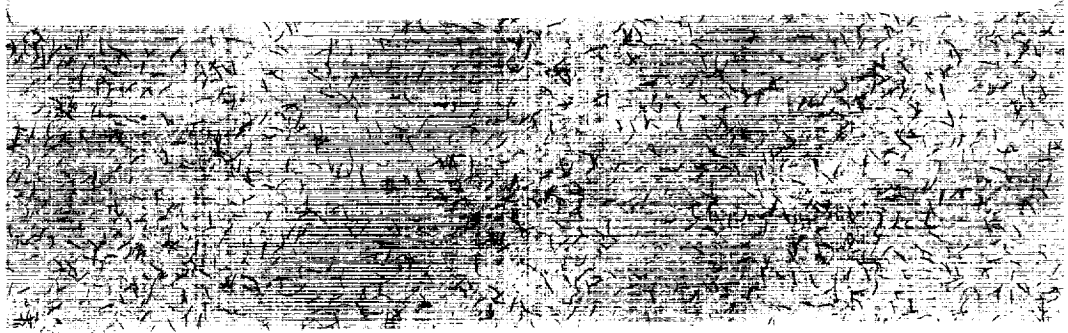

NASA

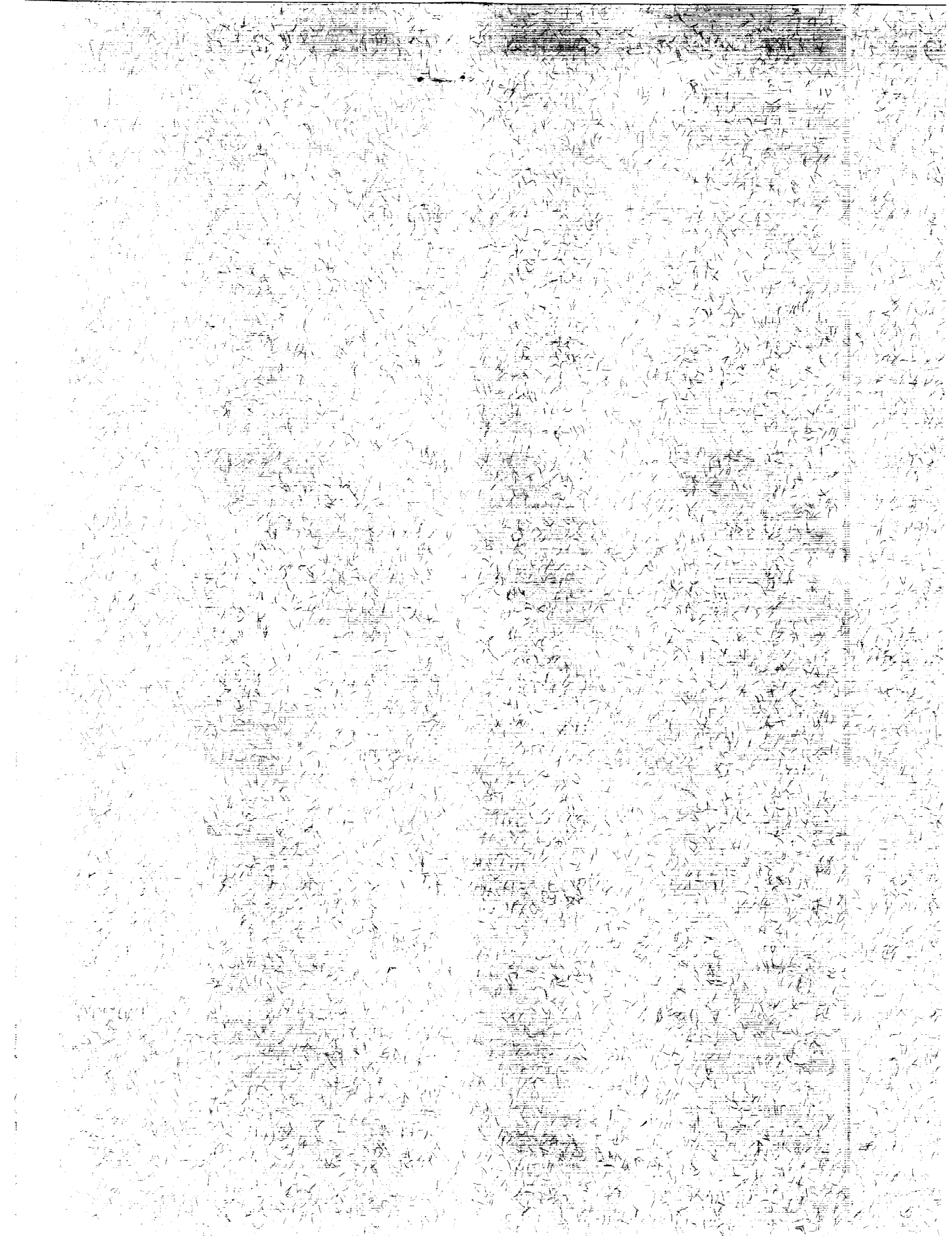

NASA Technical Paper 3325

1993

Robust Controller Design for Flexible Structures Using Normalized Coprime Factor Plant Descriptions

Ernest S. Armstrong
Langley Research Center
Hampton, Virginia

NASA
National Aeronautics and Space Administration
Office of Management
Scientific and Technical Information Program

Nomenclature

$\mathbf{A}^c$	matrix defined by equation (B21)
$\mathbf{A}_\delta$	system matrix for perturbed phase 0 simulation
$(\mathbf{A}, \mathbf{B}, \mathbf{C}, \mathbf{D})$	minimal state-variable realization matrices for $\mathbf{G}(s)$
$(\tilde{\mathbf{A}}, \tilde{\mathbf{B}}, \tilde{\mathbf{C}}, \tilde{\mathbf{D}})$	balanced realization matrices used to define optimal compensator in appendix B
$(\hat{\mathbf{A}}, \hat{\mathbf{B}}, \hat{\mathbf{C}}, \hat{\mathbf{D}})$	realization matrices employed in defining optimal robust compensator in appendix B
$(\mathbf{A}_f, \mathbf{B}_f, \mathbf{C}_f, \mathbf{D}_f)$	state-variable realization matrices of 25-mode model in phase 0 simulation
$(\mathbf{A}_t, \mathbf{B}_t, \mathbf{C}_t, \mathbf{D}_t)$	state-variable realization matrices for truncated system $\Delta\mathbf{G}(s)$ in phase 0 simulation
$(\mathbf{A}_W^{(i)}, \mathbf{B}_W^{(i)}, \mathbf{C}_W^{(i)}, \mathbf{D}_W^{(i)})$	state-variable realization matrices for loop-shaping functions (i = 1,2), defined by equations (55) to (61)
C	field of complex numbers
$\mathbf{C}_\delta$	output matrix in state-variable realization of perturbed phase 0 system
$\mathbf{d}$	disturbance vector (see fig. 2)
$\mathbf{F}$	generalized control gain matrix defined by equation (A27)
$f(s)$	scalar function defined by equation (54)
$\mathcal{F}_L(\mathbf{P}, \mathbf{K})$	lower linear fractional transform
$\mathcal{F}_U(\mathbf{P}, \Delta\mathbf{P})$	upper linear fractional transform
$\mathbf{G}(s)$	$p \times m$ transfer function matrix with real-rational function elements
$\Delta\mathbf{G}(s)$	perturbation to $\mathbf{G}(s)$ matrix
$\mathbf{G}_A(s)$	$\mathbf{G}(s)$ matrix after augmentation by loop-shaping functions
$\mathbf{G}_f$	design model transfer function matrix for evolutionary model study
$\mathbf{G}_\Delta(s)$	perturbed plant matrix
$\mathbf{G}_\delta(s)$	transfer function matrix for perturbed $\mathbf{G}(s)$
$\mathbf{G}_{\delta_A}(s)$	$\mathbf{G}_\delta(s)$ matrix after augmentation by loop-shaping functions
g	acceleration due to gravity ($1g \approx 32.174$ ft/sec^2)
$\mathbf{H}$	generalized filter gain matrix defined by equation (A21)
H_∞	Hardy space of complex-valued functions ($F(s)$) of a complex variable (s) that are analytic and bounded in the open right half-plane in the sense that sup $\{\mid F(s) \mid:$ Re $(s) > 0\} < b$ where b is a real number
$\mathbf{I}$	identity matrix of appropriate order
$\mathbf{I}_m, \mathbf{I}_p$	$m \times m$ and $p \times p$ identity matrices, respectively

j	$= \sqrt{-1}$
$\mathbf{K}(s)$	feedback compensator matrix for $\mathbf{G}(s)$
$\mathbf{K}_A(s)$	feedback compensator matrix for $\mathbf{G}_A(s)$
$\mathbf{K}_c(s)$	central suboptimal compensator matrix defined by equation (B28)
(k, i, a)	positive real parameters employed in equation (54)
$\mathbf{M}$,$\mathbf{N}$	factors in right-coprime factorization of $\mathbf{G}(s)$ matrix defined by equation (A24)
$\widetilde{\mathbf{M}}, \widetilde{\mathbf{N}}$	factors in left-coprime factorization of $\mathbf{G}(s)$ matrix defined by equation (4)
$\Delta\widetilde{\mathbf{M}}, \Delta\widetilde{\mathbf{N}}$	perturbations to left-coprime factors of $\mathbf{G}(s)$ matrix
$\widetilde{\mathbf{M}}_A, \widetilde{\mathbf{N}}_A$	left-coprime factors for $\mathbf{G}_A(s)$ matrix
$\widetilde{\mathbf{M}}_{A_\delta}, \widetilde{\mathbf{N}}_{A_\delta}$	left-coprime factors for $\mathbf{G}_{A_\delta}(s)$
n	order of system matrix for minimum realization of $\mathbf{G}(s)$
n_1, n_2	orders of system matrices in state-variable realizations of $\mathbf{W}_1(s)$ and $\mathbf{W}_2(s)$, respectively
$\mathbf{P}$	generalized plant transfer function matrix (also used in appendix A to denote reachability gramian)
$\Delta\mathbf{P}$	generalized perturbation matrix
$\mathbf{Q}$	observability gramian matrix
$\mathbf{R}$	matrix defined by equation (B25)
R	field of real numbers
R^n	vector space of $n \times 1$ matrices with real elements
$R^{n\times n}$	vector space of $n \times n$ matrices with real elements
RH_∞	subset of RL_∞ made up of all asymptotically stable, proper transfer function matrices
RL_∞	space of all real-rational proper transfer function matrices that have no poles on the imaginary axis of the complex plane
r	multiplicity of largest Hankel singular value of $(\widetilde{\mathbf{A}}, \widetilde{\mathbf{B}}, \widetilde{\mathbf{C}}, \widetilde{\mathbf{D}})$ realization
$\hat{\mathbf{r}}$	exogenous inputs (see fig. 2)
$\mathbf{S}$	matrix defined by equation (B19)
s	Laplace transform variable
t	time variable, $t \in [0, \infty)$
$\mathbf{U}, \mathbf{V}$	right-coprime factors for compensator $\mathbf{K}$ matrix defined by equation (23)
$\widehat{\mathbf{U}}$	matrix defined by equation (B10)
$\mathbf{u}(s)$	Laplace transform of $\mathbf{u}(t)$ vector

$\mathbf{u}(t)$	system input vector in time domain
$(\mathbf{U}, \mathbf{V}), (\tilde{\mathbf{U}}, \tilde{\mathbf{V}})$	left- and right-coprime factors used in equations (A13) and (A23), respectively
$\mathbf{v}$	exogenous input vectors to $\mathbf{P}$ in figure 1
$\mathbf{W}_1(s), \mathbf{W}_2(s), \mathbf{W}(s)$	transfer function matrices used in loop shaping
$\widehat{\mathbf{W}}_1$	matrix defined by equation (B27)
$\mathbf{X}$	matrix solution of generalized control algebraic Riccati equation (GCARE)
$\mathbf{y}(s)$	Laplace transform of $\mathbf{y}(t)$ vector
$\mathbf{y}(t)$	system output vector in time domain
$\mathbf{Z}$	matrix solution of generalized filter algebraic Riccati equation (GFARE)
$\mathbf{z}$	error signal vector from $\mathbf{P}$ (see fig. 1)
$\mathbf{0}$	null matrix of appropriate order
$\mathbf{\Gamma}$	matrix defined by equation (B9)
γ	positive real number, $1/\epsilon$
$\gamma_{\min}$	positive real number, $1/\epsilon_{\max}$
$(\delta\zeta)_i$	random numbers uniformly distributed within $[-0.1, 0.1]$, where $i = 1, \ldots, 9$
$(\delta\omega)_i$	random numbers uniformly distributed within $[-0.01, 0.01]$, where $i = 1, \ldots, 9$
ϵ	positive real number used as a robustness measure
$\epsilon_{\max}$	largest value of ϵ achievable by choosing $\mathbf{K}$ from all compensators that stabilize $\mathbf{G}$
$\hat{\mathbf{Z}}$	diagonal matrix of damping ratios of 25-mode phase 0 simulation model
ζ_i	damping ratio for ith mode of phase 0 simulation model, where $i = 1, \ldots, 25$
$(\zeta_p)_i$	perturbed value of damping ratio ζ_i, where $i = 1, \ldots, 9$
η	measurement noise (see fig. 2)
$\lambda_i(\mathbf{A})$	ith eigenvalue of matrix $\mathbf{A}$
$\mathbf{\Sigma}$	diagonal gramian matrix occurring in balanced realization
$\sigma_i(\mathbf{A})$	ith singular value of matrix $\mathbf{A}$
$\bar{\sigma}(\mathbf{A})$	largest singular value of matrix $\mathbf{A}$
$\underline{\sigma}(\mathbf{A})$	smallest singular value of matrix $\mathbf{A}$
$\sigma_i(\mathbf{G}(s))$	ith Hankel singular value of matrix $\mathbf{G} \in RH_\infty$
$\mathbf{\Phi}$	mode shape matrix

$\hat{\mathbf{\Phi}}$	RH_∞ function satisfying matrix $\| \hat{\mathbf{\Phi}} \|_\infty \leq 1$
$\mathbf{\Omega}$	diagonal matrix of frequencies of 25-mode phase 0 simulation model, rad/sec
ω	frequency, rad/sec or Hz
ω_i	frequency of ith mode in phase 0 simulation model, rad/sec or Hz
$(\omega_p)_i$	perturbed values of ω_i, rad/sec or Hz

Abbreviations:

CSI	Control-Structures Interaction
GCARE	generalized control algebraic Riccati equation
GFARE	generalized filter algebraic Riccati equation
inf	greatest lower bound
NLCF	normalized left-coprime factorization
NRCF	normalized right-coprime factorization
sup	least upper bound

Subscripts:

cl	closed loop
H	Hankel norm
max	maximum
min	minimum

Superscripts:

T	matrix transpose
-1	matrix inverse
$*$	matrix transpose with argument s replaced by $-s$

Notations:

$\| \cdot \|_\infty$	H_∞ norm defined by equation (A12)
$\| \cdot \|_H$	Hankel norm defined by equation (A10)
$:=$	definition by equality (e.g., $\mathbf{A} := \mathbf{B}$ denotes $\mathbf{A}$ is defined by equality to $\mathbf{B}$)
$\left[\begin{array}{c\|c} \mathbf{A} & \mathbf{B} \\ \hline \mathbf{C} & \mathbf{D} \end{array}\right]$	block matrix notation: transfer function matrix $\mathbf{C}(s\mathbf{I} - \mathbf{A})^{-1}\mathbf{B} + \mathbf{D}$ for compatible matrices $(\mathbf{A}, \mathbf{B}, \mathbf{C}, \mathbf{D})$

Abstract

Stabilization is a fundamental requirement in the design of feedback compensators for flexible structures. The search for the largest neighborhood around a given design plant for which a single controller produces closed-loop stability can be formulated as an H_∞ control problem. The use of normalized coprime factor plant descriptions, in which the plant perturbations are defined as additive modifications to the coprime factors, leads to a closed-form expression for the maximum neighborhood boundary allowing optimal and suboptimal H_∞ compensators to be computed directly without the usual γ iteration. This paper gives a summary of the theory on robust stabilization using normalized coprime factor plant descriptions, and it describes the application of the theory to the computation of robustly stable compensators for the phase 0 version of the Control-Structures Interaction (CSI) Evolutionary Model. Results from the application indicate that the suboptimal version of the theory has the potential of providing the basis for the computation of low-authority compensators that are robustly stable to expected variations in design model parameters and additive unmodeled dynamics.

Introduction

In the design of controllers for physical systems, some trade-off is usually performed between design model accuracy and mathematical complexity. The more accurate analysis models often require computational time that is too excessive to qualify them as design models for control purposes. Also, many of the most widely used multivariable design techniques work best for moderate-order, linear, time-invariant design models (Maciejowski 1989). In practice, high-order nonlinear models are typically linearized about some operating condition and have their model order reduced to produce design models that conform to computational limitations or compensator implementation constraints. These practicalities introduce modeling errors in the form of unmodeled dynamics that must be accounted for in the controller design process. Additionally, parameters in the design and analysis models are not always accurately known and can cause destabilizing effects if parametric uncertainty is ignored or improperly treated.

The foregoing considerations are especially critical in the design of controllers for flexible space structures (Joshi 1989). Space structure controller design models are generally obtained through some order-reduction procedure applied to a high-order analysis model obtained from finite element techniques. The order-reduction process essentially deletes a portion of the finite element model to produce a lower order controller design model. Although the unmodeled dynamics (represented by the deleted portion) are no longer contained in the design model, they can still be influenced by control inputs. Care must be taken in the design process to avoid control and observability spillover effects (Balas 1982) that destabilize the unmodeled dynamics. Also, the high-order model contains parametric uncertainties in natural frequencies, damping ratios, and mode shapes and slopes that get passed through to the design model. A fundamental requirement of control law design for flexible space structures is then the attainment and preservation of closed-loop stability in the presence of unmodeled dynamics and parameter uncertainties.

Nonparametric uncertainties, such as unmodeled dynamics, typically occur in the high-frequency region of physical models. In controller design, unmodeled dynamics are normally treated, often at the expense of reduced performance, by rolling off the compensator over a high-frequency band. Rolling off the compensator in this manner can be especially limiting for flexible structures in which unknown elastic modes are low-frequency, closely spaced, and fall within the bandwidth of the controller. The treatment of parametric uncertainties is still an open area of research (Dorato and

Yedavalli 1990). In this study we are concerned with compensators that robustly stabilize a given system in the presence of both parametric and nonparametric uncertainties.

Uncertainties may be viewed as perturbations about a nominal design model. If a single compensator stabilizes the nominal plant and, in addition, all systems within some neighborhood of the plant generated by the perturbations, the compensator is said to robustly stabilize the overall family of systems. The search for the largest neighborhood around a given design plant for which a single controller produces closed-loop stability can be formulated as an H_∞ control problem. Glover and McFarlane (1989) show that the use of normalized coprime factor plant descriptions, in which the plant perturbations are defined as additive modifications to the coprime factors, leads to a closed-form expression for the maximum perturbation radius. The maximum radius can be computed directly in terms of the design model, thus allowing optimal and suboptimal robust compensators to be found without the usual γ iteration of the H_∞ design.

This paper describes an application of the Glover-McFarlane robust stabilization theory to the control of a simulated structure configured to have many of the dynamic characteristics and controller design difficulties associated with flexible space structures. We begin with a description of the general robust stabilization problem followed by an overview of its results for normalized coprime factor plant descriptions. Mathematical background material is presented in appendix A, and the major computational algorithms for computing optimal and suboptimal robust controllers are presented in appendix B. Next, these theoretical results are applied to the computation of robustly stable compensators for the phase 0 version of the NASA Control-Structures Interaction (CSI) Evolutionary Model. Analysis of the compensators indicates that for the class of applications considered, the suboptimal version of the theory has the potential of providing the basis for the computation of low-authority controllers that are robustly stable to expected variations in design model parameters and additive unmodeled dynamics.

General Robust Stabilization Problem

In terms of transfer function matrix models of the design system, plant uncertainties (unmodeled dynamics and parameter inaccuracies) can be modeled in several ways. Let $\mathbf{G}(s)$ represent a $p \times m$ transfer matrix and $\Delta\mathbf{G}(s)$ denote some perturbation to $\mathbf{G}(s)$, both with real-rational elements. A perturbation is called additive if the perturbed plant ($\mathbf{G}_\Delta$) is written as

$$\mathbf{G}_\Delta = \mathbf{G} + \Delta\mathbf{G} \tag{1}$$

and it is called multiplicative when

$$\mathbf{G}_\Delta = (\mathbf{I}_p + \Delta\mathbf{G})\mathbf{G} \tag{2}$$

or

$$\mathbf{G}_\Delta = \mathbf{G}(\mathbf{I}_m + \Delta\mathbf{G}) \tag{3}$$

A third method of modeling plant uncertainty involves the use of coprime factorizations (appendix A). Here, $\mathbf{G}$ is written in coprime factor form and the system perturbations are defined in terms of perturbations to the respective coprime factors. Any (stable or not) transfer function matrix ($\mathbf{G}(s)$) can be represented in terms of a pair of asymptotically stable, real-rational, proper transfer function matrices that are coprime. For a left-coprime factor form with ($\widetilde{\mathbf{M}} \in RH_\infty, \widetilde{\mathbf{N}} \in RH_\infty$), we have

$$\mathbf{G} = \widetilde{\mathbf{M}}^{-1}\,\widetilde{\mathbf{N}} \tag{4}$$

and the perturbed system ($\mathbf{G}_\Delta$) is given by

$$\mathbf{G}_\Delta = (\widetilde{\mathbf{M}} + \Delta\widetilde{\mathbf{M}})^{-1}\,(\widetilde{\mathbf{N}} + \Delta\widetilde{\mathbf{N}}) \tag{5}$$

with

$$\Delta \mathbf{G} = [\Delta \widetilde{\mathbf{M}}, \Delta \widetilde{\mathbf{N}}] \in RH_\infty \tag{6}$$

Controller design employing uncertainty models in equations (1) to (3) has been widely investigated; see, for example, Chen and Desoer (1982) and Doyle and Stein (1981). Design methods employing coprime factor models such as equations (4) to (6) have not been as widely accepted or employed as the additive and multiplicative forms; however, they have been shown to have many theoretical and computational benefits by Vidyasagar (1985) and by McFarlane, Glover, and Vidyasagar (1990).

Each uncertainty model can be represented as a special case of an upper linear fractional transformation

$$\mathbf{G}_\Delta = \mathcal{F}_U(\mathbf{P}, \Delta \mathbf{P}) = \mathbf{P}_{22} + \mathbf{P}_{21}\ \Delta \mathbf{P}(\mathbf{I} - \mathbf{P}_{11}\Delta \mathbf{P})^{-1}\ \mathbf{P}_{12} \tag{7}$$

where $\det(\mathbf{I} - \mathbf{P}_{11}\Delta \mathbf{P}) \neq 0$ and

$$\mathbf{P} = \left[\begin{array}{c|c} \mathbf{P}_{11} & \mathbf{P}_{12} \\ \hline \mathbf{P}_{21} & \mathbf{P}_{22} \end{array}\right] \tag{8}$$

The standard plants $\mathbf{P}$ associated with three of the foregoing uncertainty descriptions are

$$\mathbf{P} = \left[\begin{array}{c|c} \mathbf{O} & \mathbf{I} \\ \hline \mathbf{I} & \mathbf{G} \end{array}\right] \qquad \Delta \mathbf{P} = \Delta \mathbf{G} \tag{9}$$

$$\mathbf{P} = \left[\begin{array}{c|c} \mathbf{O} & \mathbf{G} \\ \hline \mathbf{I} & \mathbf{G} \end{array}\right] \qquad \Delta \mathbf{P} = \Delta \mathbf{G} \tag{10}$$

and

$$\mathbf{P} = \left[\begin{array}{c|c} \mathbf{O} & \mathbf{I} \\ \widetilde{\mathbf{M}}^{-1} & \mathbf{G} \\ \hline \widetilde{\mathbf{M}}^{-1} & \mathbf{G} \end{array}\right] \qquad \Delta \mathbf{P} = [\Delta \widetilde{\mathbf{N}}, -\Delta \widetilde{\mathbf{M}}] \tag{11}$$

for equations (1), (2), and (5), respectively. Equation (7) represents a generalized uncertainty model, and the process of using feedback to stabilize and control $\mathbf{P}$ can be represented as the block diagram shown in figure 1.

By employing figure 1, a general robust stabilization problem can be posed (McFarlane and Glover 1990). From viewing $\mathbf{G}_\Delta$ as a family of perturbed models for a given class of perturbations $\Delta \mathbf{P}$, one can seek a single compensator $\mathbf{K}(s)$ that stabilizes not only $\mathbf{G}$ (that is, $\mathbf{G}_\Delta$ with $\Delta \mathbf{P} = 0$) but all members of the $\mathbf{G}_\Delta$ family. If $\Delta \mathbf{P}$ belongs to a class of admissible perturbations defined as the union of the set of stable bounded perturbations (RH_∞) and the set of perturbations in RL_∞ for which $\mathbf{G}$ and $\mathbf{G}_\Delta$ have an equal number of closed right half-plane poles, then the following theorem can be established (McFarlane and Glover 1990).

Robust Stabilization Theorem

For any $\mathbf{P}_{22}$ of $\mathbf{P}$ given by equation (8) with stabilizable and detectable state-variable realization, the compensator $\mathbf{K}(s)$ of figure 1 stabilizes $\mathbf{G}_\Delta = \mathcal{F}_U(\mathbf{P}, \Delta \mathbf{P})$ for all admissible values of $\Delta \mathbf{P}$ such that $\| \Delta \mathbf{P} \|_\infty < \epsilon$ if, and only if,

1. $\mathbf{K}$ stabilizes $\mathbf{G}$

and

2. $\| \mathcal{F}_L(\mathbf{P}, \mathbf{K}) \|_\infty < \epsilon^{-1}$

where the lower linear fractional transform is given by

$$\mathcal{F}_L(\mathbf{P}, \mathbf{K}) = \mathbf{P}_{11} + \mathbf{P}_{12}\, \mathbf{K}(\mathbf{I} - \mathbf{P}_{22}\mathbf{K})^{-1}\, \mathbf{P}_{21} \tag{12}$$

The parameter ϵ in the theorem can be viewed as a measure of robust stability for a given closed-loop system. The problem of finding the largest level of robust stability is termed the *optimal robust stabilization problem* and is formally stated in the following discussion.

Optimal Robust Stabilization Problem

Find the largest strictly positive number $\epsilon = \epsilon_{\max}$ such that for all admissible $\Delta\mathbf{P}$ values satisfying $\| \Delta\mathbf{P} \|_\infty < \epsilon$, a single controller exists that stabilizes $\mathcal{F}_U(\mathbf{P}, \Delta\mathbf{P})$. From the robust stabilization theorem,

$$\epsilon_{\max} = \left(\inf_{\mathbf{K}} \| \mathcal{F}_L(\mathbf{P}, \mathbf{K}) \|_\infty \right)^{-1} \tag{13}$$

where $\mathbf{K}$ is chosen from all controllers that stabilize $\mathbf{G}$.

The computation of $\epsilon_{\max}$ thus involves the solution of an H_∞ optimization problem such as that discussed by Francis (1987) or Doyle et al. (1989); that is, find

$$\inf_{\mathbf{K}} \| \mathcal{F}_L(\mathbf{P}, \mathbf{K}) \|_\infty = \gamma_{\min} \tag{14}$$

over all controllers $\mathbf{K}$ that stabilize $\mathbf{G}$. This H_∞ problem can be posed for each representation of the additive, multiplicative, and coprime factorization uncertainty classes. In the additive and multiplicative cases, the solution typically involves a computationally intensive iterative procedure to find the smallest γ (whereby $\gamma = \gamma_{\min}$) such that the *suboptimal robust stabilization problem*

$$\inf_{\mathbf{K}} \| \mathcal{F}_L(\mathbf{P}, \mathbf{K}) \|_\infty \leq \gamma \tag{15}$$

is solved. The solution of the optimal robust stabilization problem for the coprime factorization uncertainty class can also be approached in a similar manner; however, if the coprime factors of $\mathbf{G}$ are normalized, the γ iteration procedure can be completely avoided and the computational effort greatly reduced.

Robust Stabilization Problem for Descriptions of the Normalized Coprime Factor Plant

Let $\mathbf{G}(s)$ have the coprime factor plant representation of equation (4). With $\mathbf{P}$ and $\Delta\mathbf{P}$ given by equations (11),

$$\mathcal{F}_L(\mathbf{P}, \mathbf{K}) = \begin{bmatrix} \mathbf{K} \\ \mathbf{I} \end{bmatrix} (\mathbf{I} - \mathbf{G}\mathbf{K})^{-1}\, \widetilde{\mathbf{M}}^{-1} \tag{16}$$

Also, because $[\Delta\widetilde{\mathbf{M}}, \Delta\widetilde{\mathbf{N}}] \in RH_\infty$, the set of admissible perturbations contains only elements within RH_∞, whereby the need to observe the equality condition on the poles of $\mathbf{G}$ and $\mathbf{G}_\Delta$ is completely eliminated.

When the coprime factors of equation (4) are normalized, that is, satisfy the relation

$$\widetilde{\mathbf{M}}(s)\ \widetilde{\mathbf{M}}^*(s) + \widetilde{\mathbf{N}}(s)\ \widetilde{\mathbf{N}}^*(s) = \mathbf{I} \tag{17}$$

the solution to the corresponding optimal or suboptimal robust stabilization problem has a surprisingly simplified form. For the problem of designing a controller $\mathbf{K}$ that robustly stabilizes a plant $\mathbf{G}$ written in normalized left-coprime factor form, the following properties hold:

1. A controller $\mathbf{K}$ is stabilizing for $\mathbf{G}$ and satisfies

$$\| \begin{bmatrix} \mathbf{K} \\ \mathbf{I} \end{bmatrix} (\mathbf{I} - \mathbf{GK})^{-1}\ \widetilde{\mathbf{M}}^{-1} \|_\infty \leq \gamma = \epsilon^{-1} \tag{18}$$

   if, and only if, $\mathbf{K}$ has a right-coprime factorization

$$\mathbf{K} = \mathbf{UV}^{-1} \tag{19}$$

   for some $(\mathbf{U} \in RH_\infty, \mathbf{V} \in RH_\infty)$ satisfying

$$\| [-\widetilde{\mathbf{N}}, \widetilde{\mathbf{M}}] + \begin{bmatrix} \mathbf{U} \\ \mathbf{V} \end{bmatrix}^* \|_\infty \leq\ (1 - \gamma^{-2})^{1/2} = (1 - \epsilon^2)^{1/2} \tag{20}$$

2. Solutions to the optimal robust stabilization problem using normalized left-coprime factorization give

$$\inf_{\mathbf{K}} \| \begin{bmatrix} \mathbf{K} \\ \mathbf{I} \end{bmatrix}\ (\mathbf{I} - \mathbf{GK})^{-1}\ \widetilde{\mathbf{M}}^{-1} \|_\infty = \left\{ 1 - \| [\widetilde{\mathbf{N}}, \widetilde{\mathbf{M}}] \|_H^2 \right\}^{-1/2} \tag{21}$$

   where the subscript H refers to the Hankel norm (which is discussed in appendix A).

3. The maximum robust stability margin is

$$\epsilon_{\max} = (\gamma_{\min})^{-1} = \left\{ 1 - \| [\widetilde{\mathbf{N}}, \widetilde{\mathbf{M}}] \|_H^2 \right\}^{1/2} > 0 \tag{22}$$

4. All optimal controllers are given by equation (19), where $\mathbf{U}$ and $\mathbf{V}$ satisfy

$$\| [-\widetilde{\mathbf{N}}, \widetilde{\mathbf{M}}] + \begin{bmatrix} \mathbf{U} \\ \mathbf{V} \end{bmatrix}^* \|_\infty = \| [\widetilde{\mathbf{N}}, \widetilde{\mathbf{M}}] \|_H < 1 \tag{23}$$

Proofs of properties 1 to 4 may be found in either Glover and McFarlane (1989) or McFarlane and Glover (1990).

Properties 2 and 3 state that for the robust stabilization problem using optimal normalized left-coprime factorizations (NLCF), a γ iteration to solve the H_∞ problem is not necessary. The value of $\gamma_{\min}$, given by the right-hand side of equation (21), can be found through the computation of the largest Hankel singular value of the stable transfer matrix $[\widetilde{\mathbf{N}}, \widetilde{\mathbf{M}}]$ obtained in the initial NLCF of $\mathbf{G}$. Properties 1 and 4 show that both the optimal (eq. (14)) and suboptimal (eq. (15)) NLCF robust stabilization problems are solved by computing the closest (in the H_∞ norm sense) completely unstable (all poles in the open complex right half-plane) rational function $\begin{bmatrix} \mathbf{U} \\ \mathbf{V} \end{bmatrix}^*$ to the stable RH_∞ function $[-\widetilde{\mathbf{N}}, \widetilde{\mathbf{M}}]$. This computation involves a version of the Nehari extension problem

(Francis 1987). By using $\begin{bmatrix} \mathbf{U} \\ \mathbf{V} \end{bmatrix}^*$, $\mathbf{U}$ and $\mathbf{V}$ in RH_∞ can be constructed for use with equation (19) to form the compensator $\mathbf{K}$. State-variable realizations for the suboptimal problem with $\gamma > \gamma_{\min}$ can be found in Glover and McFarlane (1989) or McFarlane and Glover (1990). The theoretical approach to solve the optimal problem with $\gamma = \gamma_{\min}$ can be found in Glover (1984). Algorithms for constructing state-variable realizations of the compensator $\mathbf{K}$ for both (optimal and suboptimal) problems are collected in appendix B of this paper.

Note that the results obtained from application of the foregoing robust stabilization theory can be conservative. The approach of analyzing perturbations ($\Delta\mathbf{P}$) only in terms of their H_∞ norm bounds rather than taking advantage of any known internal structure is fundamentally conservative by nature (Maciejowski 1989). Known structural properties of perturbations may be incorporated by using structured singular value techniques such as those implemented by Balas et al. (1991). In addition, a feedback controller $\mathbf{K}$ may well stabilize $\mathbf{G}$ and $\mathbf{G}_\Delta$ either for some particular structured $\Delta\mathbf{P}$ such that $\| \Delta\mathbf{P} \|_\infty > \epsilon_{\max}$ or for all structured $\Delta\mathbf{P}$ terms within a subset of $\| \Delta\mathbf{P} \|_\infty \leq \epsilon_{\max}$ containing $\Delta\mathbf{P} = 0$ while not satisfying the more restrictive condition of simultaneously stabilizing *all* elements of $\mathbf{G}_\Delta$ for $\| \Delta\mathbf{P} \|_\infty \leq \epsilon_{\max}$.

Loop-Shaping Procedure Within the NLCF Robust Stabilization Structure

Because $\mathbf{G} = \widetilde{\mathbf{M}}^{-1}\widetilde{\mathbf{N}}$ is a normalized left-coprime factorization, we can write

$$\| \begin{bmatrix} \mathbf{K} \\ \mathbf{I} \end{bmatrix} (\mathbf{I} - \mathbf{GK})^{-1} \widetilde{\mathbf{M}}^{-1} \|_\infty = \| \begin{bmatrix} \mathbf{K} \\ \mathbf{I} \end{bmatrix} (\mathbf{I} - \mathbf{GK})^{-1} \widetilde{\mathbf{M}}^{-1} \, [\widetilde{\mathbf{M}}, \widetilde{\mathbf{N}}] \|_\infty$$

$$= \| \begin{bmatrix} \mathbf{K}(\mathbf{I} - \mathbf{GK})^{-1} & \mathbf{K}(\mathbf{I} - \mathbf{GK})^{-1}\mathbf{G} \\ (\mathbf{I} - \mathbf{GK})^{-1} & (\mathbf{I} - \mathbf{GK})^{-1}\mathbf{G} \end{bmatrix} \|_\infty \leq \gamma \tag{24}$$

Thus, for either the optimal or suboptimal versions of the NLCF robust stabilization problem, the satisfaction of equation (18) for $\gamma \geq \gamma_{\min}$ also implies that (Safonov and Chiang 1988)

$$\| \mathbf{K}(\mathbf{I} - \mathbf{GK})^{-1} \|_\infty \leq \gamma \tag{25}$$

$$\| (\mathbf{I} - \mathbf{GK})^{-1} \|_\infty \leq \gamma \tag{26}$$

$$\| \mathbf{K}(\mathbf{I} - \mathbf{GK})^{-1}\mathbf{G} \|_\infty \leq \gamma \tag{27}$$

and

$$\| (\mathbf{I} - \mathbf{GK})^{-1}\mathbf{G} \|_\infty \leq \gamma \tag{28}$$

The significance of the individual transfer function matrices used in equations (25) to (28) may be seen from analyzing the feedback control loop in figure 2. The system $\mathbf{G}$ is subject to exogenous inputs in the form of reference commands or actuator noise ($\hat{\mathbf{r}}$), disturbances reflected to the output ($\mathbf{d}$), and measurement noise ($\boldsymbol{\eta}$). From figure 2 we can derive

$$\mathbf{y}(s) = (\mathbf{I} - \mathbf{GK})^{-1}\mathbf{GK}\,\boldsymbol{\eta}(s) + (\mathbf{I} - \mathbf{GK})^{-1}\mathbf{G}\,\hat{\mathbf{r}}(s) + (\mathbf{I} - \mathbf{GK})^{-1}\,\mathbf{d}(s) \tag{29}$$

$$\mathbf{u}(s) = \mathbf{K}(\mathbf{I} - \mathbf{GK})^{-1}\,[\mathbf{d}(s) + \boldsymbol{\eta}(s)] + (\mathbf{I} - \mathbf{KG})^{-1}\,\hat{\mathbf{r}}(s) \tag{30}$$

$$\mathbf{u}(s) - \hat{\mathbf{r}}(s) = \mathbf{K}(\mathbf{I} - \mathbf{GK})^{-1}\,[\mathbf{d}(s) + \boldsymbol{\eta}(s)] + \mathbf{K}(\mathbf{I} - \mathbf{GK})^{-1}\mathbf{G}\,\hat{\mathbf{r}}(s) \tag{31}$$

In equations (29) to (31) the standard notation in writing $f(s)$ to represent the Laplace transformation of $f(t)$ has been used. Equations (29) to (30) reflect the well-known inherent trade-off between attenuation of disturbances ($\mathbf{d}$) and filtering out measurement and/or actuator noise ($\boldsymbol{\eta}, \hat{\mathbf{r}}$). Because the sensitivity $\left((\mathbf{I} - \mathbf{GK})^{-1}\right)$ and complementary sensitivity $\left((\mathbf{I} - \mathbf{GK})^{-1}(-\mathbf{GK})\right)$ transfer

function matrices are related by

$$(\mathbf{I}-\mathbf{GK})^{-1}+(\mathbf{I}-\mathbf{GK})^{-1}\,(-\mathbf{GK})=\mathbf{I} \tag{32}$$

both cannot be kept small over the same frequency range. Normally, the disturbances are assumed to be large in magnitude only over a low-frequency range, and actuator and sensor noise are appreciable only over a complementary high-frequency range. The compensator $\mathbf{K}$ is typically designed to cause $\| (\mathbf{I}-\mathbf{GK})^{-1} \|_\infty$ to be small over low-frequency ranges and $\| (\mathbf{I}-\mathbf{GK})^{-1}\mathbf{GK} \|_\infty$ to be small over high-frequency ranges.

The NLCF robust stabilization compensators cause equations (25) to (28) to be satisfied over the entire frequency range, whereby the output $\mathbf{y}$ may be subject to any high-frequency noise. Such design difficulties are normally addressed through frequency-dependent weighting matrices applied directly to the sensitivity and complementary sensitivity matrices before compensator design. Only a special class of weighting matrices are shown to be allowed if the exact-solution advantage of the NLCF robust stabilization problem is to be preserved (McFarlane and Glover 1990).

Let $\mathbf{W}_1(s)$ and $\mathbf{W}_2(s)$ be system precompensator and postcompensator matrices, respectively, and define an augmented plant $\mathbf{G}_A(s)$ by

$$\mathbf{G}_A(s)=\mathbf{W}_2(s)\;\mathbf{G}(s)\;W_1(s) \tag{33}$$

Performing an NLCF robust stabilization design with $\mathbf{G}$ replaced by $\mathbf{G}_A$ yields a dynamic compensator $\mathbf{K}_A(s)$ that robustly stabilizes $\mathbf{G}_A$. Figure 3(a) gives a block diagram illustrating this loop-shaping procedure. Simple block manipulation yields figure 3(b), which shows that the corresponding compensator $\mathbf{K}$ to be applied to the unshaped plant $\mathbf{G}$ is

$$\mathbf{K}(s)=\mathbf{W}_1(s)\;\mathbf{K}_A(s)\;\mathbf{W}_2(s) \tag{34}$$

We then have

$$\epsilon_{A,\max}^{-1}=\left(1-\|\,[\widetilde{\mathbf{N}}_A,\widetilde{\mathbf{M}}_A]\,\|_H^2\right)^{-1/2}=\inf_{\mathbf{K}_A}\|\begin{bmatrix}\mathbf{K}_A\\ \mathbf{I}\end{bmatrix}\,(\mathbf{I}-\mathbf{G}_A\mathbf{K}_A)^{-1}[\mathbf{I},\mathbf{G}_A]\,\|_\infty$$

$$=\inf_{\mathbf{K}}\|\begin{bmatrix}\mathbf{W}_1^{-1}\mathbf{K}(\mathbf{I}-\mathbf{GK})^{-1}\mathbf{W}^{-1} & \mathbf{W}_1^{-1}\mathbf{K}(\mathbf{I}-\mathbf{GK})^{-1}\mathbf{GW}_1\\ \mathbf{W}_2(\mathbf{I}-\mathbf{GK})^{-1}\mathbf{W}_2^{-1} & \mathbf{W}_2(\mathbf{I}-\mathbf{GK})^{-1}\mathbf{GW}_1\end{bmatrix}\|_\infty \tag{35}$$

which indicates the weighting configuration that can be applied to the elements of equation (24) if the exact-solution structure is to be preserved. In general, if other weighting configurations are desired, the normal γ iteration procedure is required.

The introduction of dynamic weighting matrices always increases the order of the compensator. Let n be the order of a minimal realization of $\mathbf{G}(s), n_1$ be the order of $\mathbf{W}_1(s)$, and n_2 be the order of $\mathbf{W}_2(s)$. Given state-variable realizations for $\mathbf{W}_1(s), \mathbf{W}_2(s)$, and $\mathbf{K}_A(s)$, repeated application of equation (A5) yields a state-variable realization for $\mathbf{K}(s)$. The order of the realization for $\mathbf{K}(s)$ will be $\leq\; n+2(n_1+n_2)$ after elimination of any uncontrollable and unobservable modes. Lower order compensators can be obtained through application of compensator order-reduction methods such as that described by Anderson and Liu (1989). However, compensator order-reduction methods should be used with caution because they can attenuate robust stability.

Stability Robustness to Unmodeled Dynamics

In flexible space structures, perturbations in the form of unmodeled dynamics occur naturally in the additive form (eq. (1)). A direct relationship does not seem to exist in defining $[\Delta\widetilde{\mathbf{N}},\Delta\widetilde{\mathbf{M}}]$ as a

function of a given additive $\Delta\mathbf{G}$ in equation (1). Setting

$$\mathbf{G}_\Delta = \widetilde{\mathbf{M}}^{-1}\widetilde{\mathbf{N}} + \Delta\mathbf{G} = (\widetilde{\mathbf{M}} + \Delta\widetilde{\mathbf{M}})^{-1}(\widetilde{\mathbf{N}} + \Delta\widetilde{\mathbf{N}}) \tag{36}$$

yields

$$(\widetilde{\mathbf{M}} + \Delta\widetilde{\mathbf{M}})\Delta\mathbf{G} = [\Delta\widetilde{\mathbf{N}}, \Delta\widetilde{\mathbf{M}}] \begin{bmatrix} \mathbf{I}_m \\ -\mathbf{G} \end{bmatrix} \tag{37}$$

For small $\| \Delta\widetilde{\mathbf{M}}\Delta\mathbf{G} \|_\infty$, equation (37) becomes

$$\Delta\mathbf{G} = \widetilde{\mathbf{M}}^{-1}[\Delta\widetilde{\mathbf{N}}, \Delta\widetilde{\mathbf{M}}] \begin{bmatrix} \mathbf{I}_m \\ -\mathbf{G} \end{bmatrix} \tag{38}$$

for which a solution is

$$[\Delta\widetilde{\mathbf{N}}, \Delta\widetilde{\mathbf{M}}] = \widetilde{\mathbf{M}}\ \Delta\mathbf{G}(\mathbf{I}_m + \mathbf{G}^*\mathbf{G})^{-1}(\mathbf{I}_m, -\mathbf{G}^*) \tag{39}$$

Then, robust stability is preserved if

$$\| \widetilde{\mathbf{M}}\ \Delta\mathbf{G}(\mathbf{I}_m + \mathbf{G}^*\mathbf{G})^{-1}(\mathbf{I}_m, \mathbf{G}^*) \|_\infty < \epsilon_{\max}$$

Rigorous use of equation (39) is likely to produce conservative designs. In the application of the NLCF robust stabilization theory that follows, stability robustness to additive unmodeled dynamics in the form of equation (1) is incorporated by use of the weighting matrices in equation (34) and is analyzed through the examination of closed-loop conditions for stability robustness (Francis 1987)

$$\| \Delta\mathbf{G}\ \mathbf{K}(\mathbf{I} - \mathbf{G}\mathbf{K})^{-1} \|_\infty < 1 \tag{40}$$

or the more conservative sufficient condition for inequality (40)

$$\bar{\sigma}[\Delta\mathbf{G}(s)]\bar{\sigma}[\mathbf{K}(\mathbf{I} - \mathbf{G}\mathbf{K})^{-1}(s)] < 1 \tag{41}$$

for $s = j\omega$ and $\omega \in [0, \infty)$.

In figure 2, let

$$\mathbf{K}(s) = \left[\begin{array}{c|c} \mathbf{A}_c & \mathbf{B}_c \\ \hline \mathbf{C}_c & \mathbf{D}_c \end{array}\right] \tag{42}$$

and

$$\mathbf{G}(s) = \left[\begin{array}{c|c} \mathbf{A} & \mathbf{B} \\ \hline \mathbf{C} & \mathbf{D} \end{array}\right] \tag{43}$$

Then, state-variable realizations for the transfer matrices in equations (29) to (31) can be formed, wherein each has the same system matrix given by

$$\mathbf{A}_{cl} = \begin{bmatrix} \mathbf{A} + \mathbf{B}(\mathbf{I} - \mathbf{D}_c\mathbf{D})^{-1}\mathbf{D}_c\mathbf{C} & \mathbf{B}(\mathbf{I} - \mathbf{D}_c\mathbf{D})^{-1}\mathbf{C}_c \\ \mathbf{B}_c(\mathbf{I} - \mathbf{D}\mathbf{D}_c)^{-1}\mathbf{C} & \mathbf{A}_c + \mathbf{B}_c\mathbf{D}(\mathbf{I} - \mathbf{D}_c\mathbf{D})^{-1}\mathbf{C}_c \end{bmatrix} \tag{44}$$

An eigenvalue analysis of $\mathbf{A}_{cl}$ often gives an indication of the effect of the compensator on the open-loop eigenvalues of $\mathbf{A}$. An eigenvalue analysis of $\mathbf{A}_{cl}$ can occasionally give a measure of stability robustness to additive perturbations when the realization ($\mathbf{A}$, $\mathbf{B}$, $\mathbf{C}$, $\mathbf{D}$) in equation (44) is replaced by a state-variable realization of $\mathbf{G}_\Delta$.

Robust Stabilization of the Phase 0 Evolutionary Model

In this section, the previously discussed theory and algorithms for the robust stabilization of a plant modeled in normalized left-coprime factorization form are applied to produce compensators for the control of a model of a laboratory structure that has many of the characteristics and design difficulties associated with flexible space structures. Except for certain high-order transient response simulations, all computations were performed using a 486 personal computer employing the 386 MATLAB^{TM} computational environment in Anon. (1990). Use was also made of software from the MATLAB Control System Toolbox (Little and Laub 1986) and Robust-Control Toolbox (Chiang and Safonov 1988). Balanced realizations were computed by using the algorithm based on Singular Value Decomposition described by Laub et al. (1987). The H_∞ norms were calculated by using the bisection algorithm of Boyd, Balakrishnan, and Kabamba (1989).

Description of Phase 0 Model

The Control-Structures Interaction (CSI) Evolutionary Model is a laboratory testbed concept in which a sequence of testbeds is evolved with each new facility having more challenging dynamics and control characteristics than the previous one. The testbeds are to be designed and constructed at the Langley Research Center for the experimental validation of control techniques and integrated design methodology developed under the CSI program at Langley (Newsom et al. 1990). The phase 0 model was the first testbed to be constructed under this program, but, unfortunately, the phase 0 model is no longer in existence at Langley. However, many useful studies were performed using the phase 0 model (for example, see Lim, Maghami, and Joshi (1992); Maghami, Joshi, and Armstrong (1993); Lim and Balas (1992), and its data base has been archived and is still available for this and future studies. A schematic of the phase 0 structure is shown in figure 4, and a detailed description can be found in Belvin et al. (1991).

The phase 0 structure consisted of two vertical towers and two horizontal booms attached to a central 62-bay-truss main section with each bay being a 10-in. cube. (See fig. 4.) The structure was suspended from the laboratory ceiling by springs and two long cables designed to minimize the interaction between the suspension and the structural modes. A laser source was mounted at the top of the taller vertical tower, and a 16-ft reflector with a mirrored surface was mounted on the shorter tower. The laser beam was reflected by the mirrored surface onto a detector surface 660 in. above the reflector. The total structural weight was 741 lb. Eight proportional bidirectional gas thrusters (air jets) provided the input force actuation, and eight nearly collocated servo accelerometers provided output measurements.

Global line-of-sight pointing studies using the laser targeting system have been performed by Lim and Balas (1992). The present study is directly concerned with only vibration suppression about a given operating point and does not treat laser targeting as such. However, vibration suppression of the laser tower modes is a critical part of our design requirements because damping of the laser tower structure was a troublesome issue in previous laboratory tests.

The phase 0 model had six nonstructural modes (due to suspension) and many significant elastic modes. The NASTRAN finite element model (Belvin et al. 1991) consisted of 3560 degrees of freedom. A total of 86 modes with frequencies below 50 Hz were selected as a truth or evaluation model. For this study, as in previous studies (Lim, Maghami, and Joshi 1992), a reduced-order model consisting of 25 modes (selected from the 86 modes through a controllability and observability analysis) was used for the controller design model. Table I shows the frequency range of these 25 modes in hertz. Frequencies of the first six pendulum/suspension modes, brought about by the cable suspension in a $1g$ environment, range from 0.147 to 0.874 Hz. The first two elastic modes (7 and 8) are truss beam bending in the XY- and XZ-planes (defined in fig. 4) with frequencies of 1.474 Hz and 1.738 Hz, respectively. A uniform damping ratio of 0.5 percent is assumed for all the modes.

By using data from the finite element analysis, a dynamic mathematical model in the modal coordinate system can be constructed. A 50th-order state-variable realization of this model in (block) phase-canonical form will appear as $(\mathbf{A}_f, \mathbf{B}_f, \mathbf{C}_f, \mathbf{D}_f)$ where

$$\mathbf{A}_f = \begin{bmatrix} \mathbf{0} & \mathbf{I} \\ -\mathbf{\Omega}^2 & -\hat{\mathbf{Z}} \end{bmatrix} \qquad \mathbf{B}_f = \begin{bmatrix} \mathbf{0} \\ \mathbf{\Phi}^T \end{bmatrix} \qquad \mathbf{C}_f = [\mathbf{0}, \mathbf{\Phi}]\mathbf{A}_f \qquad \mathbf{D}_f = \mathbf{\Phi}\mathbf{\Phi}^T \tag{45}$$

with

$$\mathbf{\Omega} = \text{diag}(\omega_1,\ \omega_2,\ \ldots,\ \omega_{25}) \tag{46}$$

$$\hat{\mathbf{Z}} = \text{diag}(2\zeta_1\omega_1,\ 2\zeta_2\omega_2,\ \ldots,\ 2\zeta_{25}\omega_{25}) \tag{47}$$

and $\mathbf{\Phi}$ is an 8×25 matrix of mode shapes obtained from a finite element analysis (Belvin et al. 1991). In equations (46) and (47), ω_i denotes frequency and ζ_i denotes a damping ratio of 0.005 for $i = 1, \ldots, 25$. Eigenvalues of $\mathbf{A}_f$ are given in table I. Because the damping ratios are small, the frequencies in radians per second are closely approximated by the imaginary parts of the eigenvalues. Figure 5 shows an open-loop frequency response plot of the singular value bounds of the transfer matrix $\mathbf{G}_f$ defined by the $(\mathbf{A}_f, \mathbf{B}_f, \mathbf{C}_f, \mathbf{D}_f)$ system.

In flexible structures, higher frequency modes are more difficult to measure and compute accurately. For the phase 0 structure, the finite element model provided reasonably accurate natural frequency and damping values for modes below 2 Hz. However, higher frequency modes, beginning with the 10th mode at 2.301 Hz, are not accurately known (Lim and Balas 1992). In this design, only modes with frequencies up to 14 rad/sec are used to form the compensator design model, and modes with higher frequencies are used to represent unmodeled dynamics. Therefore, modes above mode 9 are truncated from the 25-mode model and are accounted for as an additive uncertainty in the design process. The matrix $\mathbf{G}_f$ now appears as in equation (1) with

$$\mathbf{G}_\Delta = \mathbf{G}_f = \mathbf{G} + \Delta\mathbf{G} \tag{48}$$

$$\mathbf{G} = \mathbf{C}(s\mathbf{I}_{18} - \mathbf{A})^{-1}\mathbf{B} + \mathbf{D} \tag{49}$$

and

$$\Delta\mathbf{G} = \mathbf{C}_t(s\mathbf{I}_{32} - \mathbf{A}_t)^{-1}\mathbf{B}_t + \mathbf{D}_t \tag{50}$$

The realizations $(\mathbf{A}, \mathbf{B}, \mathbf{C}, \mathbf{D})$ and $(\mathbf{A}_t, \mathbf{B}_t, \mathbf{C}_t, \mathbf{D}_t)$ are obtained by collecting and rearranging appropriate rows and columns of $(\mathbf{A}_f, \mathbf{B}_f, \mathbf{C}_f, \mathbf{D}_f)$. Numerical data for $\mathbf{G}$ and $\Delta\mathbf{G}$ are given in appendix C, and figure 6 shows individual frequency response plots for $\mathbf{G}$ and $\Delta\mathbf{G}$.

Design Objectives

The objective of the control system design is to increase the damping of all the pseudo rigid-body and structural modes of the design model $\mathbf{G}$. The designs must also possess stability robustness with respect to unmodeled structural modes, of which $\Delta\mathbf{G}$ from equation (50) is taken as a representative sample, and, if possible, possess stability robustness to parametric uncertainties such as errors expected in frequency, damping, and mode shapes in the design model.

Loop-Shaping Procedures

By using the numerical data for the 18th-order system ($\mathbf{A}$, $\mathbf{B}$, $\mathbf{C}$, $\mathbf{D}$) found in appendix C, the construction given by equations (A18) to (A22) leads to a state-variable realization for $[\widetilde{\mathbf{N}}, \widetilde{\mathbf{M}}]$ with a Hurwitz system matrix. Computing the Hankel norm of $[\widetilde{\mathbf{N}}, \widetilde{\mathbf{M}}]$, as outlined in appendix A, gives $\| [\widetilde{\mathbf{N}}, \widetilde{\mathbf{M}}] \|_H = 0.8972$, whereby, from equation (22), $\epsilon_{\max} = 0.4417$ and $\gamma_{\min} = 1/\epsilon_{\max} = 2.264$. An optimal compensator (using eq. (B16) with $r = 1$) and a central suboptimal compensator (using eq. (B28) with $\epsilon = 0.9\epsilon_{\max}$) were obtained following the algorithms in appendix B. Frequency

response plots for the compensators are shown in figure 7. Both compensators, when applied to $\mathbf{G}$ in the feedback fashion of figure 2, enhanced the stability of $\mathbf{G}$ but grossly violated the condition stated in inequality (40) with $\Delta\mathbf{G}$ given by equation (50). Violation of inequality (40) indicates that the compensator

$$\mathbf{u}(s) = \mathbf{K}(s)\ \mathbf{y}(s) \tag{51}$$

applied to $\mathbf{G}_\Delta$, given by equation (48), has the potential of a destabilizing spillover effect (Joshi 1989) on the $\Delta\mathbf{G}$ dynamics. The failure to satisfy the condition in inequality (40) was primarily caused by the lack of free parameters for adjustment in the algorithms and the fact that $\mathbf{G}(s)$ is not strictly proper, in which case both optimal and suboptimal compensators will not be strictly proper as can be seen from figure 7.

The spillover problem could be resolved through incorporation of loop-shaping functions of the form given in equation (33). The weighting functions employed were

$$\mathbf{W}_1(s) = \mathbf{I}_8 \tag{52}$$

and

$$\mathbf{W}_2(s) = \mathbf{W}(s) = f(s)\ \mathbf{I}_8 \tag{53}$$

where the scalar function $f(s)$ is given by

$$f(s) = k/(s+a)^i \tag{54}$$

The positive real parameters a, i, and k are adjusted from observation of the condition given by inequality (41) with the compensator in equation (34). The parameter a is chosen such that a plot of the inverse of $\bar{\sigma}[\mathbf{K}(\mathbf{I}-\mathbf{GK})^{-1}(j\omega)]$ versus $\omega \in [0,\infty)$ breaks upward before $\omega = 14$ rad/sec, the approximate frequency at which the $\Delta\mathbf{G}$ dynamics become predominant. The parameter i roughly controls the slope of the upward break and was taken as $i = 1$ or 2. The quantity k adjusts the magnitude of $\mathbf{W}(s)$ and ranges between 0.08 and 4.0 in the following discussion. Minimal-order state-variable realizations for $\mathbf{W}(s)$ for $i = 1$ are

$$\mathbf{W} = \left[\begin{array}{c|c} \mathbf{A}_W^{(1)} & \mathbf{B}_W^{(1)} \\ \hline \mathbf{C}_W^{(1)} & \mathbf{D}_W^{(1)} \end{array}\right] = \left[\begin{array}{c|c} -a\mathbf{I}_8 & \mathbf{B}_W^{(1)} \\ \hline k\mathbf{B}_W^{(1)} & \mathbf{0}_{8\times 8} \end{array}\right] \tag{55}$$

where

$$\mathbf{B}_W^{(1)} = \begin{pmatrix} 0 & 0 & 0 & \dots & 0 & 0 & 1 \\ 0 & 0 & 0 & \dots & 0 & 1 & 0 \\ \vdots & \vdots & \vdots & & \vdots & \vdots & \vdots \\ 0 & 1 & 0 & \dots & 0 & 0 & 0 \\ 1 & 0 & 0 & \dots & 0 & 0 & 0 \end{pmatrix}_{8\times 8} \tag{56}$$

and, for $i = 2$, are

$$\mathbf{W} = \left[\begin{array}{c|c} \mathbf{A}_W^{(2)} & \mathbf{B}_W^{(2)} \\ \hline \mathbf{C}_W^{(2)} & \mathbf{D}_W^{(2)} \end{array}\right] \tag{57}$$

where

$$\mathbf{A}_W^{(2)} = \left[\begin{array}{c|c} -2a\mathbf{I}_8 & -a^2\mathbf{B}_W^{(1)} \\ \hline \mathbf{B}_W^{(1)} & \mathbf{0}_{8\times 8} \end{array}\right] \tag{58}$$

$$\mathbf{B}_W^{(2)} = \begin{pmatrix} \mathbf{I}_8 \\ - - \\ \mathbf{0}_{8\times 8} \end{pmatrix} \tag{59}$$

$$\mathbf{C}_W^{(2)} = \left(\mathbf{0}_{8\times 8} \;\vdots\; k\mathbf{B}_W^{(1)} \right) \tag{60}$$

and

$$\mathbf{D}_W^{(2)} = \mathbf{0}_{8\times 8} \tag{61}$$

Realizations of equations (55) to (61) were obtained from the Control System Toolbox function entitled "tf2ss.m."

Increasing the parameter k not only moves the closed-loop eigenvalues of the controllable modes of the design model farther into the complex left-hand plane but also increases the potential of destabilizing spillover into the modes of $\mathbf{A}_t$. Observing the real parts of modes 10 and 11 shows that these modes need stability augmentation as much as modes 1 to 9. However, of the first 11 modes, modes 10 and 11 are the least controllable (with mode 11 more controllable than mode 10). A Hankel singular value analysis of the 11-mode model yields the mode numbers ordered in decreasing controllability and/or observability as 8, 7, 3, 2/9 (tie), 6, 4, 1, 5, 11, and 10. Including modes 10 and 11 in the design model and increasing k to provide the added stability invariably produces compensators (optimal and suboptimal) that violate conditions given in inequalites (40) and (41). By using the methodology and weighting described herein, modes 10 and 11 will necessarily remain relatively unchanged when stability to additive perturbations is a design requirement.

Robustness to Structured Perturbations

For modes 1 to 9 below 2 Hz, the accuracy of values of natural frequency and damping ratio are within 1 percent and 10 percent, respectively. (See Lim and Balas 1992.) In order to evaluate the compensators for perturbations in frequencies and damping ratios within these ranges, the frequencies ω_i and damping ratios ζ_i in the $\mathbf{A}$ matrix of the 9-mode design model were replaced by perturbed values $(\omega_p)_i$ and $(\zeta_p)_i$ given, respectively, by

$$(\omega_p)_i = \omega_i + (\delta\omega)_i\omega_i \tag{62}$$

and

$$(\zeta_p)_i = \zeta_i + (\delta\zeta)_i\zeta_i \tag{63}$$

for $i = 1, \ldots, 9$. In equations (62) and (63), $(\delta\omega)_i$ and $(\delta\zeta)_i$ are random variables uniformly distributed within $[-0.01, 0.01]$ and $[-0.1, 0.1]$, respectively. The new perturbed system matrix is denoted by $\mathbf{A}_\delta$. If $\mathbf{G}(s)$ is given by equation (49), the transfer matrix for the perturbed system is given by

$$\mathbf{G}_\delta(s) = \mathbf{C}_\delta(s\mathbf{I}_{18} - \mathbf{A}_\delta)^{-1}\mathbf{B} + \mathbf{D} \tag{64}$$

where

$$\mathbf{C}_\delta = \mathbf{C}\mathbf{A}^{-1}\mathbf{A}_\delta \tag{65}$$

to reflect acceleration measurements.

With

$$\mathbf{G}_A(s) = \mathbf{W}_2(s)\ \mathbf{G}(s)\ \mathbf{W}_1(s) \tag{66}$$

and

$$\mathbf{G}_{\delta_A}(s) = \mathbf{W}_2(s)\ \mathbf{G}_\delta(s)\ \mathbf{W}_1(s) \tag{67}$$

normalized left-coprime factors are found such that

$$\mathbf{G}_A(s) = (\widetilde{\mathbf{M}}_A)^{-1}\widetilde{\mathbf{N}}_A \tag{68}$$

and

$$\mathbf{G}_{\delta_A}(s) = (\widetilde{\mathbf{M}}_{\delta_A})^{-1}\widetilde{\mathbf{N}}_{\delta_A} \tag{69}$$

Define

$$\Delta\mathbf{P} = [\Delta\widetilde{\mathbf{N}}_A, -\Delta\widetilde{\mathbf{M}}_A] \tag{70}$$

where

$$\Delta\widetilde{\mathbf{M}}_A = \widetilde{\mathbf{M}}_{\delta_A} - \widetilde{\mathbf{M}}_A \tag{71}$$

and

$$\Delta\widetilde{\mathbf{N}}_A = \widetilde{\mathbf{N}}_{\delta_A} - \widetilde{\mathbf{N}}_A \tag{72}$$

If $\| \Delta\mathbf{P} \|_\infty < \epsilon_A < \epsilon_{A,\max}$, the compensators also stabilize the perturbed system in addition to stabilizing $\mathbf{G}(s)$.

Compensator Design

Optimal compensator. The parameters (k, i, a) in equation (54) were adjusted to meet the design objectives. Because the optimal compensator was not strictly proper, $i = 2$ was found to provide faster roll-off and to best allow the satisfaction of conditions in inequalities (40) and (41). A representative optimal compensator used $(k, i, a) = (0.1,\ 2,\ 0.5)$. After scaling each channel of $\mathbf{G}$ by $0.1/(s + 0.5)^2$, the result was $\epsilon_{A,\max} = 0.6749$. Figure 8 shows the scaled version of $\mathbf{G}(s)$, and figures 9 and 10 show singular value bounds for the corresponding compensators $\mathbf{K}_A(s)$ and $\mathbf{K}(s)$, respectively. Table II gives the eigenvalues of the Hurwitz system matrix from a state-variable realization of $\mathbf{K}_A(s)$. The order of the compensator $\mathbf{K}_A$ is 33 (corresponding to $n = 18, n_1 = 0, n_2 = 16, r = 1$, and $i = 2$), whereby the final compensator $\mathbf{K}$ is on the order of 49.

Over 2000 realizations of equations (62) and (63) were computed for the optimal compensator and corresponding $\Delta\mathbf{P}$ transfer matrices (given by eq. (70)) tested for satisfaction of $\| \Delta\mathbf{P} \|_\infty < \epsilon_{A,\max}$. No violations were encountered. Values of $\| \Delta\mathbf{P} \|_\infty$ ranged between 0.1728 and 0.5888 with a mean of 0.4627, and the standard deviation was 0.0726. Satisfaction of conditions in inequalities (40) and (41) is depicted in figure 11, which indicates that mode 20 (the laser tower mode) at 41.9 rad/sec (6.7 Hz) is the mode most likely to experience destabilizing spillover. (In this report, frequency is expressed in radians per second or Hertz (or in both) for comparison purposes with the literature.) This property has also been observed experimentally in previous studies. The peak value (H_∞ norm) of the curve in figure 11(b) is 0.024 at 41.9 rad/sec, which indicates an additive stability robustness margin of about 97 percent.

This ultraconservative margin for additive stability robustness was forced by the desire to *also* have a compensator that guarantees stability robustness to expected parametric uncertainties in frequencies and damping ratios. If k is increased to 2.0 for the same values of i and a, the peak value of the curve in the corresponding figure 11(b) is 0.570, which indicates a more reasonable margin of 43 percent. However, $k = 2.0$ produced $\epsilon_{A,\max} = 0.4856$, and this reduced value of $\epsilon_{A,\max}$ leads to the occurrence of violations greater than 40 percent of the time in the random tests for $\| \Delta\mathbf{P} \|_\infty < \epsilon_{A,\max}$. For fixed values of i and a, decreasing k increases $\epsilon_{A,\max}$ and decreases $\| \Delta\mathbf{P} \|_\infty$. A value of k allowing a sufficiently wide "gap" between the two quantities is required when specific ranges of parametric variations are considered.

A state-variable realization $(\mathbf{A}_c, \mathbf{B}_c, \mathbf{C}_c, \mathbf{D}_c)$ of the optimal compensator $\mathbf{K}$ was formed, and the controller was applied (in the manner of fig. 2) to the 50th-order system $\mathbf{G}_\Delta$. The closed-loop system matrix appears as $\mathbf{A}_{cl}$ in equation (44), but with (**A**, **B**, **C**, **D**) replaced by $(\mathbf{A}_f, \mathbf{B}_f, \mathbf{C}_f, \mathbf{D}_f)$. When comparing the imaginary parts of the eigenvalues of $\mathbf{A}_{cl}$ with the imaginary parts of the open-loop eigenvalues (given in table I), certain $\mathbf{A}_{cl}$ eigenvalues can be identified as the closed-loop modifications of the eigenvalues of $\mathbf{A}_f$. These eigenvalues and corresponding damping ratios (which are correlated with open-loop mode numbers) are given in table III. The compensator leaves the

open-loop eigenvalues essentially unchanged except for modes 1 to 3. Optimal compensators with better stability augmentation can be obtained at the expense of violations in robust stability because of parametric variations in frequencies and damping ratios of the design model.

Suboptimal compensators. Suboptimal compensators computed from strictly proper systems $\mathbf{G}_A(s)$ are strictly proper, whereby lower order weighting functions (other than those used in the foregoing optimal compensator studies) can be employed without difficulty in satisfying the additive robustness conditions. Suboptimal compensator studies were performed using $i = 1$ and $\epsilon_A = 0.9\epsilon_{A,\max}$ from which a representative result had $(k, i, a) = (0.5, 1, 0.1)$. After scaling each channel of $\mathbf{G}$ by $0.5/(s + 0.1)$, the result was found to be $\epsilon_{A,\max} = 0.667$. Figure 12 shows the scaled version of $\mathbf{G}$, and figures 13 and 14 show singular value bounds for the compensators $\mathbf{K}_A(s)$ and $\mathbf{K}(s)$, respectively. Table IV gives the eigenvalues of the Hurwitz system matrix from a state variable realization of $\mathbf{K}_A(s)$. The order of the compensator $\mathbf{K}_A$ is 26 (corresponding to $n = 18, n_1 = 0, n_2 = 8$, and $i = 1$), whereby the order of the final compensator $\mathbf{K}$ is 34.

Again, over 2000 realizations of equations (62) and (63) were computed for the suboptimal compensator and the corresponding $\Delta\mathbf{P}$ transfer matrices tested for satisfaction of $\| \Delta\mathbf{P} \|_\infty < \epsilon_{A,\max}$ with no violations encountered. Values of $\| \Delta\mathbf{P} \|_\infty$ ranged between 0.0561 and 0.5595 with a mean of 0.2798 and a standard deviation of 0.0907. The expected variations in frequency and damping ratio of 1 percent and 10 percent, respectively, are apparently close to the upper bounds for robust stability for $k = 0.5$. Increasing these variations to 1.5 percent and 15 percent causes violations about 6 percent of the time.

Satisfaction of conditions in inequalities (40) and (41) is shown in figure 15. An interesting note is that figure 15(a) indicates that mode 20 (the same mode as that indicated by fig. 11) is the mode most likely to be troublesome, whereas figure 15(b) flags mode 15 at 27.6 rad/sec. The peak value of the curve in figure 15(b) is 0.562, which indicates an additive stability robustness margin of about 44 percent.

The suboptimal compensator was also applied to the control of the 50th-order system $\mathbf{G}_\Delta$, and an eigenvalue analysis was performed on the resulting $\mathbf{A}_{cl}$ matrix. The results are given in table V. The fact that the real parts of the eigenvalues for modes 10 to 25 are not significantly changed from the corresponding values of table I indicates that the additive robustness conditions are satisfied. Modes 3 to 9 all have enhanced stability except for possibly mode 5. The eigenvalue data give two eigenvalues with imaginary parts close to the imaginary part of open-loop mode 5. Both are shown in table V. The entry with the largest real part is possibly the closed-loop eigenvalue of mode 5 because this mode is the least controllable and observable of the first nine modes. No correlation could be made for modes 1 and 2.

For comparative purposes, a calculation was performed with $(k, i, a) = (0.5, 1, 0.1)$ and $\epsilon_A = 0$. Compensator equations for this calculation are given by the $\gamma \to \infty$ case found at the end of appendix B. Figures 16 to 18 and tables VI and VII provide the same information as previously provided for the optimal and other suboptimal compensators. Figure 18 indicates that robustness to additive perturbations measured by conditions in inequalities (40) and (41) is somewhat improved. The peak value of the curve in figure 18(b) is 0.184 at 27.6 rad/sec with a robustness stability margin of about 81 percent.

For fixed values of the parameters (k, i, a) as ϵ_A increased from 0 toward $\epsilon_{A,\max}$ within the suboptimal structure, the magnitudes of the imaginary parts of the eigenvalues of a state-variable realization of $\mathbf{K}_A(s)$ generally decreased, whereas the magnitudes of the real parts generally increased. Thus, for small values of ϵ_A, a relatively slower compensator was produced; this caused smaller values on the left side of inequality (41) which, in turn, created larger values of additive robustness stability margin.

Evaluation model simulations. The four compensators discussed were applied to the control of the full 86-mode-evaluation phase 0 model subjected to a transient input disturbance. Although not directly considered in the robust stability design process, this application gave an indication of the relative merit of the compensators in the area of closed-loop performance. The simulation consisted of (1) applying an excitation input sequence for the first 9 sec, (2) allowing 1 sec of free decay, and then (3) applying a controller at the 10-sec mark for a total duration of 30 sec. The input sequence consisted of harmonic forces designed to excite two pendulum modes (1 and 3) and the first two bending modes (7 and 8) using a single actuator for each mode. Specifically, actuators 1 (mode 7), 2 (mode 8), 6 (mode 3), and 7 (mode 1) were excited with signals of 1.474 Hz, 1.738 Hz, 0.155 Hz, and 0.147 Hz, respectively. No actuator dynamics were considered.

The compensators were discretized at a sampling rate of 133 Hz. The input sequence and sampling rate are the same as those employed by Lim, Maghami, and Joshi (1992) in their experimental investigation using the actual phase 0 structure. The format for the presentation of the results herein parallels that of the experimental study. Figures 19 to 34 show input and output responses for collocated thrusters and accelerometers 7 and 8 (laser tower) for the optimal and suboptimal controllers. The best performance is obtained by the suboptimal compensator with $\epsilon_{A,\max} = 0.667$ followed closely by the suboptimal compensator with $\epsilon_A = 0$. The optimal (2.0, 2, 0.5) compensator had marginal performance characteristics, and the highly conservative robust (0.1, 2, 0.5) compensator had almost no effect. The suboptimal responses compare favorably with those of Lim et al. which were designed with performance issues in mind.

Concluding Remarks

In this report the application of a robust stabilization methodology to the control of a simulated model of an actual laboratory apparatus has been considered. The apparatus, known as the Control-Structures Interaction (CSI) Phase 0 Evolutionary Model, was built at the Langley Research Center for the purpose of investigating some of the problems and solution approaches involved in the control of flexible space structures.

With the view that system uncertainties are perturbations about a nominal design model, a single robustly stabilizing compensator was sought that not only enhanced the stability of the nominal plant but, in addition, stabilized all systems within some neighborhood of the plant generated by the perturbations. The computation of the largest neighborhood around a given design plant for which a single controller produces closed-loop stability was shown to be formulated as an H_∞ control problem. Several formulations of the H_∞ problem were possible depending on the character of the perturbation space. A formulation based on the Glover-McFarlane theory (1989) was employed wherein descriptions of the normalized coprime factor plant were used and the plant perturbations were defined as additive modifications to the coprime factors. An attractive feature of the normalized coprime factorization approach is that it leads to a closed-form expression for the maximum perturbation radius. The maximum radius can be directly computed in terms of the open-loop design model, thus allowing optimal and suboptimal robust compensators to be found without the usual γ iteration of the H_∞ design.

Computational algorithms for both the optimal and suboptimal versions of the McFarlane-Glover theory (1990) were summarized, and representative compensators were computed and analyzed for the control of the simulated Langley phase 0 structure. Through incorporation of weighting functions, the compensators were made to roll off in such a way as to cause the closed-loop system to be robust to additive unmodeled dynamics. A Monte Carlo approach was employed to test the robust stability of the compensators against expected structured parametric perturbations in the compensator design model. Even though these calculations offer no mathematical proof, they do give a degree of confidence that the compensators robustly stabilize the nominal system for expected perturbations in frequencies and damping ratios of the system matrix of the design model. The compensators were tested through application to a full-order evaluation model.

Results from the study indicate that when requiring the compensators to satisfy all design objectives of stability augmentation, robust stability to unmodeled dynamics appearing as additive perturbations, and robustness to structured parametric variations, the optimal robust compensators can be overly conservative with marginal stability augmentation, whereas the suboptimal compensators are not. For the class of flexible structure applications considered, the suboptimal version of the McFarlane-Glover theory provides a viable approach for the computation of low-authority controllers providing robust stability augmentation for variations in design model parameters and additive unmodeled dynamics. These controllers may need to be supplemented with high-authority loops to provide additional performance.

NASA Langley Research Center
Hampton, VA 23681-0001
March 29, 1993

Appendix A

Nomenclature and Definitions

This appendix offers a compilation of certain fundamental results from linear systems theory that are employed in the body of this report.

State-Variable and Transfer Matrix Representations

Assume that a dynamic system is modeled by a real, linear, finite-dimensional, time-invariant, continuous set of ordinary differential equations written in vector-matrix form as

$$\dot{\mathbf{x}}(t) = \mathbf{A}\ \mathbf{x}(t) + \mathbf{B}\ \mathbf{u}(t) \tag{A1}$$

$$\mathbf{y}(t) = \mathbf{C}\ \mathbf{x}(t) + \mathbf{D}\ \mathbf{u}(t) \tag{A2}$$

where, for $t \in [0, \infty)$,

$\mathbf{x}(t) \in R^n$	state vector
$\mathbf{y}(t) \in R^p$	output vector
$\mathbf{u}(t) \in R^m$	control vector
$\mathbf{A} \in R^{n \times n}$	system matrix
$\mathbf{B} \in R^{n \times m}$	control-effectiveness matrix
$\mathbf{C} \in R^{p \times n}$	output matrix
$\mathbf{D} \in R^{p \times m}$	control-feedthrough matrix

The transfer $p \times m$ function matrix ($\mathbf{G}(s)$) for the ($\mathbf{A}$, $\mathbf{B}$, $\mathbf{C}$, $\mathbf{D}$) system is given for $s \in C$ by

$$\mathbf{G}(s) = \mathbf{C}(s\mathbf{I} - \mathbf{A})^{-1}\mathbf{B} + \mathbf{D} := \left[\begin{array}{c|c} \mathbf{A} & \mathbf{B} \\ \hline \mathbf{C} & \mathbf{D} \end{array}\right] \tag{A3}$$

If $\mathbf{D}$ is square and nonsingular,

$$\mathbf{G}^{-1}(s) = \left[\begin{array}{c|c} \mathbf{A} - \mathbf{B}\mathbf{D}^{-1}\mathbf{C} & \mathbf{B}\mathbf{D}^{-1} \\ \hline -\mathbf{D}^{-1}\mathbf{C} & \mathbf{D}^{-1} \end{array}\right] \tag{A4}$$

If

$$\mathbf{G}_1 = \left[\begin{array}{c|c} \mathbf{A}_1 & \mathbf{B}_1 \\ \hline \mathbf{C}_1 & \mathbf{D}_1 \end{array}\right]$$

$$\mathbf{G}_2 = \left[\begin{array}{c|c} \mathbf{A}_2 & \mathbf{B}_2 \\ \hline \mathbf{C}_2 & \mathbf{D}_2 \end{array}\right]$$

then state-variable realizations (not necessarily minimal) for the cascaded system $\mathbf{G}_1\mathbf{G}_2$ are

$$\mathbf{G}_1\mathbf{G}_2 = \left[\begin{array}{cc|c} \mathbf{A}_1 & \mathbf{B}_1\mathbf{C}_2 & \mathbf{B}_1\mathbf{D}_2 \\ \mathbf{0} & \mathbf{A}_2 & \mathbf{B}_2 \\ \hline \mathbf{C}_1 & \mathbf{D}_1\mathbf{C}_2 & \mathbf{D}_1\mathbf{D}_2 \end{array}\right]$$

$$= \left[\begin{array}{cc|c} \mathbf{A}_2 & \mathbf{0} & \mathbf{B}_2 \\ \mathbf{B}_1\mathbf{C}_2 & \mathbf{A}_1 & \mathbf{B}_1\mathbf{D}_2 \\ \hline \mathbf{D}_1 & \mathbf{C}_2\mathbf{C}_1 & \mathbf{D}_1\mathbf{D}_2 \end{array}\right] \tag{A5}$$

where **0** represents a null matrix of appropriate size.

When **A** is Hurwitz, that is, has eigenvalues only in the open, complex left half-plane, the reachability gramian (**P**) and the observability gramian (**Q**) are given (Kwakernaak and Sivan 1972) as the unique symmetric nonnegative definite solutions to the Lyapunov equations

$$\mathbf{A}\mathbf{P} + \mathbf{P}\mathbf{A}^T + \mathbf{B}\mathbf{B}^T = 0 \tag{A6}$$

$$\mathbf{A}^T\mathbf{Q} + \mathbf{Q}\mathbf{A} + \mathbf{C}^T\mathbf{C} = 0 \tag{A7}$$

If (**A**, **B**) and (**C**, **A**) are, respectively, completely controllable and completely observable, then **P** and **Q** are symmetric and positive definite.

Denote the ith eigenvalue of a square matrix **E** by $\lambda_i(\mathbf{E})$. When $\mathrm{Re}[\lambda_i(\mathbf{A})] < 0$ for $i = 1, 2, \ldots, n$, the Hankel singular values of the transfer function matrix **G**(s) are defined as (Glover 1984)

$$\sigma_i[\mathbf{G}(s)] = \{\lambda_i(\mathbf{P}\mathbf{Q})\}^{1/2} \tag{A8}$$

where **P** and **Q** satisfy equations (A6) and (A7), respectively, and, by convention,

$$\sigma_i[\mathbf{G}(s)] \geq \sigma_{i+1}[\mathbf{G}(s)] \tag{A9}$$

for $i = 1, 2, \ldots, n-1$. The Hankel norm of **G**(s), denoted by $\| \mathbf{G} \|_H$, is defined as

$$\| \mathbf{G} \|_H = \sigma_1[\mathbf{G}(s)] \tag{A10}$$

which is the largest Hankel singular value of $\mathbf{G}(s)$. The eigenvalues of the product **PQ** are invariant under coordinate transformations on $\mathbf{x}(t)$ in equations (A1) and (A2). When **A** is Hurwitz, a particular coordinate transformation called a balancing transformation exists (Moore 1981) such that

$$\mathbf{P} = \mathbf{Q} = \mathrm{diag}(\sigma_1, \sigma_2, \ldots, \sigma_n) \tag{A11}$$

Computational aspects of balancing transformations are discussed in Laub et al. (1987), and applications to model-order reduction are surveyed in Anderson and Liu (1989).

Let RL_∞ denote the space of all real-rational proper transfer function matrices that have no poles on the imaginary ($s = j\omega$) axis of the complex plane and $RH_\infty \subset RL_\infty$ denote the subset of all asymptotically stable (no poles in the closed right half-plane) proper transfer function matrices. With $\mathbf{G}(s) \in RH_\infty$, the H_∞ norm of $\mathbf{G}(s)$ is

$$\| \mathbf{G} \|_\infty = \sup_{\omega \in R} \bar{\sigma}[\mathbf{G}(j\omega)] \tag{A12}$$

where $\bar{\sigma}$ denotes the largest singular value (not the Hankel singular value) of the complex matrix $\mathbf{G}(j\omega)$ for a given real ω. For a discussion of matrix singular values and their applications in linear systems theory, see Golub and Van Loan (1989) and Klema and Laub (1980). Computational aspects

of H_∞ norms are discussed in Boyd, Balakrishnan, and Kabamba (1989) and Boyd and Balakrishnan (1990).

Coprime Factor Representations

In addition to state-variable and transfer-function matrix representations, all time-invariant linear systems have coprime factor representations (Vidyasagar 1985). Suppose that $\widetilde{\mathbf{M}} \in RH_\infty$ and $\widetilde{\mathbf{N}} \in RH_\infty$ have the same number of rows. Then $\widetilde{\mathbf{M}}$ and $\widetilde{\mathbf{N}}$ are left coprime if, and only if, $\widetilde{\mathbf{U}} \epsilon RH_\infty$ and $\widetilde{\mathbf{V}} \epsilon RH_\infty$ exist such that

$$\widetilde{\mathbf{M}}(s)\widetilde{\mathbf{V}}(s) + \widetilde{\mathbf{N}}(s)\ \widetilde{\mathbf{U}}(s) = \mathbf{I}_p \tag{A13}$$

for all $s \in C$. Equivalently, $\widetilde{\mathbf{M}}$ and $\widetilde{\mathbf{N}}$ are left coprime if, and only if, $[\widetilde{\mathbf{N}}, \widetilde{\mathbf{M}}]$ has a right inverse in RH_∞. Any (stable or not) transfer function matrix $\mathbf{G}(s)$ can be represented in terms of a pair of asymptotically stable, real-rational, proper transfer function matrices that are left coprime. This representation, termed a left-coprime factorization of $\mathbf{G}(s)$, is given by

$$\mathbf{G}(s) = \widetilde{\mathbf{M}}(s)^{-1}\widetilde{\mathbf{N}}(s) \tag{A14}$$

where $\widetilde{\mathbf{M}} \in RH_\infty$ is square with $\det(\widetilde{\mathbf{M}}) \neq 0$, and $\widetilde{\mathbf{N}} \in RH_\infty$ and $\widetilde{\mathbf{M}}$ are left coprime. A particular left-coprime factorization, called a normalized left-coprime factorization (NLCF), is one in which

$$\widetilde{\mathbf{N}}(s)\widetilde{\mathbf{N}}^*(s) + \widetilde{\mathbf{M}}(s)\ \widetilde{\mathbf{M}}^*(s) = \mathbf{I}_p \tag{A15}$$

for all $s \in C$ where

$$\widetilde{\mathbf{N}}^*(s) = \widetilde{\mathbf{N}}^T(-s) \tag{A16}$$

$$\widetilde{\mathbf{M}}^*(s) = \widetilde{\mathbf{M}}^T(-s) \tag{A17}$$

A state-variable realization for a normalized left-coprime factorization can be formed from a minimal ($\mathbf{A}$, $\mathbf{B}$, $\mathbf{C}$, $\mathbf{D}$) realization of $\mathbf{G}(s)$ (Vidyasagar 1988). First, solve the generalized filter algebraic Riccati equation (GFARE)

$$(\mathbf{A} - \mathbf{B}\mathbf{S}^{-1}\mathbf{D}^T\mathbf{C})\mathbf{Z} + \mathbf{Z}(\mathbf{A} - \mathbf{B}\mathbf{S}^{-1}\mathbf{D}^T\mathbf{C})^T - \mathbf{Z}\mathbf{C}^T\mathbf{R}^{-1}\mathbf{C}\mathbf{Z} + \mathbf{B}\mathbf{S}^{-1}\mathbf{B}^T = 0 \tag{A18}$$

for the unique symmetric positive definite matrix $\mathbf{Z}$ where

$$\mathbf{S} = \mathbf{I}_m + \mathbf{D}^T\mathbf{D} \tag{A19}$$

$$\mathbf{R} = \mathbf{I}_p + \mathbf{D}\mathbf{D}^T \tag{A20}$$

Then, with

$$\mathbf{H} = -(\mathbf{Z}\mathbf{C}^T + \mathbf{B}\mathbf{D}^T)\mathbf{R}^{-1} \tag{A21}$$

and

$$[\widetilde{\mathbf{N}} \ \vdots \ \widetilde{\mathbf{M}}] = \left[\begin{array}{c|c|c} \mathbf{A} + \mathbf{H}\mathbf{C} & \mathbf{B} + \mathbf{H}\mathbf{D} & \mathbf{H} \\ \hline \mathbf{R}^{-1/2}\mathbf{C} & \mathbf{R}^{-1/2}\mathbf{D} & \mathbf{R}^{-1/2} \end{array}\right] \tag{A22}$$

$\widetilde{\mathbf{N}}$ and $\widetilde{\mathbf{M}}$ form a normalized left-coprime factorization of $\mathbf{G}(s)$ constructed as in equation (A14).

Similar to left-coprime factorizations, all rational transfer matrices also have right-coprime factorizations (Vidyasagar 1985). Suppose that $\mathbf{M} \in RH_\infty$ and $\mathbf{N} \in RH_\infty$ have the same number of columns. Then, $\mathbf{M}$ and $\mathbf{N}$ are defined to be right coprime if, and only if, $\mathbf{U} \in RH_\infty$ and $\mathbf{V} \in RH_\infty$ exist such that

$$\mathbf{V}(s)\mathbf{M}(s) + \mathbf{U}(s)\mathbf{N}(s) = \mathbf{I}_m \tag{A23}$$

for all $s \in C$. That is, the matrix $\begin{bmatrix} \mathbf{N} \\ \mathbf{M} \end{bmatrix}$ has a left inverse in RH_∞. The transfer matrix $\mathbf{G}(s)$ is said to have a right-coprime factorization when

$$\mathbf{G}(s) = \mathbf{N}\mathbf{M}^{-1} \tag{A24}$$

where $\mathbf{M} \in RH_\infty$ is square with $\det(\mathbf{M}) \neq 0$, and $\mathbf{N} \in RH_\infty$ and $\mathbf{M}$ are right coprime. A particular right-coprime factorization, called a normalized right-coprime factorization (NRCF), is one in which

$$\mathbf{M}^*(s)\ \mathbf{M}(s) + \mathbf{N}^*(s)\ \mathbf{N}(s) = \mathbf{I}_m \tag{A25}$$

for $s \in C$, where $\mathbf{N}^*$ and $\mathbf{M}^*$ are as defined by equations (A16) and (A17), respectively. For a minimal ($\mathbf{A}$, $\mathbf{B}$, $\mathbf{C}$, $\mathbf{D}$) realization of $\mathbf{G}(s)$, a state-variable realization for an NRCF of $\mathbf{G}(s)$ is given by

$$\begin{bmatrix} \mathbf{N} \\ \mathbf{M} \end{bmatrix} = \left[\begin{array}{c|c} \mathbf{A}+\mathbf{BF} & \mathbf{B}\mathbf{S}^{-1/2} \\ \hline \mathbf{C}+\mathbf{DF} & \mathbf{D}\mathbf{S}^{-1/2} \\ \hline \mathbf{F} & \mathbf{S}^{-1/2} \end{array}\right] \tag{A26}$$

where $\mathbf{S}$ and $\mathbf{R}$ are given by equations (A19) and (A20), respectively,

$$\mathbf{F} = -\mathbf{S}^{-1}(\mathbf{D}^T\mathbf{C} + \mathbf{B}^T\mathbf{X}) \tag{A27}$$

and $\mathbf{X}$ is the unique symmetric positive definite solution of the generalized control algebraic Riccati equation (GCARE)

$$(\mathbf{A} - \mathbf{B}\mathbf{S}^{-1}\mathbf{D}^T\mathbf{C})^T\mathbf{X} + \mathbf{X}(\mathbf{A} - \mathbf{B}\mathbf{S}^{-1}\mathbf{D}^T\mathbf{C}) - \mathbf{X}\mathbf{B}\mathbf{S}^{-1}\mathbf{B}^T\mathbf{X} + \mathbf{C}^T\mathbf{R}^{-1}\mathbf{C} = 0 \tag{A28}$$

Both the NLCF and NRCF realizations are minimal given a minimal ($\mathbf{A}$, $\mathbf{B}$, $\mathbf{C}$, $\mathbf{D}$) realization (Meyer 1988).

Appendix B

Algorithms for the NLCF Robust Stabilization Problems

In this section, computational procedures are presented for determining state-variable realizations of the compensators resulting from the optimal ($\gamma = \gamma_{\min}$) and suboptimal ($\gamma > \gamma_{\min}$) NLCF robust stabilization problems.

Optimal Compensator

From equation (23), construction of the optimal compensator involves the approximation of a function $[-\tilde{\mathbf{N}}, \widetilde{\mathbf{M}}] \in RH_\infty$ by a completely unstable (all poles in the open complex right half-plane) rational transfer function $\begin{bmatrix} \mathbf{U} \\ \mathbf{V} \end{bmatrix}^*$. This type of problem is referred to as a Nehari extension problem. Its solution, as has been shown in section 6 of Glover (1984), can be constructed through the use of balanced realizations and Hankel norm approximations. In this paper, the version of Glover's theory found in section 6.6.2 of Maciejowski (1989) is employed.

If $\mathbf{G}$ is a $p \times m$ matrix, then $[-\tilde{\mathbf{N}}, \widetilde{\mathbf{M}}]$ will be $p \times (p+m)$. Place an $m \times (p+m)$ null matrix beneath $[-\tilde{\mathbf{N}}, \widetilde{\mathbf{M}}]$ such that the resulting augmented square matrix is of size $\tilde{n} = m + p$. A state-variable realization for the augmented matrix can be found through the use of equations (A18) to (A22). The realization will have a system matrix with the same size as the system of a minimum realization of $\mathbf{G}$, which is denoted by n. Let $(\tilde{\mathbf{A}}, \tilde{\mathbf{B}}, \tilde{\mathbf{C}}, \tilde{\mathbf{D}})$ be a balanced realization of the augmented matrix realization. The balanced realization will be such that

$$\tilde{\mathbf{A}}\boldsymbol{\Sigma} + \boldsymbol{\Sigma}\tilde{\mathbf{A}}^T + \tilde{\mathbf{B}}\tilde{\mathbf{B}}^T = 0 \tag{B1}$$

and

$$\tilde{\mathbf{A}}^T\boldsymbol{\Sigma} + \boldsymbol{\Sigma}\tilde{\mathbf{A}} + \tilde{\mathbf{C}}^T\tilde{\mathbf{C}} = 0 \tag{B2}$$

where

$$\boldsymbol{\Sigma} = \begin{bmatrix} \sigma_1 \mathbf{I}_r & \mathbf{0} \\ \mathbf{0} & \boldsymbol{\Sigma}_1 \end{bmatrix} \tag{B3}$$

$$\boldsymbol{\Sigma}_1 = \mathrm{diag}(\sigma_{r+1}, \sigma_{r+2}, \ldots, \sigma_n) \tag{B4}$$

and $r \geq 1$ is the multiplicity of σ_1. In equations (B3) and (B4), the Hankel singular values of $[-\tilde{\mathbf{N}}, \widetilde{\mathbf{M}}]$ are ordered such that

$$\sigma_i \geq \sigma_{i+1} \qquad (i = 1, 2, \ldots, n-1)$$

and

$$\sigma_1 = \| [-\tilde{\mathbf{N}}, \widetilde{\mathbf{M}}] \|_H = \| [\tilde{\mathbf{N}}, \widetilde{\mathbf{M}}] \|_H \tag{B5}$$

Unique solutions to equations (B1) and (B2) exist because $\tilde{\mathbf{A}}$ is Hurwitz.

Next, partition $\tilde{\mathbf{A}}, \tilde{\mathbf{B}}$, and $\tilde{\mathbf{C}}$ conformally with $\boldsymbol{\Sigma}$ to obtain

$$\tilde{\mathbf{A}} = \begin{bmatrix} \tilde{\mathbf{A}}_{11} & \tilde{\mathbf{A}}_{12} \\ \tilde{\mathbf{A}}_{21} & \tilde{\mathbf{A}}_{22} \end{bmatrix} \tag{B6}$$

$$\tilde{\mathbf{B}} = \begin{bmatrix} \tilde{\mathbf{B}}_1 \\ \tilde{\mathbf{B}}_2 \end{bmatrix} \tag{B7}$$

and

$$\tilde{\mathbf{C}} = [\tilde{\mathbf{C}}_1, \tilde{\mathbf{C}}_2] \tag{B8}$$

Define

$$\boldsymbol{\Gamma} = \boldsymbol{\Sigma}_1 - \sigma_1 \mathbf{I}_{n-r} \tag{B9}$$

and find $\hat{\mathbf{U}}$ such that $\hat{\mathbf{U}}\hat{\mathbf{U}}^T = \mathbf{I}_{\tilde{n}}$ and

$$\tilde{\mathbf{B}}_1 = -\tilde{\mathbf{C}}_1^T\hat{\mathbf{U}} \tag{B10}$$

The matrix $\hat{\mathbf{U}}$ may be found as follows. Let $\tilde{\mathbf{C}}_1^T$ have singular value decomposition $\mathbf{U}_1\hat{\mathbf{\Sigma}}\mathbf{V}_1^T$. From equations (B1), (B2), and the construction of $\mathbf{\Sigma}$, we have $\tilde{\mathbf{B}}_1\tilde{\mathbf{B}}_1^T = \tilde{\mathbf{C}}_1^T\tilde{\mathbf{C}}_1$, whereby $\mathbf{U}_1\hat{\mathbf{\Sigma}}\mathbf{V}_2^T$ is a singular value decomposition of $-\tilde{\mathbf{B}}_1$. Then, a solution of equation (B10) is

$$\hat{\mathbf{U}} = \mathbf{V}_1\mathbf{V}_2^T \tag{B11}$$

Thereafter, construct

$$\hat{\mathbf{A}} = \mathbf{\Gamma}^{-1}(\sigma_1^2\tilde{\mathbf{A}}_{22}^T + \mathbf{\Sigma}_1\tilde{\mathbf{A}}_{22}\mathbf{\Sigma}_1 - \sigma_1\tilde{\mathbf{C}}_2^T\hat{\mathbf{U}}\tilde{\mathbf{B}}_2^T) \tag{B12}$$

$$\hat{\mathbf{B}} = \mathbf{\Gamma}^{-1}(\mathbf{\Sigma}_1\tilde{\mathbf{B}}_2 + \sigma_1\tilde{\mathbf{C}}_2^T\hat{\mathbf{U}}) \tag{B13}$$

$$\hat{\mathbf{C}} = -\tilde{\mathbf{C}}_2\mathbf{\Sigma}_1 - \sigma_1\hat{\mathbf{U}}\tilde{\mathbf{B}}_2^T \tag{B14}$$

$$\hat{\mathbf{D}} = -\tilde{\mathbf{D}} + \sigma_1\hat{\mathbf{U}} \tag{B15}$$

Glover (1984) shows that after deleting the lower m rows of $\hat{\mathbf{C}}$ and $\hat{\mathbf{D}}$ (corresponding to those initially added), a state-variable realization for $\begin{bmatrix}\mathbf{U}\\ \mathbf{V}\end{bmatrix}^*$ in equation (23) is $(\hat{\mathbf{A}}, \hat{\mathbf{B}}, \hat{\mathbf{C}}, \hat{\mathbf{D}})$. Applying the definition in equation (A16) indicates that the corresponding realization for $\begin{bmatrix}\mathbf{U}\\ \mathbf{V}\end{bmatrix}$ is $(-\hat{\mathbf{A}}^T, -\hat{\mathbf{C}}^T, \hat{\mathbf{B}}^T, \hat{\mathbf{D}}^T)$. In other words,

$$\begin{bmatrix}\mathbf{U}\\ \mathbf{V}\end{bmatrix} = -\hat{\mathbf{B}}^T(s\mathbf{I}_{n-r} + \hat{\mathbf{A}}^T)^{-1}\hat{\mathbf{C}}^T + \hat{\mathbf{D}}^T \tag{B16}$$

where

$$\hat{\mathbf{A}}^T \in R^{(n-r)\times(n-r)}$$

$$\hat{\mathbf{B}}^T \in R^{(p+m)\times(n-r)}$$

$$\hat{\mathbf{C}}^T \in R^{(n-r)\times p}$$

and

$$\hat{\mathbf{D}} \in R^{(p+m)\times p}$$

The matrices $\mathbf{U}$ and $\mathbf{V}$ are the upper $m \times p$ and lower $p \times p$ portions of equation (B16), respectively. The optimal compensator $\mathbf{K}$ is given by equation (19) for which a state-variable realization can be constructed through application of equations (A4) and (A5).

The system matrix corresponding to a state-variable realization of $\mathbf{K}$ will be on the order of $(n - r)$, where r is the multiplicity of the largest singular value of $[\tilde{\mathbf{N}}, \widetilde{\mathbf{M}}]$. Here, n is the order of a minimal realization of $[\tilde{\mathbf{N}}, \widetilde{\mathbf{M}}]$ and also the order of a minimal realization of $\mathbf{G}$. Thus, the optimal compensator is of a lower order than $\mathbf{G}$. However, even if $\mathbf{G}$ is strictly proper, the compensator will generally only be proper. (See eq. (B15).) If a strictly proper compensator is desired for a strictly proper $\mathbf{G}$, the suboptimal compensator may be employed.

Suboptimal Compensator

Utilization of the compensator from the previous section always yields

$$\| \begin{bmatrix}\mathbf{K}\\ \mathbf{I}\end{bmatrix} (\mathbf{I} - \mathbf{GK})^{-1}\widetilde{\mathbf{M}}^{-1} \|_\infty = \epsilon_{\max}^{-1} = \gamma_{\min} \tag{B17}$$

If one wishes to specify that $\gamma > \gamma_{\min}$ such that

$$\| \begin{bmatrix} \mathbf{K} \\ \mathbf{I} \end{bmatrix} (\mathbf{I} - \mathbf{GK})^{-1} \widetilde{\mathbf{M}}^{-1} \|_\infty \leq \gamma \tag{B18}$$

a suboptimal version of the optimal NLCF robust stabilization problem can be posed as finding all compensators that simultaneously stabilize $\mathbf{G}$ and satisfy equation (B18).

Let $\mathbf{G}$ have state-variable realization ($\mathbf{A}$, $\mathbf{B}$, $\mathbf{C}$, $\mathbf{D}$) and $\mathbf{Z}$ and $\mathbf{X}$ denote the solutions of equations (A18) and (A28), respectively. Also let

$$\mathbf{S} = \mathbf{I}_m + \mathbf{D}^T\mathbf{D} \tag{B19}$$

$$\mathbf{F} = -\mathbf{S}^{-1}(\mathbf{B}^T\mathbf{X} + \mathbf{D}^T\mathbf{C}) \tag{B20}$$

and

$$\mathbf{A}^c = \mathbf{A} + \mathbf{BF} \tag{B21}$$

Then, as shown in Glover and McFarlane (1989) or McFarlane and Glover (1990), all controllers satisfying the suboptimal robust stabilization problem for selected

$$\gamma > \gamma_{\min} = (1 - \| [\widetilde{\mathbf{N}}, \widetilde{\mathbf{M}}] \|_H^2)^{-1/2} \tag{B22}$$

are given by

$$\mathbf{K} = (\mathbf{L}_{11}\hat{\mathbf{\Phi}} + \mathbf{L}_{12})(\mathbf{L}_{21}\hat{\mathbf{\Phi}} + \mathbf{L}_{22})^{-1} \tag{B23}$$

where

$$\left[\begin{array}{c|c} \mathbf{L}_{11} & \mathbf{L}_{12} \\ \hline \mathbf{L}_{21} & \mathbf{L}_{22} \end{array}\right] = \left[\begin{array}{c|c|c} \mathbf{A}^c & -\gamma^2\widehat{\mathbf{W}}_1^{-T}\mathbf{BS}^{-1/2} & \gamma^2\hat{\zeta}^{-T}\mathbf{ZC}^T\mathbf{R}^{-1/2} \\ \hline \mathbf{F} & \mathbf{S}^{-1/2} & \zeta^{-1}\mathbf{D}^T\mathbf{R}^{-1/2} \\ \hline \mathbf{C} + \mathbf{DF} & \mathbf{DS}^{-1/2} & -\zeta^{-1}\mathbf{R}^{-1/2} \end{array}\right] \tag{B24}$$

$$\mathbf{R} = \mathbf{I}_p + \mathbf{DD}^T \tag{B25}$$

$$\zeta = (\gamma^2 - 1)^{1/2} \tag{B26}$$

$$\widehat{\mathbf{W}}_1 = \mathbf{I}_n + (\mathbf{XZ} - \gamma^2\mathbf{I}_n) \tag{B27}$$

and $\hat{\mathbf{\Phi}}$ is arbitrary in RH_∞ so long as $\| \hat{\mathbf{\Phi}} \|_\infty \leq 1$.

The central ($\hat{\mathbf{\Phi}} = 0$), or lowest order, suboptimal compensator is

$$\mathbf{K}_c = \left[\begin{array}{c|c} \mathbf{A}^c + \gamma^2\widehat{\mathbf{W}}_1^{-T}\mathbf{ZC}^T(\mathbf{C} + \mathbf{DF}) & \gamma^2\widehat{\mathbf{W}}_1^{-T}\mathbf{ZC}^T \\ \hline \mathbf{B}^T\mathbf{X} & -\mathbf{D}^T \end{array}\right] \tag{B28}$$

Comparing the orders of the optimal and central suboptimal controllers shows that the central controller always has an order equal to that of the original design model ($\mathbf{G}$), whereas the order of an optimal compensator is $n - r(r \geq 1)$. The central controller gives a strictly proper compensator for a strictly proper $\mathbf{G}$, whereas the optimal compensator typically does not.

McFarlane and Glover (1990) show that

$$1 - \gamma_{\min}^2 = -\lambda_{\max}(\mathbf{ZX}) \tag{B29}$$

whereby $\widehat{\mathbf{W}}_1$ of equation (B27) becomes singular as $\gamma \rightarrow \gamma_{\min}$. As $\gamma \rightarrow \infty$, the central solution approaches

$$\left[\begin{array}{c|c} \mathbf{A}^c - \mathbf{Z}\mathbf{C}^T(\mathbf{C}+\mathbf{D}\mathbf{F}) & -\mathbf{Z}\mathbf{C}^T \\ \hline \mathbf{B}^T\mathbf{X} & -\mathbf{D}^T \end{array}\right]$$

which is easily recognized as a Linear-Quadratic-Gaussian (LQG) compensator construction.

Appendix C

Numerical Data

Matrices Defining Controller Design Model

Numerical data for $\mathbf{G} = \mathbf{C}(s\mathbf{I}_{18} - \mathbf{A})^{-1}\mathbf{B} + \mathbf{D}$ for equation (49) are given in the following matrices for (**A**, **B**, **C**, **D**).

A =

Columns 1 through 6

0	0	0	0	0	0
0	0	0	0	0	0
0	0	0	0	0	0
0	0	0	0	0	0
0	0	0	0	0	0
0	0	0	0	0	0
0	0	0	0	0	0
0	0	0	0	0	0
0	0	0	0	0	0
−8.5437E−01	0	0	0	0	0
0	−8.7713E−01	0	0	0	0
0	0	−9.5105E−01	0	0	0
0	0	0	−2.1042E+01	0	0
0	0	0	0	−2.2077E+01	0
0	0	0	0	0	−3.0155E+01
0	0	0	0	0	0
0	0	0	0	0	0
0	0	0	0	0	0

Columns 7 through 12

0	0	0	1.0000E+00	0	0
0	0	0	0	1.0000E+00	0
0	0	0	0	0	1.0000E+00
0	0	0	0	0	0
0	0	0	0	0	0
0	0	0	0	0	0
0	0	0	0	0	0
0	0	0	0	0	0
0	0	0	0	0	0
0	0	0	−9.2432E−03	0	0
0	0	0	0	−9.3655E−03	0
0	0	0	0	0	−9.7522E−03
0	0	0	0	0	0
0	0	0	0	0	0
0	0	0	0	0	0
−8.5712E+01	0	0	0	0	0
0	−1.1927E+02	0	0	0	0
0	0	−1.3997E+02	0	0	0

A =

Columns 13 through 18

0	0	0	0	0	0
0	0	0	0	0	0
0	0	0	0	0	0
1.0000E+00	0	0	0	0	0
0	1.0000E+00	0	0	0	0
0	0	1.0000E+00	0	0	0
0	0	0	1.0000E+00	0	0
0	0	0	0	1.0000E+00	0
0	0	0	0	0	1.0000E+00
0	0	0	0	0	0
0	0	0	0	0	0
0	0	0	0	0	0
−4.5872E−02	0	0	0	0	0
0	−4.6986E−02	0	0	0	0
0	0	−5.4914E−02	0	0	0
0	0	0	−9.2581E−02	0	0
0	0	0	0	−1.0921E−01	0
0	0	0	0	0	−1.1831E−01

B =

Columns 1 through 6

0	0	0	0	0	0
0	0	0	0	0	0
0	0	0	0	0	0
0	0	0	0	0	0
0	0	0	0	0	0
0	0	0	0	0	0
0	0	0	0	0	0
0	0	0	0	0	0
0	0	0	0	0	0
0	0	0	0	0	0
−9.0412E−02	−1.7503E−03	−2.2032E−03	8.6983E−04	7.2204E−01	7.6707E−02
−7.2842E−01	2.1216E−04	−7.4012E−01	1.9792E−04	2.8522E−03	−7.0804E−01
1.1157E+00	−2.6799E−04	6.2103E−02	9.7330E−05	5.9780E−02	−8.8555E−01
−2.3142E−04	−1.1076E+00	−1.5399E−04	−3.9490E−02	−8.7477E−02	2.3484E−04
5.9439E−05	−7.5943E−01	1.9928E−04	−7.4550E−01	−3.0950E−03	−3.4298E−04
−6.8777E−02	2.3805E−03	−2.5082E−01	2.0583E−03	8.2306E−04	3.0302E−01
−9.0841E−01	−9.2293E−04	4.7562E−01	4.0256E−03	9.0757E−04	−4.3450E−01
2.9426E−02	1.2695E+00	−2.6966E−02	−1.0421E+00	−3.8239E−01	1.0193E−02
9.4147E−01	−4.7622E−02	−9.0573E−01	4.2744E−02	1.2593E−02	3.8921E−01

Columns 7 through 8

0	0
0	0
0	0
0	0
0	0
0	0
0	0
0	0
0	0
7.2043E−01	−4.6856E−02
2.8556E−03	−6.2905E−01
5.9586E−02	5.9095E−01
−2.7368E−01	1.0451E−03
3.9825E−03	−1.1842E−03
5.0834E−04	1.3185E+00
−7.0441E−03	1.1182E+00
9.5012E−01	1.6953E−02
−2.2581E−02	3.1281E−01

C =

Columns 1 through 6

7.7245E−02	6.3892E−01	−1.0611E+00	4.8696E−03	−1.3122E−03	2.0740E+00
1.4954E−03	−1.8609E−04	2.5487E−04	2.3307E+01	1.6766E+01	−7.1785E−02
1.8823E−03	6.4918E−01	−5.9063E−02	3.2403E−03	−4.3995E−03	7.5636E+00
−7.4315E−04	−1.7360E−04	−9.2566E−05	8.3096E−01	1.6458E+01	−6.2069E−02
−6.1689E−01	−2.5017E−03	−5.6854E−02	1.8407E+00	6.8328E−02	−2.4820E−02
−6.5536E−02	6.2104E−01	8.4221E−01	−4.9416E−03	7.5719E−03	−9.1377E+00
−6.1551E−01	−2.5047E−03	−5.6670E−02	5.7589E+00	−8.7921E−02	−1.5329E−02
4.0032E−02	5.5176E−01	−5.6203E−01	−2.1991E−02	2.6143E−02	−3.9760E+01

Columns 7 through 12

7.7862E+01	−3.5096E+00	−1.3178E+02	8.3570E−04	6.8220E−03	−1.0881E−02
7.9107E−02	−1.5141E+02	6.6658E+00	1.6178E−05	−1.9870E−06	2.6135E−06
−4.0767E+01	3.2162E+00	1.2678E+02	2.0365E−05	6.9316E−03	−6.0564E−04
−3.4504E−01	1.2429E+02	−5.9830E+00	−8.0400E−06	−1.8536E−06	−9.4918E−07
−7.7790E−02	4.5607E+01	−1.7627E+00	−6.6740E−03	−2.6712E−05	−5.8299E−04
3.7242E+01	−1.2157E+00	−5.4479E+01	−7.0902E−04	6.6311E−03	8.6361E−03
6.0377E−01	−1.1332E+02	3.1607E+00	−6.6591E−03	−2.6744E−05	−5.8109E−04
−9.5844E+01	−2.0220E+00	−4.3785E+01	4.3310E−04	5.8914E−03	−5.7631E−03

Columns 13 through 18

1.0616E−05	−2.7928E−06	3.7768E−03	8.4102E−02	−3.2136E−03	−1.1139E−01
5.0808E−02	3.5683E−02	−1.3072E−04	8.5446E−05	−1.3864E−01	5.6342E−03
7.0638E−06	−9.3634E−06	1.3774E−02	−4.4033E−02	2.9450E−03	1.0716E−01
1.8115E−03	3.5028E−02	−1.1303E−04	−3.7269E−04	1.1381E−01	−5.0570E−03
4.0127E−03	1.4542E−04	−4.5198E−05	−8.4024E−05	4.1761E−02	−1.4899E−03
−1.0773E−05	1.6115E−05	−1.6640E−02	4.0226E−02	−1.1132E−03	−4.6047E−02
1.2554E−02	−1.8712E−04	−2.7915E−05	6.5215E−04	−1.0376E−01	2.6716E−03
−4.7941E−05	5.5641E−05	−7.2404E−02	−1.0352E−01	−1.8514E−03	−3.7009E−02

D =

Columns 1 through 6

3.5007E+00	−6.8878E−03	−6.5971E−01	5.6295E−03	−9.1940E−04	2.6140E−01
−6.8878E−03	3.4174E+00	7.7127E−03	−7.1509E−01	−3.8808E−01	−4.5194E−03
−6.5971E−01	7.7127E−03	1.6618E+00	−9.4997E−03	−8.4551E−04	−1.6658E−01
5.6295E−03	−7.1509E−01	−9.4997E−03	1.6452E+00	4.0543E−01	4.9757E−03
−9.1940E−04	−3.8808E−01	−8.4551E−04	4.0543E−01	6.7897E−01	1.2671E−03
2.6140E−01	−4.5194E−03	−1.6658E−01	4.9757E−03	1.2671E−03	1.7236E+00
1.2391E−02	1.5061E+00	−8.6038E−03	−9.8264E−01	1.8407E−01	4.5186E−03
3.1031E−01	8.2638E−03	4.1973E−01	3.6531E−03	−8.3024E−04	−4.5921E−02

Columns 7 through 8

1.2391E−02	3.1031E−01
1.5061E+00	8.2638E−03
−8.6038E−03	4.1973E−01
−9.8264E−01	3.6531E−03
1.8407E−01	−8.3024E−04
4.5186E−03	−4.5921E−02
1.5008E+00	1.2062E−03
1.2062E−03	3.8341E+00

Matrices Defining Truncated System

Numerical data for $\Delta \mathbf{G} = \mathbf{C}_t(s\mathbf{I}_{32} - \mathbf{A}_t)^{-1}\mathbf{B}_t + \mathbf{D}_t$ for equation (50) are given in the following matrices for $(\mathbf{A}_t, \mathbf{B}_t, \mathbf{C}_t, \mathbf{D}_t)$.

$\mathbf{A}_t =$

Columns 1 through 6

0	0	0	0	0	0
0	0	0	0	0	0
0	0	0	0	0	0
0	0	0	0	0	0
0	0	0	0	0	0
0	0	0	0	0	0
0	0	0	0	0	0
0	0	0	0	0	0
0	0	0	0	0	0
0	0	0	0	0	0
0	0	0	0	0	0
0	0	0	0	0	0
0	0	0	0	0	0
0	0	0	0	0	0
0	0	0	0	0	0
0	0	0	0	0	0
−2.0909E+02	0	0	0	0	0
0	−3.1809E+02	0	0	0	0
0	0	−6.3630E+02	0	0	0
0	0	0	−6.4186E+02	0	0
0	0	0	0	−6.9828E+02	0
0	0	0	0	0	−7.6148E+02
0	0	0	0	0	0
0	0	0	0	0	0
0	0	0	0	0	0
0	0	0	0	0	0
0	0	0	0	0	0
0	0	0	0	0	0
0	0	0	0	0	0
0	0	0	0	0	0
0	0	0	0	0	0
0	0	0	0	0	0

Columns 7 through 12

0	0	0	0	0	0
0	0	0	0	0	0
0	0	0	0	0	0
0	0	0	0	0	0
0	0	0	0	0	0
0	0	0	0	0	0
0	0	0	0	0	0
0	0	0	0	0	0
0	0	0	0	0	0
0	0	0	0	0	0
0	0	0	0	0	0
0	0	0	0	0	0
0	0	0	0	0	0
0	0	0	0	0	0
0	0	0	0	0	0
0	0	0	0	0	0
0	0	0	0	0	0
0	0	0	0	0	0
0	0	0	0	0	0
0	0	0	0	0	0
0	0	0	0	0	0
0	0	0	0	0	0
−1.1948E+03	0	0	0	0	0
0	−1.5075E+03	0	0	0	0
0	0	−1.5326E+03	0	0	0
0	0	0	−1.6531E+03	0	0
0	0	0	0	−1.7563E+03	0
0	0	0	0	0	−2.1457E+03
0	0	0	0	0	0
0	0	0	0	0	0
0	0	0	0	0	0
0	0	0	0	0	0

Columns 13 through 18

0	0	0	0	1.0000E+00	0
0	0	0	0	0	1.0000E+00
0	0	0	0	0	0
0	0	0	0	0	0
0	0	0	0	0	0
0	0	0	0	0	0
0	0	0	0	0	0
0	0	0	0	0	0
0	0	0	0	0	0
0	0	0	0	0	0
0	0	0	0	0	0
0	0	0	0	0	0
0	0	0	0	0	0
0	0	0	0	0	0
0	0	0	0	0	0
0	0	0	0	0	0
0	0	0	0	−1.4460E−01	0
0	0	0	0	0	−1.7835E−01
0	0	0	0	0	0
0	0	0	0	0	0
0	0	0	0	0	0
0	0	0	0	0	0
0	0	0	0	0	0
0	0	0	0	0	0
0	0	0	0	0	0
0	0	0	0	0	0
0	0	0	0	0	0
0	0	0	0	0	0
−2.7152E+03	0	0	0	0	0
0	−3.1739E+03	0	0	0	0
0	0	−6.1546E+03	0	0	0
0	0	0	−1.1213E+04	0	0

Columns 19 through 24

0	0	0	0	0	0
0	0	0	0	0	0
1.0000E+00	0	0	0	0	0
0	1.0000E+00	0	0	0	0
0	0	1.0000E+00	0	0	0
0	0	0	1.0000E+00	0	0
0	0	0	0	1.0000E+00	0
0	0	0	0	0	1.0000E+00
0	0	0	0	0	0
0	0	0	0	0	0
0	0	0	0	0	0
0	0	0	0	0	0
0	0	0	0	0	0
0	0	0	0	0	0
0	0	0	0	0	0
0	0	0	0	0	0
0	0	0	0	0	0
0	0	0	0	0	0
−2.5225E−01	0	0	0	0	0
0	−2.5335E−01	0	0	0	0
0	0	−2.6425E−01	0	0	0
0	0	0	−2.7595E−01	0	0
0	0	0	0	−3.4566E−01	0
0	0	0	0	0	−3.8827E−01
0	0	0	0	0	0
0	0	0	0	0	0
0	0	0	0	0	0
0	0	0	0	0	0
0	0	0	0	0	0
0	0	0	0	0	0
0	0	0	0	0	0
0	0	0	0	0	0

Columns 25 through 30

0	0	0	0	0	0
0	0	0	0	0	0
0	0	0	0	0	0
0	0	0	0	0	0
0	0	0	0	0	0
0	0	0	0	0	0
0	0	0	0	0	0
0	0	0	0	0	0
1.0000E+00	0	0	0	0	0
0	1.0000E+00	0	0	0	0
0	0	1.0000E+00	0	0	0
0	0	0	1.0000E+00	0	0
0	0	0	0	1.0000E+00	0
0	0	0	0	0	1.0000E+00
0	0	0	0	0	0
0	0	0	0	0	0
0	0	0	0	0	0
0	0	0	0	0	0
0	0	0	0	0	0
0	0	0	0	0	0
0	0	0	0	0	0
0	0	0	0	0	0
0	0	0	0	0	0
0	0	0	0	0	0
−3.9149E−01	0	0	0	0	0
0	−4.0658E−01	0	0	0	0
0	0	−4.1908E−01	0	0	0
0	0	0	−4.6322E−01	0	0
0	0	0	0	−5.2108E−01	0
0	0	0	0	0	−5.6337E−01
0	0	0	0	0	0
0	0	0	0	0	0

Columns 31 through 32

0	0
0	0
0	0
0	0
0	0
0	0
0	0
0	0
0	0
0	0
0	0
0	0
0	0
0	0
0	0
1.0000E+00	0
0	1.0000E+00
0	0
0	0
0	0
0	0
0	0
0	0
0	0
0	0
0	0
0	0
0	0
0	0
0	0
−7.8451E−01	0
0	−1.0589E+00

$\mathbf{B}_t$ =

Columns 1 through 6

0	0	0	0	0	0
0	0	0	0	0	0
0	0	0	0	0	0
0	0	0	0	0	0
0	0	0	0	0	0
0	0	0	0	0	0
0	0	0	0	0	0
0	0	0	0	0	0
0	0	0	0	0	0
0	0	0	0	0	0
0	0	0	0	0	0
0	0	0	0	0	0
0	0	0	0	0	0
0	0	0	0	0	0
0	0	0	0	0	0
0	0	0	0	0	0
−1.7116E−01	−5.8049E−03	2.0869E−01	3.2349E−03	−1.0585E−03	1.0457E−01
−2.9829E−03	−3.5789E−01	−1.2875E−03	2.5253E−01	−3.8650E−02	−3.3579E−03
−2.0542E−01	−7.2812E−02	−9.5226E−03	7.2871E−03	−5.5209E−02	6.7861E−02
−8.3452E−01	−1.7241E−02	−4.2512E−02	−2.1983E−02	−2.8225E−03	2.8268E−01
−2.7311E−01	−1.0499E−01	−4.2532E−02	−5.3459E−03	−5.4968E−02	1.0531E−01
8.3909E−02	−1.0430E+00	−4.9171E−03	−6.5816E−02	−4.8285E−01	−3.5314E−02
3.0662E−01	−4.5815E−02	4.1271E−01	−1.2829E−02	6.0601E−03	−8.9994E−02
1.5476E−02	−5.8067E−01	−3.6281E−02	−3.9609E−01	−1.8812E−01	−3.4468E−02
1.1892E−01	−3.9154E−02	3.6029E−01	−9.2921E−02	2.3797E−02	3.5179E−01
−2.0457E−02	3.3652E−01	1.9963E−01	2.5025E−02	−1.8725E−02	−2.1458E−01
−6.8681E−02	1.0751E+00	−1.2244E−01	−1.4175E−01	6.5808E−02	3.4202E−02
5.4524E−03	5.4087E−01	1.5533E−01	1.0847E+00	−6.6816E−01	2.2399E−02
−2.0571E−01	2.7394E−02	−9.8462E−01	1.0100E−01	−4.6903E−02	4.6728E−02
−1.5396E+00	−1.0585E−01	−1.7445E−01	−6.0191E−03	−1.5392E−03	−1.2358E−03
−1.0503E−02	1.9177E−01	3.6153E−02	6.2227E−01	4.0364E−01	5.9594E−03
1.7533E−01	1.5125E−01	1.1805E−01	7.5504E−01	−2.2316E−02	2.6324E−02

Columns 7 through 8

0	0
0	0
0	0
0	0
0	0
0	0
0	0
0	0
0	0
0	0
0	0
0	0
0	0
0	0
0	0
0	0
−7.9081E−03	−2.1884E−01
−2.0767E−01	3.3597E−03
−4.1550E−02	1.1263E−01
−5.3852E−02	4.5806E−01
−6.0046E−02	1.5792E−01
−4.0749E−01	−4.2931E−02
1.0370E−02	−5.1029E−01
1.6912E−01	8.8657E−02
−1.0616E−01	−1.1353E+00
−5.2492E−01	−1.2112E+00
−2.2117E+00	3.0859E−01
5.2024E−01	5.3702E−02
1.0856E−01	−3.1874E−01
1.1115E−01	−2.4079E−01
3.7390E−01	1.3817E−02
1.0209E−01	−7.8110E−03

$\mathbf{C}_t =$

Columns 1 through 6

3.5788E+01	9.4882E−01	1.3071E+02	5.3565E+02	1.9071E+02	−6.3895E+01
1.2138E+00	1.1384E+02	4.6330E+01	1.1066E+01	7.3312E+01	7.9423E+02
−4.3635E+01	4.0954E−01	6.0592E+00	2.7287E+01	2.9699E+01	3.7443E+00
−6.7639E−01	−8.0327E+01	−4.6368E+00	1.4110E+01	3.7329E+00	5.0118E+01
2.2132E−01	1.2294E+01	3.5130E+01	1.8117E+00	3.8383E+01	3.6768E+02
−2.1865E+01	1.0681E+00	−4.3180E+01	−1.8144E+02	−7.3536E+01	2.6891E+01
1.6535E+00	6.6057E+01	2.6438E+01	3.4566E+01	4.1929E+01	3.1030E+02
4.5758E+01	−1.0687E+00	−7.1667E+01	−2.9401E+02	−1.1027E+02	3.2691E+01

Columns 7 through 12

−3.6635E+02	−2.3331E+01	−1.8226E+02	3.3817E+01	1.2062E+02	−1.1699E+01
5.4740E+01	8.7538E+02	6.0009E+01	−5.5629E+02	−1.8882E+03	−1.1606E+03
−4.9311E+02	5.4695E+01	−5.5220E+02	−3.3000E+02	2.1504E+02	−3.3330E+02
1.5328E+01	5.9712E+02	1.4241E+02	−4.1368E+01	2.4895E+02	−2.3275E+03
−7.2407E+00	2.8360E+02	−3.6472E+01	3.0954E+01	−1.1558E+02	1.4337E+03
1.0753E+02	5.1962E+01	−5.3917E+02	3.5472E+02	−6.0068E+01	−4.8062E+01
−1.2390E+01	−2.5495E+02	1.6271E+02	8.6773E+02	3.8844E+03	−1.1163E+03
6.0970E+02	−1.3365E+02	1.7400E+03	2.0022E+03	−5.4197E+02	−1.1523E+02

Columns 13 through 18

5.5855E+02	4.8865E+03	6.4641E+01	−1.9659E+03	2.4750E−02	5.3200E−04
−7.4381E+01	3.3595E+02	−1.1803E+03	−1.6959E+03	8.3939E−04	6.3830E−02
2.6735E+03	5.5368E+02	−2.2251E+02	−1.3237E+03	−3.0177E−02	2.2963E−04
−2.7424E+02	1.9104E+01	−3.8298E+03	−8.4660E+03	−4.6777E−04	−4.5039E−02
1.2735E+02	4.8852E+00	−2.4842E+03	2.5022E+02	1.5306E−04	6.8932E−03
−1.2688E+02	3.9223E+00	−3.6677E+01	−2.9516E+02	−1.5121E−02	5.9888E−04
−2.9477E+02	−3.5277E+02	−2.3012E+03	−1.1447E+03	1.1435E−03	3.7038E−02
8.6546E+02	7.6423E+02	−8.5038E+01	8.7582E+01	3.1644E−02	−5.9920E−04

Columns 19 through 24

5.1817E−02	2.1143E−01	7.2169E−02	−2.3155E−02	−1.0599E−01	−6.0089E−03
1.8367E−02	4.3680E−03	2.7744E−02	2.8782E−01	1.5836E−02	2.2546E−01
2.4021E−03	1.0770E−02	1.1239E−02	1.3569E−03	−1.4266E−01	1.4087E−02
−1.8382E−03	5.5694E−03	1.4127E−03	1.8162E−02	4.4345E−03	1.5379E−01
1.3926E−02	7.1508E−04	1.4525E−02	1.3324E−01	−2.0947E−03	7.3041E−02
−1.7118E−02	−7.1617E−02	−2.7828E−02	9.7449E−03	3.1107E−02	1.3383E−02
1.0481E−02	1.3643E−02	1.5867E−02	1.1245E−01	−3.5845E−03	−6.5664E−02
−2.8411E−02	−1.1605E−01	−4.1730E−02	1.1847E−02	1.7639E−01	−3.4423E−02

Columns 25 through 30

−4.6556E−02	8.3174E−03	2.8783E−02	−2.5257E−03	1.0719E−01	8.6736E−01
1.5328E−02	−1.3682E−01	−4.5055E−01	−2.5054E−01	−1.4274E−02	5.9633E−02
−1.4105E−01	−8.1166E−02	5.1312E−02	−7.1952E−02	5.1307E−01	9.8280E−02
3.6378E−02	−1.0175E−02	5.9405E−02	−5.0245E−01	−5.2629E−02	3.3910E−03
−9.3163E−03	7.6132E−03	−2.7579E−02	3.0951E−01	2.4440E−02	8.6714E−04
−1.3772E−01	8.7244E−02	−1.4333E−02	−1.0376E−02	−2.4349E−02	6.9621E−04
4.1561E−02	2.1342E−01	9.2688E−01	−2.4099E−01	−5.6568E−02	−6.2619E−02
4.4446E−01	4.9245E−01	−1.2932E−01	−2.4876E−02	1.6609E−01	1.3565E−01

Columns 31 through 32

8.2397E−03	−1.8566E−01
−1.5045E−01	−1.6016E−01
−2.8362E−02	−1.2500E−01
−4.8818E−01	−7.9951E−01
−3.1666E−01	2.3630E−02
−4.6752E−03	−2.7874E−02
−2.9333E−01	−1.0810E−01
−1.0840E−02	8.2711E−03

$\mathbf{D}_t$ =

Columns 1 through 6

3.4067E+00	4.8934E−02	6.7837E−01	1.1984E−01	−1.3647E−02	−2.8674E−01
4.8934E−02	3.2066E+00	3.4160E−02	8.9253E−01	4.1129E−01	1.0130E−02
6.7837E−01	3.4160E−02	1.4429E+00	1.8143E−01	−3.4086E−02	9.6979E−03
1.1984E−01	8.9253E−01	1.8143E−01	2.3992E+00	−4.1076E−01	2.0039E−02
−1.3647E−02	4.1129E−01	−3.4086E−02	−4.1076E−01	8.9345E−01	1.1979E−02
−2.8674E−01	1.0130E−02	9.6979E−03	2.0039E−02	1.1979E−02	2.9147E−01
1.6819E−02	−1.7796E+00	1.1186E−01	1.1030E+00	−1.6368E−01	4.2827E−03
−2.6614E−01	−4.1046E−05	−6.1139E−01	2.5951E−02	−1.3970E−02	3.2796E−02

Columns 7 through 8

1.6819E−02	−2.6614E−01
−1.7796E+00	−4.1046E−05
1.1186E−01	−6.1139E−01
1.1030E+00	2.5951E−02
−1.6368E−01	−1.3970E−02
4.2827E−03	3.2796E−02
5.8696E+00	3.4138E−02
3.4138E−02	3.5793E+00

References

Anon. 1990: *MATLAB™—User's Guide.* MathWorks, Inc.

Anderson, Brian D. O.; and Liu, Yi 1989: Controller Reduction: Concepts and Approaches. *IEEE Trans. Autom. Control*, vol. 34, no. 8, pp. 802–812.

Balas, Gary J.; Doyle, John C.; Glover, Keith; Packard, Andy; and Smith, Roy 1991: *μ-Analysis and Synthesis Toolbox (μ-Tools)—MATLAB™ Functions for the Analysis and Design of Robust Control Systems.* MathWorks, Inc.

Balas, Mark J. 1982: Trends in Large Space Structure Control Theory: Fondest Hopes, Wildest Dreams. *IEEE Trans. Autom. Control*, vol. AC-27, no. 3, pp. 522–535.

Belvin, W. Keith; Elliott, Kenny B.; Horta, Lucas G.; Bailey, Jim; Bruner, Anne; Sulla, Jeff; Won, John; and Ugoletti, Roberto 1991: *Langley's CSI Evolutionary Model: Phase 0.* NASA TM-104165.

Boyd, S.; Balakrishnan, V.; and Kabamba, P. 1989: A Bisection Method for Computing the H_∞ Norm of a Transfer Matrix and Related Problems. *Math. Control, Signals, & Syst.*, vol. 2, pp. 207–219.

Boyd, S.; and Balakrishnan, V. 1990: A Regularity Result for the Singular Values of a Transfer Matrix and a Quadratically Convergent Algorithm for Computing Its L_∞-Norm. *Syst. and Control Lett.*, vol. 15, pp. 1–7.

Chen, M. J.; and Desoer, C. A. 1982: Necessary and Sufficient Condition for Robust Stability of Linear Distributed Systems. *Int. J. Control*, vol. 35, no. 2, pp. 255–267.

Chiang, Richard Y.; and Safonov, Michael G. 1988: *Robust-Control Toolbox for Use With MATLAB™—User's Guide.* MathWorks, Inc.

Dorato, Peter; and Yedavalli, Rama C. 1990: *Recent Advances in Robust Control.* IEEE Press.

Doyle, John C.; and Stein, Gunter 1981: Multivariable Feedback Design: Concepts for a Classical/Modern Synthesis. *IEEE Trans. Autom. Control*, vol. AC-26, no. 1, pp. 4–16.

Doyle, John C.; Glover, Keith; Khargonekar, Pramod P.; and Francis, Bruce A. 1989: State-Space Solutions to Standard H_2 and H_∞ Control Problems. *IEEE Trans. Autom. Control*, vol. AC-34, no. 8, pp. 831–847.

Francis, Bruce A. 1987: *A Course in H_∞ Control Theory.* Volume 88 of *Lecture Notes in Control and Information Sciences*, M. Thoma and A. Wyner, eds., Springer-Verlag.

Glover, Keith 1984: All Optimal Hankel-Norm Approximations of Linear Multivariable Systems and Their L^∞-Error Bounds. *Int. J. Control*, vol. 39, no. 6, pp. 1115–1193.

Glover, Keith; and McFarlane, Duncan 1989: Robust Stabilization of Normalized Coprime Factor Plant Descriptions With H_∞-Bounded Uncertainty. *IEEE Trans. Autom. Control*, vol. 34, no. 8, pp. 821–830.

Golub, Gene H.; and Van Loan, Charles F. 1989: *Matrix Computations, Second ed.* Johns Hopkins Univ. Press.

Joshi, S. M. 1989: *Control of Large Flexible Space Structures.* Volume 131 of *Lecture Notes in Control and Information Sciences*, M. Thoma and A. Wyner, eds., Springer-Verlag.

Klema, Virginia C.; and Laub, Alan J. 1980: The Singular Value Decomposition: Its Computation and Some Applications. *IEEE Trans. Autom. Control*, vol. AC-25, no. 2, pp. 164–176.

Kwakernaak, Huibert; and Sivan, Raphael 1972: *Linear Optimal Control Systems.* John Wiley & Sons, Inc.

Laub, Alan J.; Heath, Michael T.; Paige, Chris C.; and Ward, Robert C. 1987: Computation of System Balancing Transformations and Other Applications of Simultaneous Diagonalization Algorithms. *IEEE Trans. Autom. Control*, vol. AC-32, no. 2, pp. 115–122.

Lim, K. B.; and Balas, G. J. 1992: Line-of-Sight Control of the CSI Evolutionary Model: μ Control. *Proceedings of the 1992 American Control Conference*, Vol. 3 of 4, IEEE Catalog No. 92CH3072-6, American Automatic Control Council, pp. 1996–2000.

Lim, K. B.; Maghami, P. G.; and Joshi, S. M. 1992: Comparison of Controller Designs for an Experimental Flexible Structure. *IEEE Control Syst.*, vol. 12, no. 3, pp. 108–118.

Little, John N.; and Laub, Alan J. 1986: *Control System Toolbox—User's Guide.* MathWorks, Inc.

Maciejowski, Jan Marian 1989: *Multivariable Feedback Design.* Addison-Wesley.

Maghami, Peiman G.; Joshi, Suresh M.; and Armstrong, Ernest S. 1993: *An Optimization-Based Integrated Controls-Structures Design Methodology for Flexible Space Structures.* NASA TP-3283.

McFarlane, D. C.; and Glover, K. 1990: *Robust Controller Design Using Normalized Coprime Factor Plant Descriptions.* Volume 138 of *Lecture Notes in Control and Information Sciences*, M. Thoma and A. Wyner, eds., Springer-Verlag.

McFarlane, Duncan; Glover, Keith; and Vidyasagar, M. 1990: Reduced-Order Controller Design Using Coprime Factor Model Reduction. *IEEE Trans. Autom. Control*, vol. 35, no. 3, pp. 369–373.

Meyer, David G. 1988: A Fractional Approach to Model Reduction. *Proceedings of 1988 American Control Conference*, Volume 2, IEEE Catalog No. 88CH2601-3, American Automatic Control Council, pp. 1041–1047.

Moore, Bruce C. 1981: Principal Component Analysis in Linear Systems: Controllability, Observability, and Model Reduction. *IEEE Trans. Autom. Control*, vol. AC-26, no. 1, pp. 17–32.

Newsom, Jerry R.; Layman, W. E.; Waites, H. B.; and Hayduk, R. J. 1990: *The NASA Controls-Structures Interaction Technology Program.* NASA TM-102752.

Safonov, M. G.; and Chiang, R. Y. 1988: CACSD Using the State-Space L^∞ Theory – A Design Example. *IEEE Trans. Autom. Control*, vol. 33, no. 5, pp. 477–479.

Vidyasagar, M. 1985: *Control System Synthesis: A Factorization Approach.* MIT Press.

Vidyasagar, M. 1988: Normalized Coprime Factorizations for Nonstrictly Proper Systems. *IEEE Trans. Autom. Control*, vol. 33, no. 3, pp. 300–301.

Table I. Open-Loop-System Characteristics of Phase 0 Model

Mode	Eigenvalues		Frequency, Hz
	Real	±Imaginary	
1	−4.622E−3	9.243E−1	0.147
2	−4.682E−3	9.365E−1	.149
3	−4.876E−3	9.752E−1	.155
4	−2.294E−2	4.587E+0	.730
5	−2.349E−2	4.698E+0	.748
6	−2.746E−2	5.491E+0	.874
7	−4.629E−2	9.258E+0	1.474
8	−5.460E−2	1.092E+1	1.738
9	−5.916E−2	1.183E+1	1.883
10	−7.230E−2	1.446E+1	2.301
11	−8.918E−2	1.783E+1	2.838
12	−1.261E−1	2.522E+1	4.015
13	−1.267E−1	2.534E+1	4.032
14	−1.321E−1	2.642E+1	4.206
15	−1.380E−1	2.760E+1	4.392
16	−1.728E−1	3.457E+1	5.501
17	−1.941E−1	3.883E+1	6.180
18	−1.958E−1	3.915E+1	6.231
19	−2.033E−1	4.066E+1	6.471
20	−2.095E−1	4.191E+1	6.670
21	−2.316E−1	4.632E+1	7.372
22	−2.605E−1	5.211E+1	8.293
23	−2.817E−1	5.634E+1	8.966
24	−3.922E−1	7.845E+1	12.49
25	−5.294E−1	1.059E+2	16.85

Table II. Eigenvalues of $\mathbf{K}_A(s)$ Optimal Compensator System Matrix With $\epsilon_A = \epsilon_{A,\max}$

$\left[(k, i, a) = (0.1, 2, 0.5); \epsilon_{A,\max} = 0.6749\right]$

Real	Complex	
	Real	±Imaginary
−1.2941	−1.857E−1	1.115E−1
−.7197	−2.983E−1	7.433E−1
−.7088	−1.342E−1	8.200E−1
−.5482	−3.402E−2	4.579E+0
−.5462	−2.898E−2	4.685E+0
−.5361	−3.684E−2	5.468E+0
−.5283	−5.027E−2	9.245E+1
−.5066	−6.042E−2	1.090E+1
−.4936	−5.962E−2	1.183E+1
−.4746		
−.4684		
−.4610		
−.4595		
−.3868		
−.3723		

Table III. Closed-Loop Eigenvalues of Design Model Controlled by Optimal Compensator $\mathbf{K}(s)$ With $\epsilon_A = \epsilon_{A,\max}$

$\left[(k, i, a) = (0.1, 2, 0.5); \epsilon_{A,\max} = 0.6749\right]$

Open-loop mode	Complex		Damping ratio, ζ
	Real	±Imaginary	
1	−4.426E−2	9.246E−1	0.0478
2	−7.079E−2	9.485E−1	.0744
3	−1.096E−1	9.645E−1	.1291
4	−2.716E−2	4.588E+0	.0059
5	−2.658E−2	4.698E+0	.0057
6	−3.237E−2	5.491E+0	.0059
7	−4.820E−2	9.258E+0	.0052
8	−5.723E−2	1.092E+1	.0052
9	−5.968E−2	1.183E+1	.0054
10	−7.234E−2	1.446E+1	.0050
11	−8.920E−2	1.784E+1	.0050
12	−1.261E−1	2.523E+1	.0050
13	−1.268E−1	2.534E+1	.0050
14	−1.321E−1	2.643E+1	.0050
15	−1.380E−1	2.760E+1	.0050
16	−1.729E−1	3.457E+1	.0050
17	−1.941E−1	3.883E+1	.0050
18	−1.958E−1	3.915E+1	.0050
19	−2.033E−1	4.066E+1	.0050
20	−2.097E−1	4.191E+1	.0050
21	−2.316E−1	4.632E+1	.0050
22	−2.606E−1	5.211E+1	.0050
23	−2.818E−1	5.634E+1	.0050
24	−3.923E−1	7.845E+1	.0050
25	−5.295E−1	1.059E+2	.0050

Table IV. Eigenvalues of $\mathbf{K}_A(s)$ Suboptimal Compensator System Matrix With $\epsilon_A = 0.9\epsilon_{A,\max}$

$\left[(k, i, a) = (0.5, 1, 0.1); \epsilon_{A,\max} = 0.6670\right]$

Real	Complex	
	Real	±Imaginary
[a]−0.1000	−2.296E+0	4.230E+0
−.1612	−2.366E−1	4.690E+0
−.2945	−1.859E+0	5.232E+0
−.4769	−2.339E+0	8.859E+0
−1.8518	−3.535E+0	9.659E+0
−3.1977	−1.408E+0	1.103E+1
−6.8123		

[a]Repeated eigenvalues of multiplicity 8.

Table V. Closed-Loop Eigenvalues of Design Model Controlled by Suboptimal Compensator $\mathbf{K}(s)$ With $\epsilon_A = 0.9\epsilon_{A,\max}$

$\left[(k, i, a) = (0.5, 1, 0.1); \epsilon_{A,\max} = 0.6670\right]$

Open-loop mode	Complex		Damping ratio, ζ
	Real	±Imaginary	
[a]1			
[a]2			
3	−2.610E−1	8.872E−1	0.2822
4	−5.216E−1	4.620E+0	.1122
5	−1.767E−1 or −9.510E−2	4.671E+0 or 4.653E+0	.0378 or .0204
6	−4.760E−1	5.480E+0	.0865
7	−6.248E−1	9.237E+0	.0675
8	−9.416E−1	1.086E+1	.0838
9	−4.921E−1	1.178E+1	.0417
10	−8.062E−2	1.447E+1	.0056
11	−1.056E−1	1.785E+1	.0059
12	−1.266E−1	2.522E+1	.0050
13	−1.391E−1	2.538E+1	.0055
14	−1.336E−1	2.643E+1	.0051
15	−1.606E−1	2.766E+1	.0058
16	−1.747E−1	3.458E+1	.0050
17	−1.953E−1	3.884E+1	.0050
18	−2.038E−1	3.919E+1	.0052
19	−2.133E−1	4.071E+1	.0052
20	−2.122E−1	4.194E+1	.0051
21	−2.334E−1	4.634E+1	.0050
22	−2.623E−1	5.212E+1	.0050
23	−2.895E−1	5.639E+1	.0051
24	−3.924E−1	7.845E+1	.0050
25	−5.295E−1	1.059E+2	.0050

[a]Not discernible from data.

Table VI. Eigenvalues of $\mathbf{K}_A(s)$ Suboptimal Compensator System Matrix With $\epsilon_A = 0$

$\left[(k, i, a) = (0.5, 1, 0.1); \epsilon_{A,\max} = 0.6670\right]$

Real	Complex	
	Real	±Imaginary
[a]−0.1000	−7.687E−1	5.570E−1
−.3663	−5.185E−1	7.661E−1
−2.5134	−1.039E+0	4.555E+0
	−1.568E−1	4.661E+0
	−9.240E−1	5.427E+0
	−1.188E+0	9.153E+0
	−1.808E+0	1.063E+1
	−8.976E−1	1.161E+1

[a]Repeated eigenvalues of multiplicity 8.

Table VII. Closed-Loop Eigenvalues of Design Model Controlled by Suboptimal Compensator $\mathbf{K}(s)$ With $\epsilon_A = 0$

$\left[(k, i, a) = (0.5, 1, 0.1); \epsilon_{A,\max} = 0.6670\right]$

Open-loop mode	Complex		Damping ratio, ζ
	Real	±Imaginary	
[a]1			
[a]2			
3	−2.578E−1	8.945E−1	0.2769
4	−5.448E−1	4.581E+0	.1181
5	−4.956E−1	4.647E+0	.1060
	or	or	or
	−9.308E−2	4.653E+0	.0200
6	−4.497E−1	5.503E+0	.0814
7	−5.895E−1	9.275E+0	.0634
8	−8.884E−1	1.092E+1	.0811
9	−4.683E−1	1.181E+1	.0396
10	−7.423E−2	1.446E+1	.0051
11	−9.251E−2	1.784E+1	.0052
12	−1.262E−1	2.523E+1	.0050
13	−1.287E−1	2.535E+1	.0051
14	−1.324E−1	2.643E+1	.0050
15	−1.417E−1	2.762E+1	.0051
16	−1.731E−1	3.457E+1	.0050
17	−1.943E−1	3.883E+1	.0050
18	−1.971E−1	3.916E+1	.0050
19	−2.048E−1	4.067E+1	.0050
20	−2.100E−1	4.192E+1	.0050
21	−2.319E−1	4.633E+1	.0050
22	−2.608E−1	5.211E+1	.0050
23	−2.828E−1	5.635E+1	.0050
24	−3.923E−1	7.845E+1	.0050
25	−5.295E−1	1.059E+2	.0050

[a]Not discernible from data.

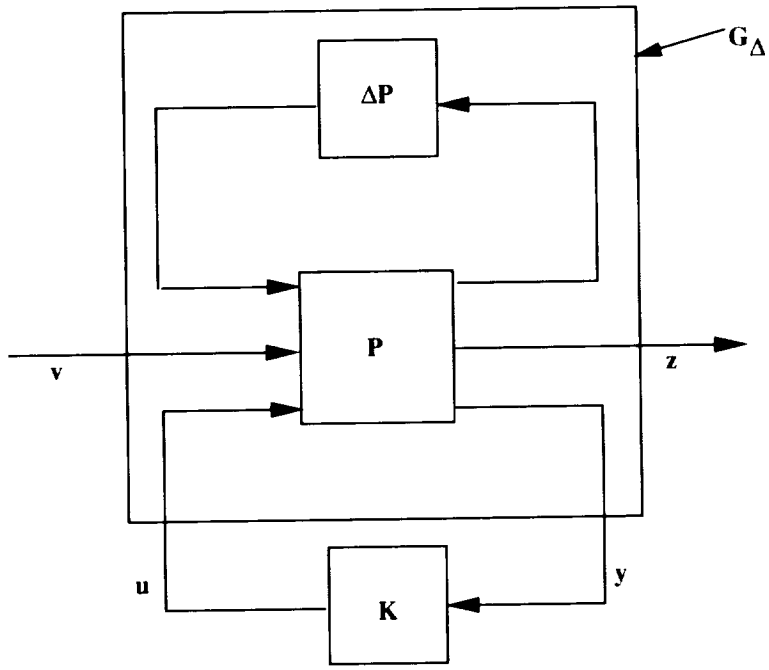

Figure 1. Feedback control of generalized uncertainty model.

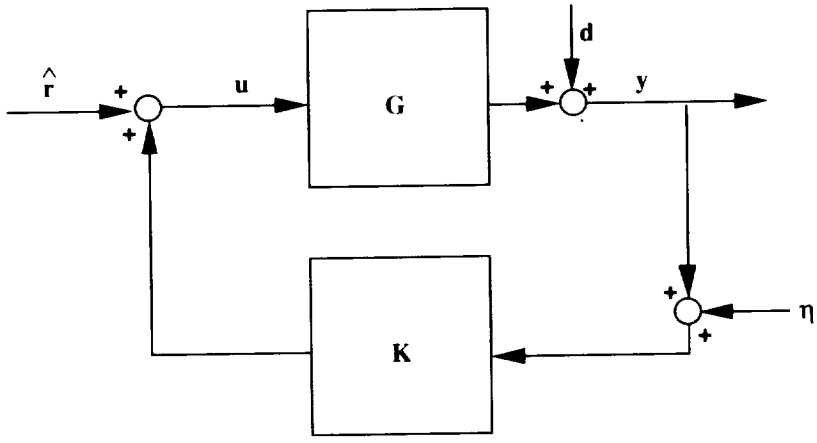

Figure 2. Closed-loop system with exogenous inputs.

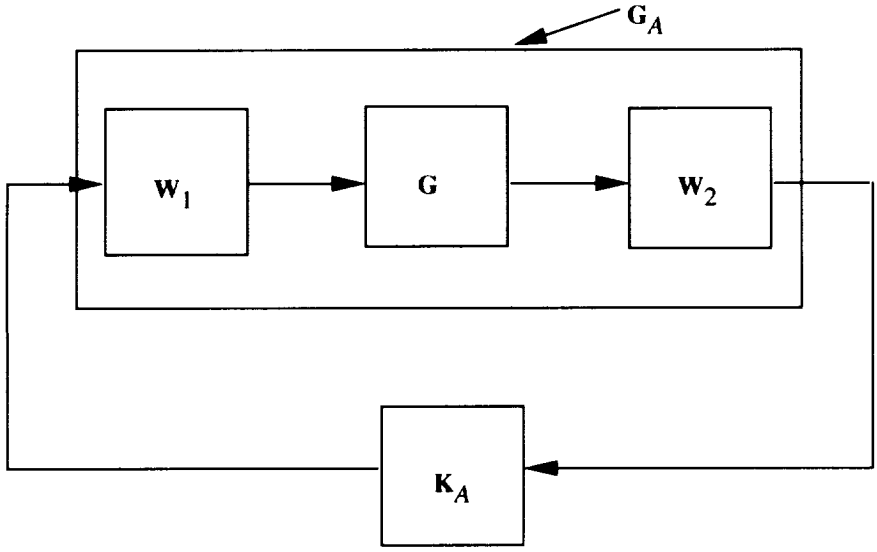

(a) Compensator for shaped plant ($\mathbf{G}_A$).

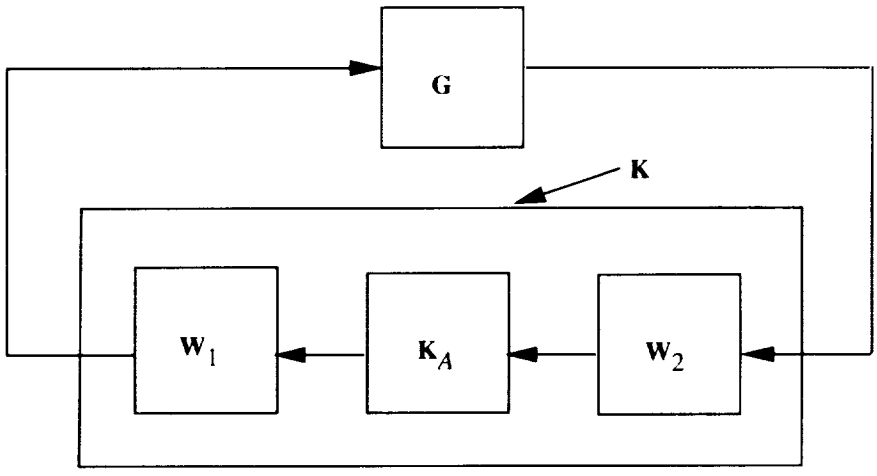

(b) Equivalent compensator for unshaped plant ($\mathbf{G}$).

Figure 3. Loop-shaping procedure.

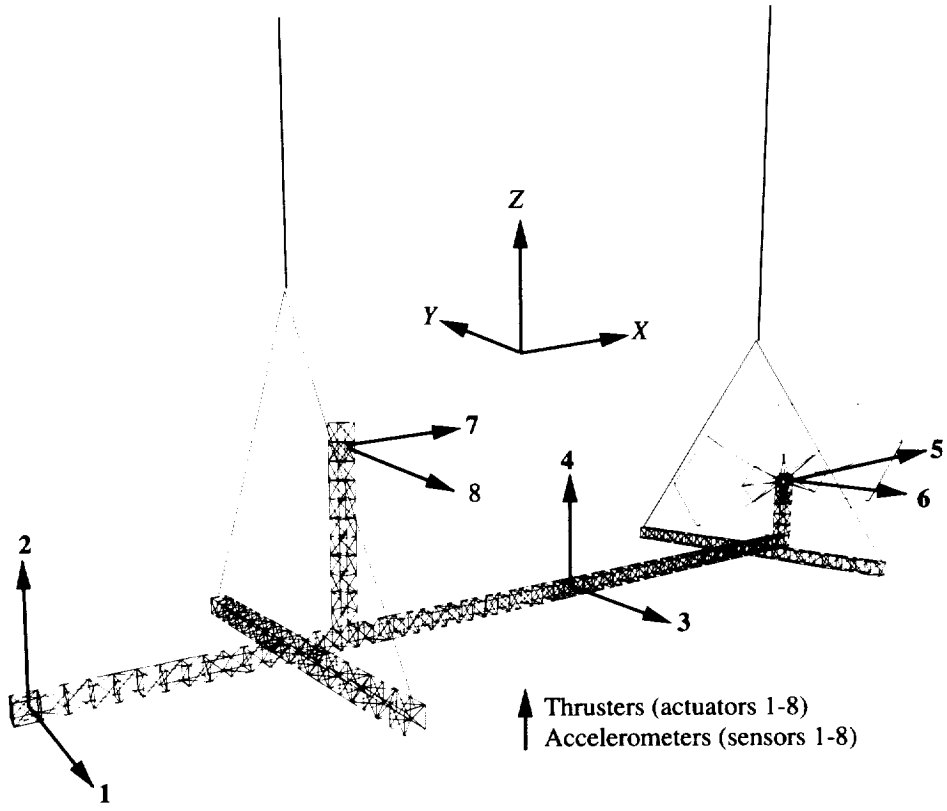

Figure 4. Schematic of CSI Phase 0 Evolutionary Model.

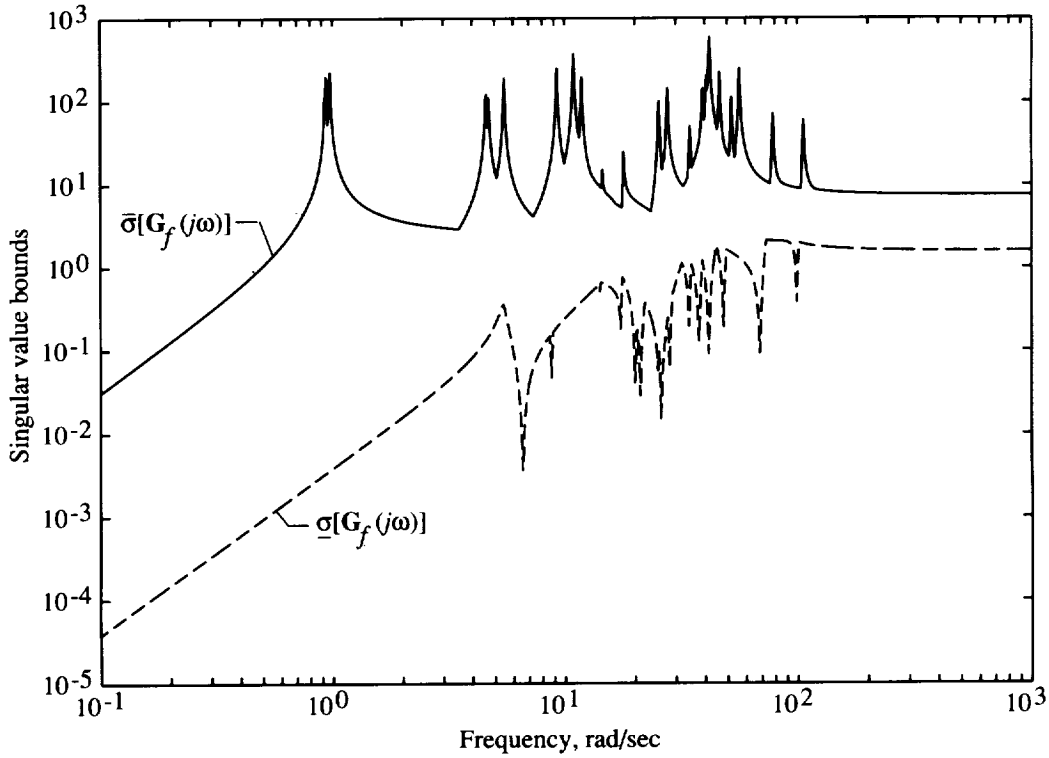

Figure 5. Open-loop 25-mode nominal system ($\mathbf{G}_f(s)$).

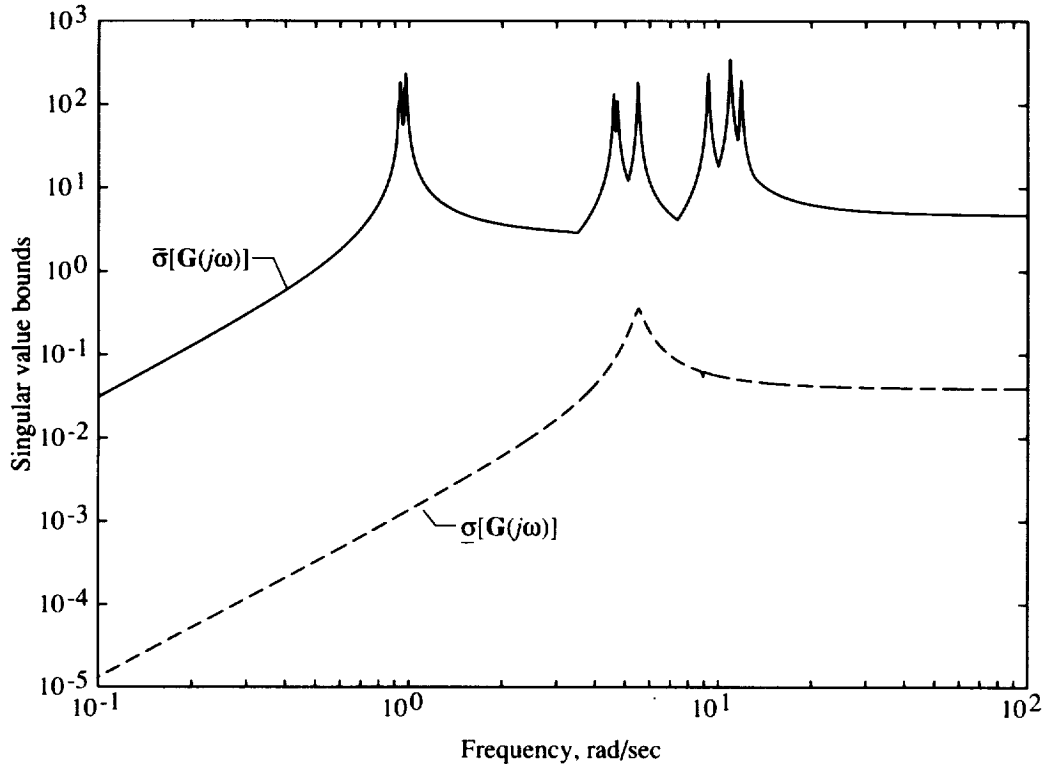

(a) 9-mode nominal system ($\mathbf{G}(s)$).

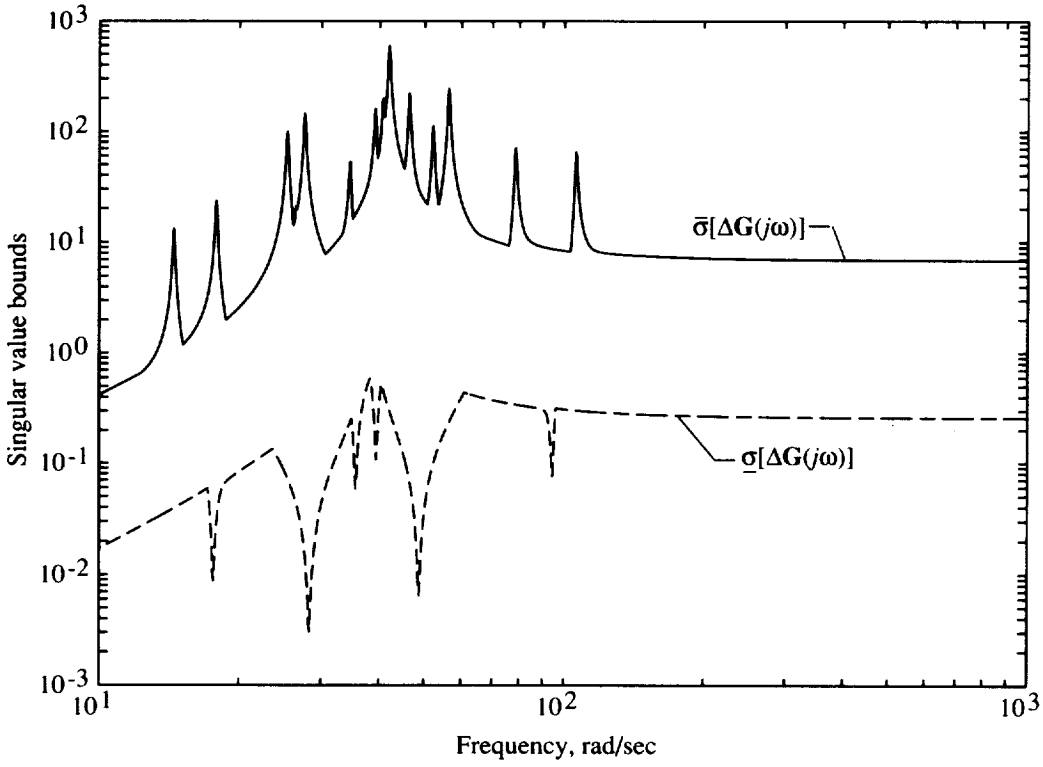

(b) 16-mode truncated system ($\Delta\mathbf{G}(s)$).

Figure 6. Unweighted open-loop nominal and truncated systems.

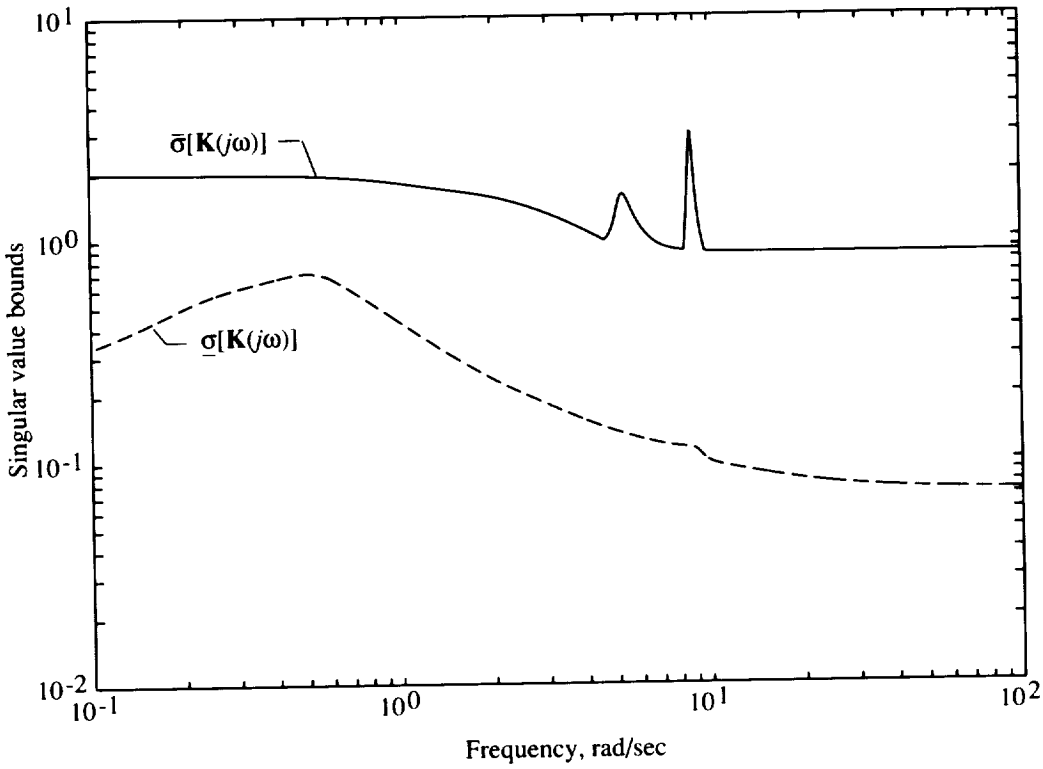

(a) Optimal compensator ($\mathbf{K}(s)$) with $\epsilon = \epsilon_{\max}$.

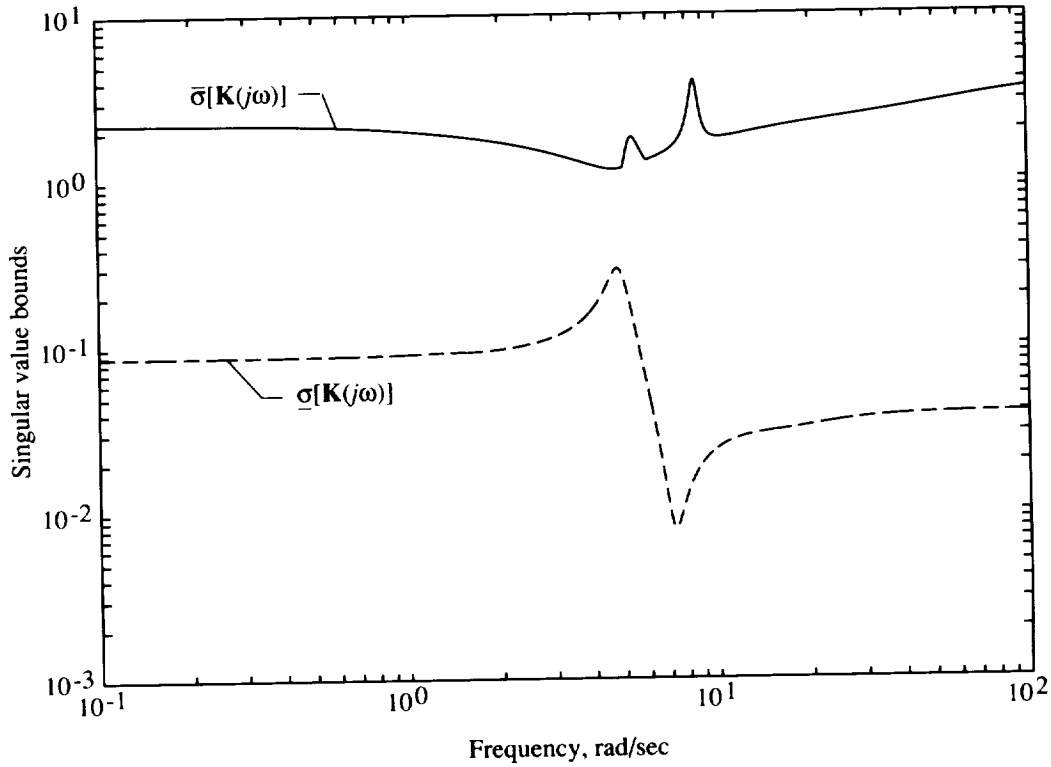

(b) Suboptimal compensator ($\mathbf{K}(s)$) with $\epsilon = 0.9\epsilon_{\max}$.

Figure 7. Unweighted optimal and suboptimal compensators ($\mathbf{K}(s)$) with $\epsilon_{\max} = 0.4417$.

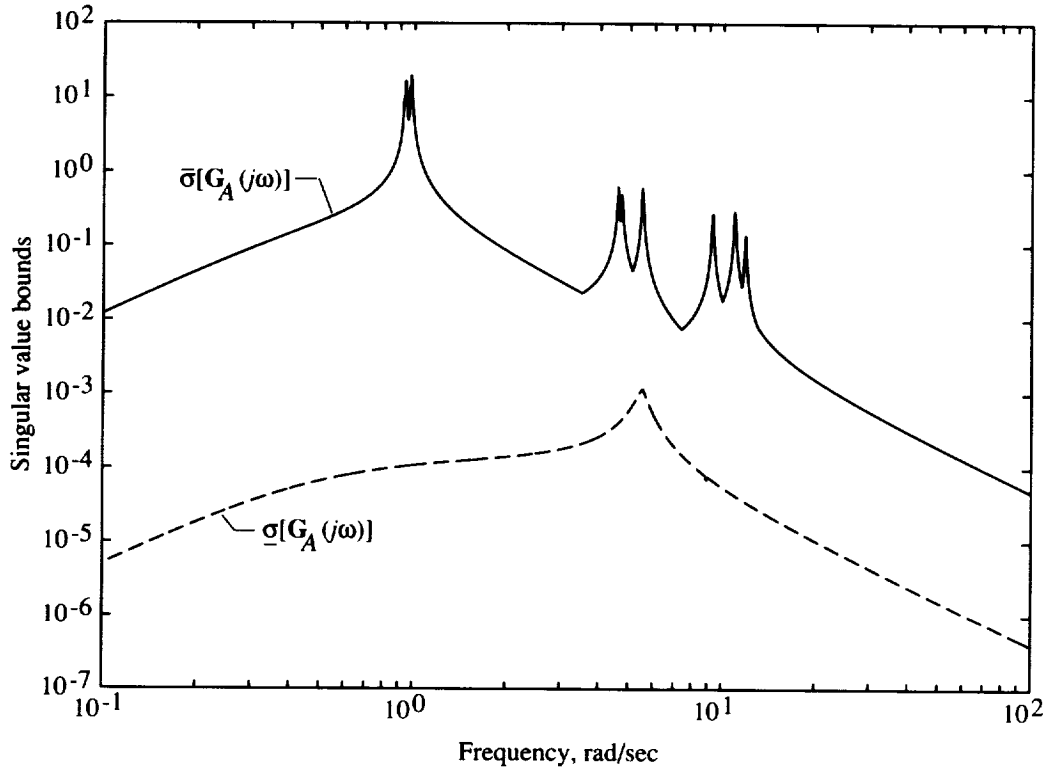

Figure 8. Weighted open-loop 9-mode system ($\mathbf{G}_A(s)$) with $\mathbf{G}_A(s) = \frac{0.1}{(s+0.5)^2}\mathbf{G}(s)$.

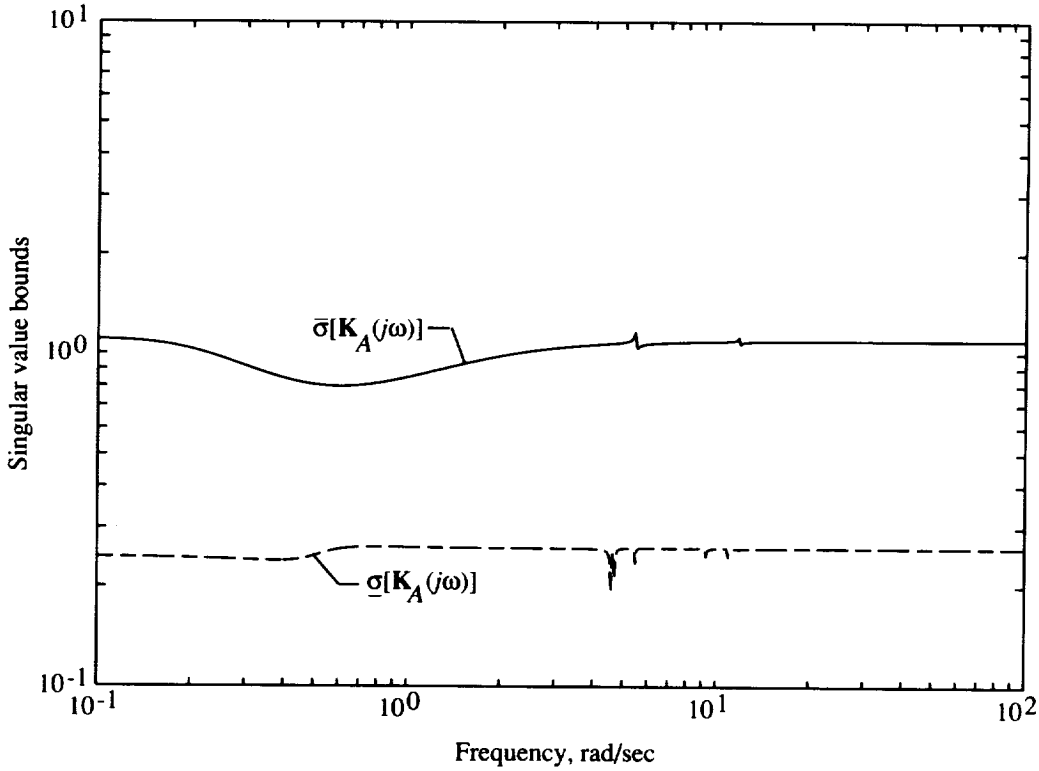

Figure 9. Weighted optimal compensator ($\mathbf{K}_A(s)$) with $(k, i, a) = (0.1, 2, 0.5)$ and $\epsilon_A = \epsilon_{A,\max} = 0.6749$.

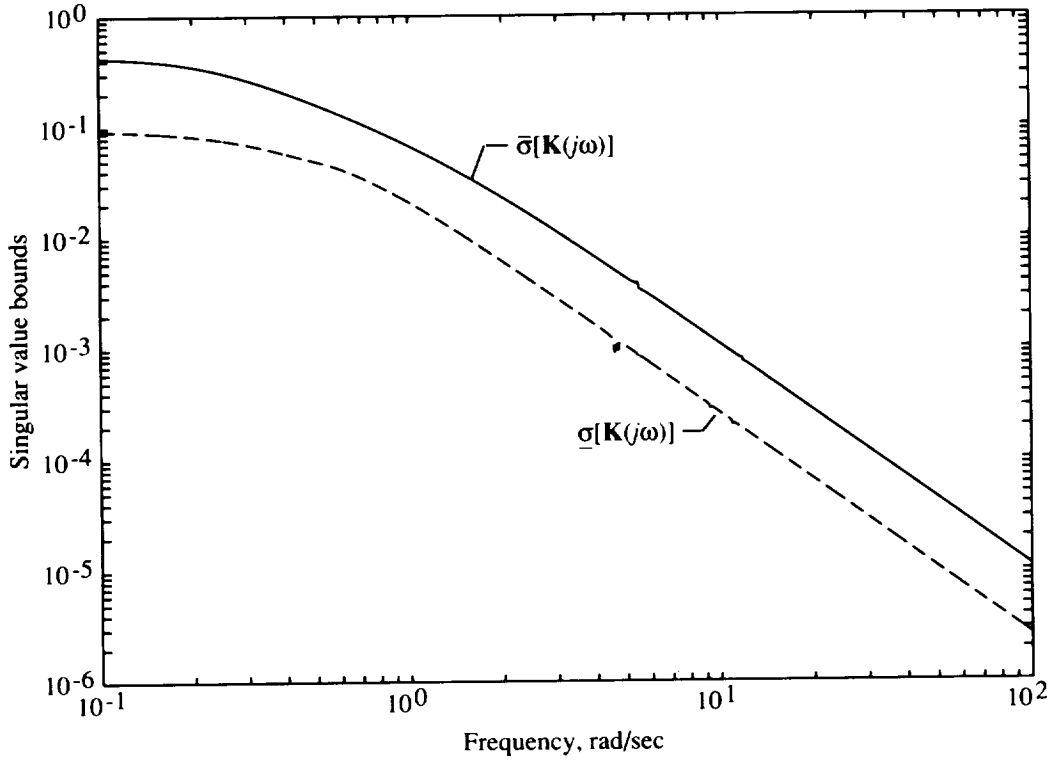

Figure 10. Weighted optimal compensator ($\mathbf{K}(s)$) with $(k, i, a) = (0.1, 2, 0.5)$, $\epsilon_A = \epsilon_{A,\max} = 0.6749$, and $\mathbf{K}(s) = \frac{0.1}{(s + 0.5)^2}\mathbf{K}_A(s)$.

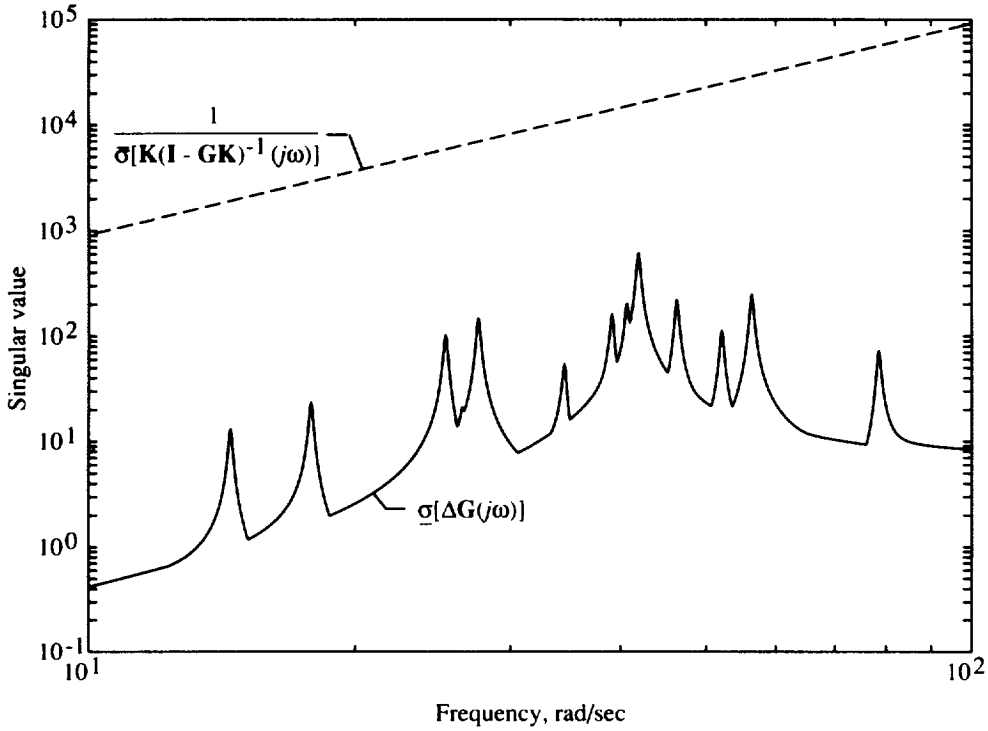

(a) Condition from inequality (41).

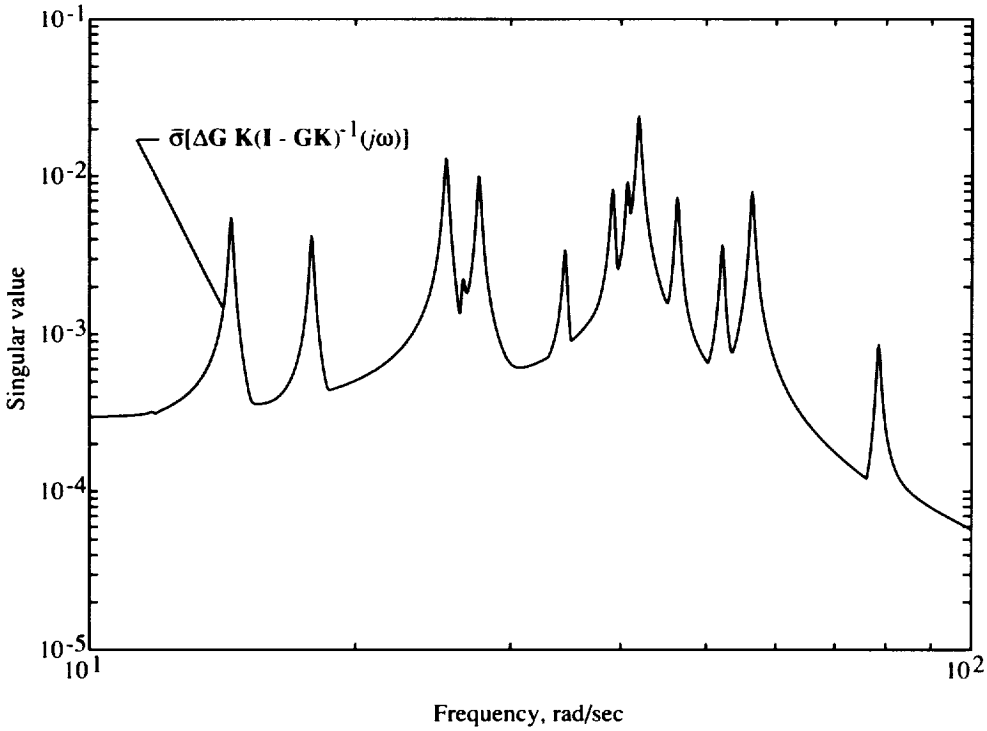

(b) Condition from inequality (40).

Figure 11. Robustness conditions for inequalities (40) and (41) for weighted optimal compensator ($\mathbf{K}(s)$) with $\epsilon_A = \epsilon_{A,\max} = 0.6749$ and $\mathbf{K}(s) = \frac{0.1}{(s + 0.5)^2}\mathbf{K}_A(s)$.

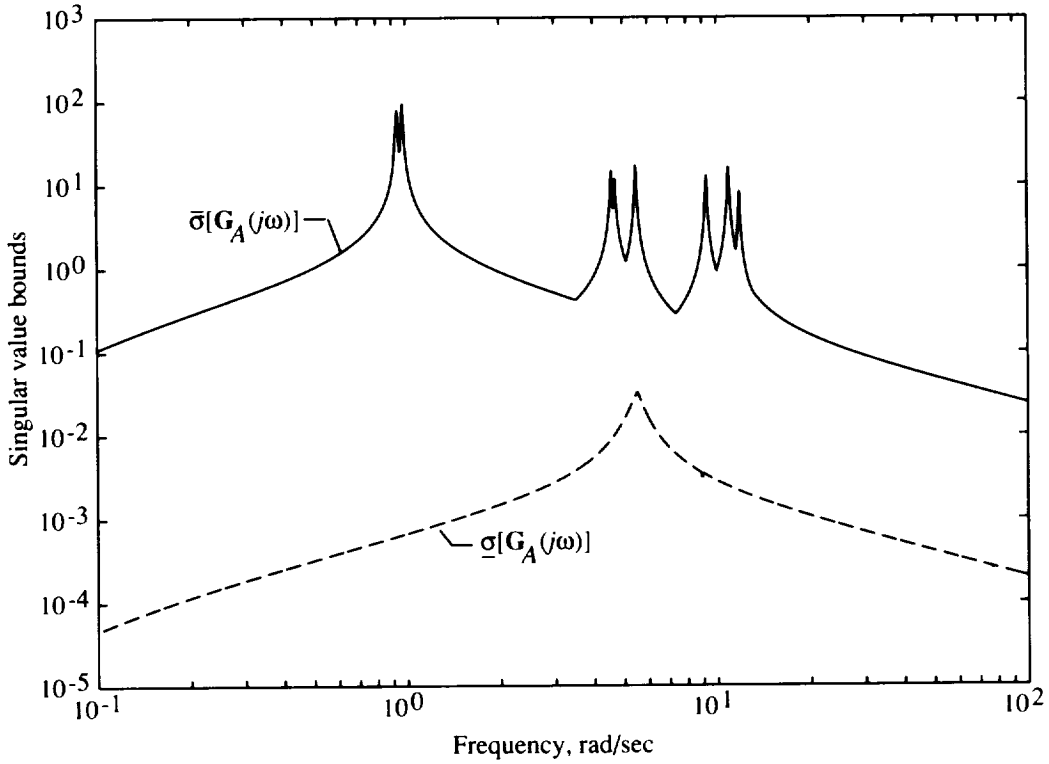

Figure 12. Weighted open-loop 9-mode nominal system ($\mathbf{G}_A(s)$) with $\mathbf{G}_A(s) = \frac{0.5}{(s+0.1)}\mathbf{G}(s)$.

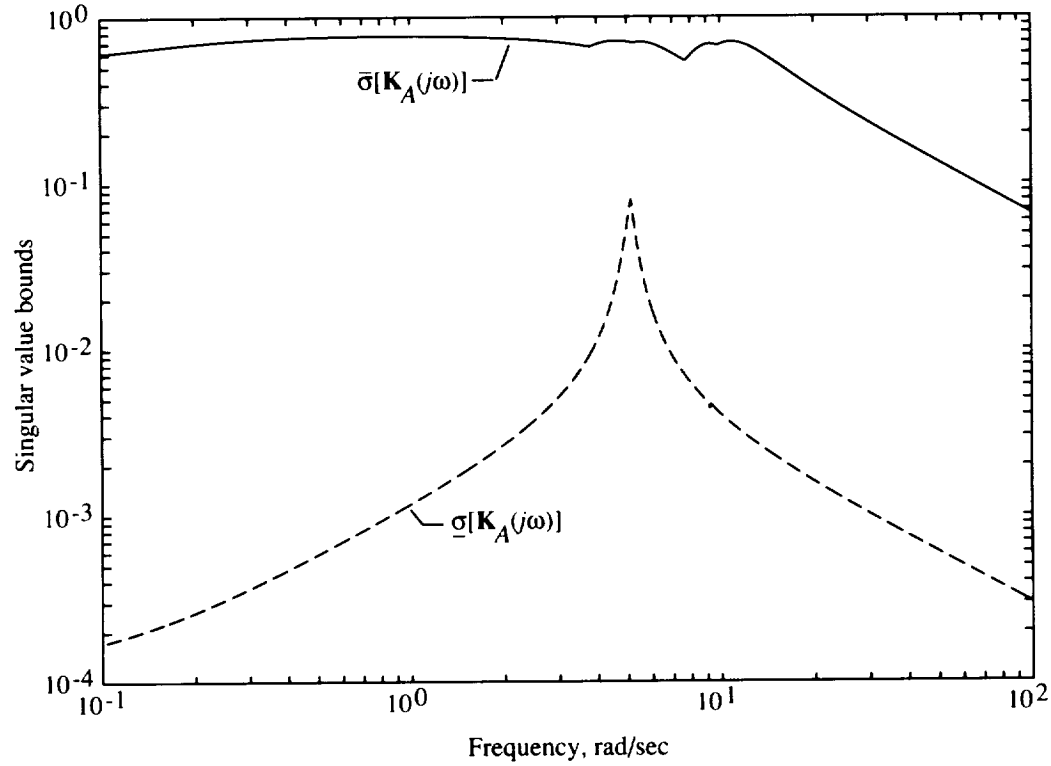

Figure 13. Weighted suboptimal compensator ($\mathbf{K}_A(s)$) with $(k, i, a) = (0.5, 1, 0.1)$, $\epsilon_A = 0.9\epsilon_{A,\max}$, and $\epsilon_{A,\max} = 0.667$.

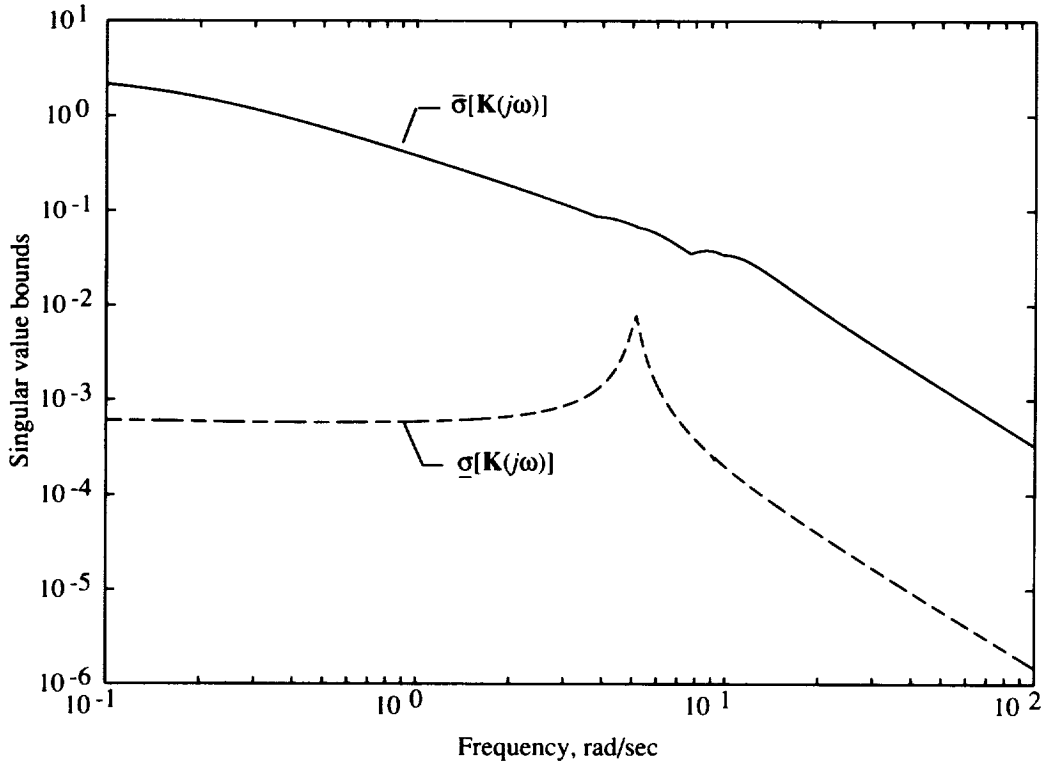

Figure 14. Weighted suboptimal compensator ($\mathbf{K}(s)$) with $\epsilon_A = 0.9\epsilon_{A,\max}$, $\epsilon_{A,\max} = 0.667$, and $\mathbf{K}(s) = \frac{0.5}{(s+0.1)}\mathbf{K}_A(s)$.

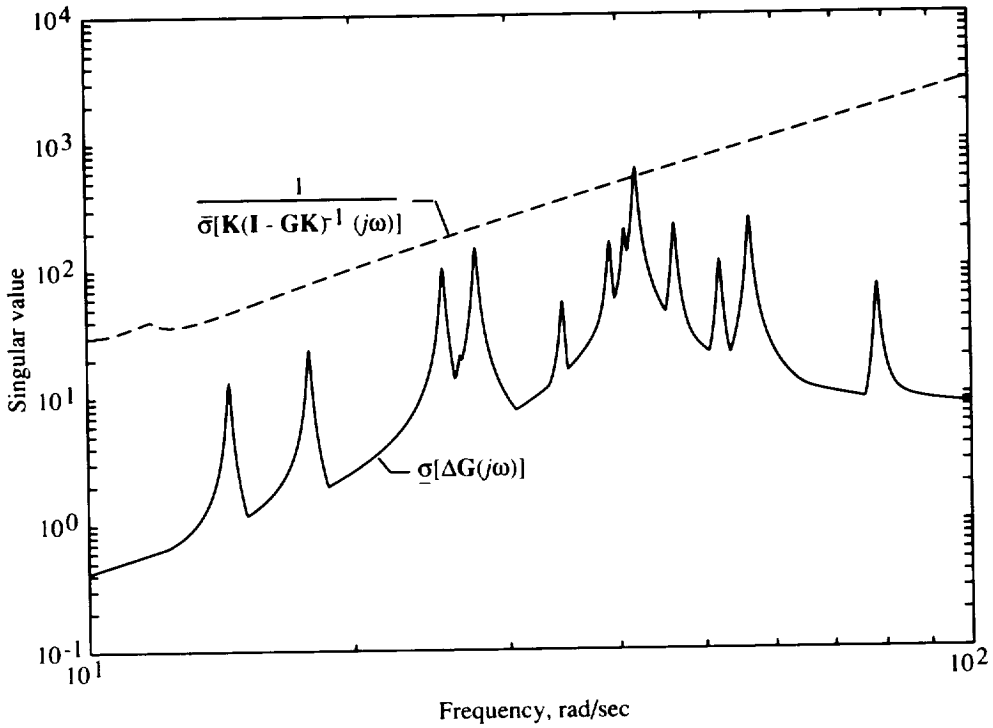

(a) Condition from inequality (41).

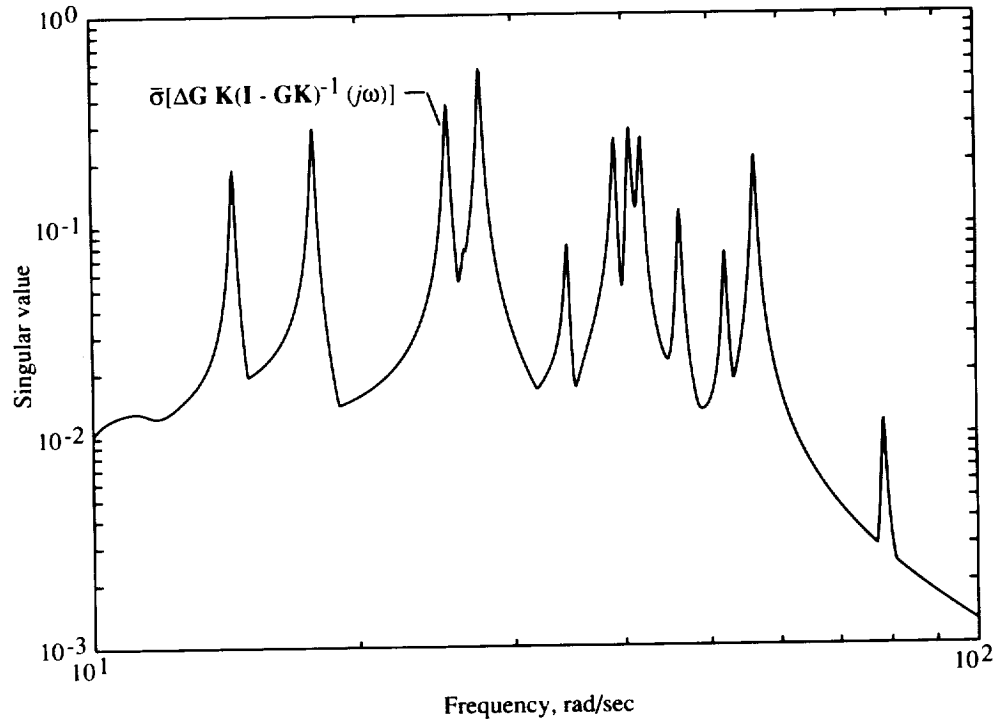

(b) Condition from inequality (40).

Figure 15. Robustness conditions for inequalities (40) and (41) for weighted suboptimal compensator ($\mathbf{K}(s)$) with $\epsilon_A = 0.9\epsilon_{A,\max}$, $\epsilon_{A,\max} = 0.667$, and $\mathbf{K}(s) = \frac{0.5}{(s + 0.1)}\mathbf{K}_A(s)$.

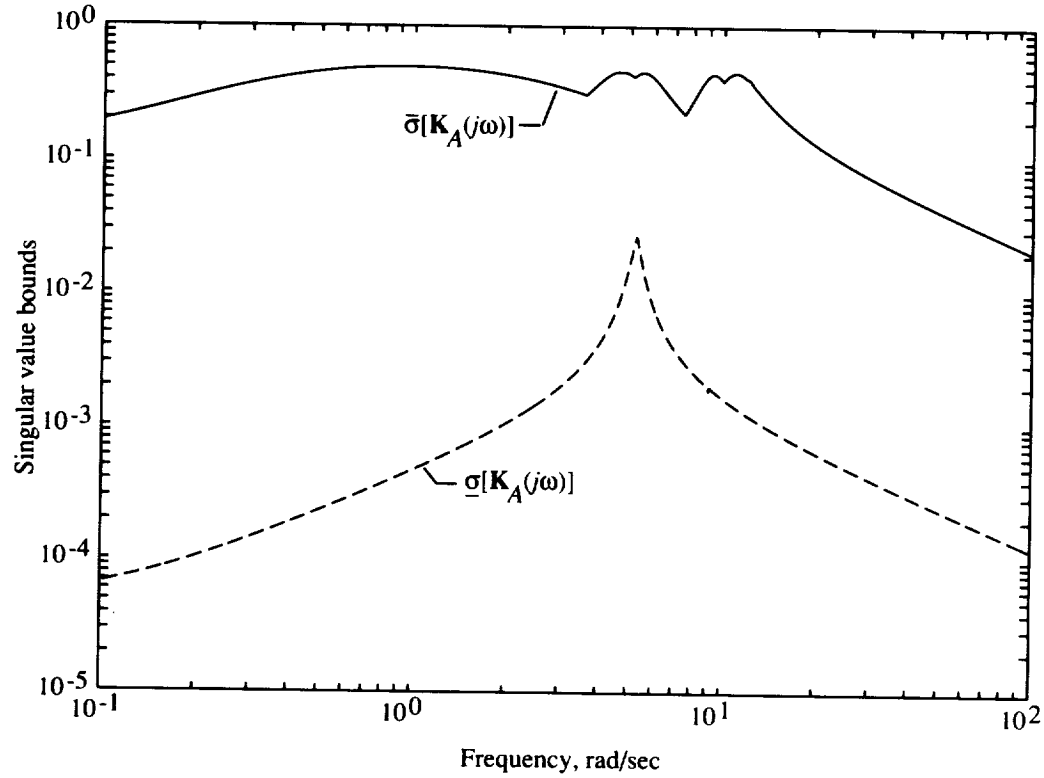

Figure 16. Weighted suboptimal compensator $(\mathbf{K}_A(s))$ with $(k, i, a) = (0.5, 1, 0.1)$ and $\epsilon_A = 0$.

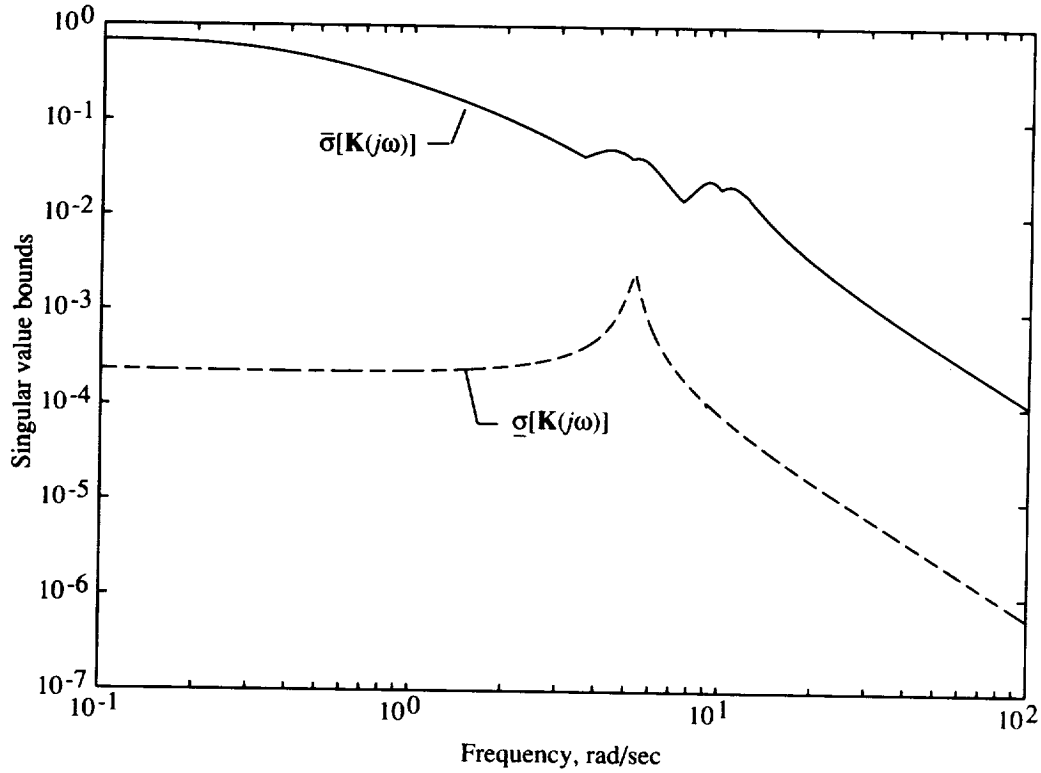

Figure 17. Weighted suboptimal compensator $(\mathbf{K}(s))$ with $\epsilon_A = 0$ and $\mathbf{K}(s) = \frac{0.5}{(s + 0.1)}\mathbf{K}_A(s)$.

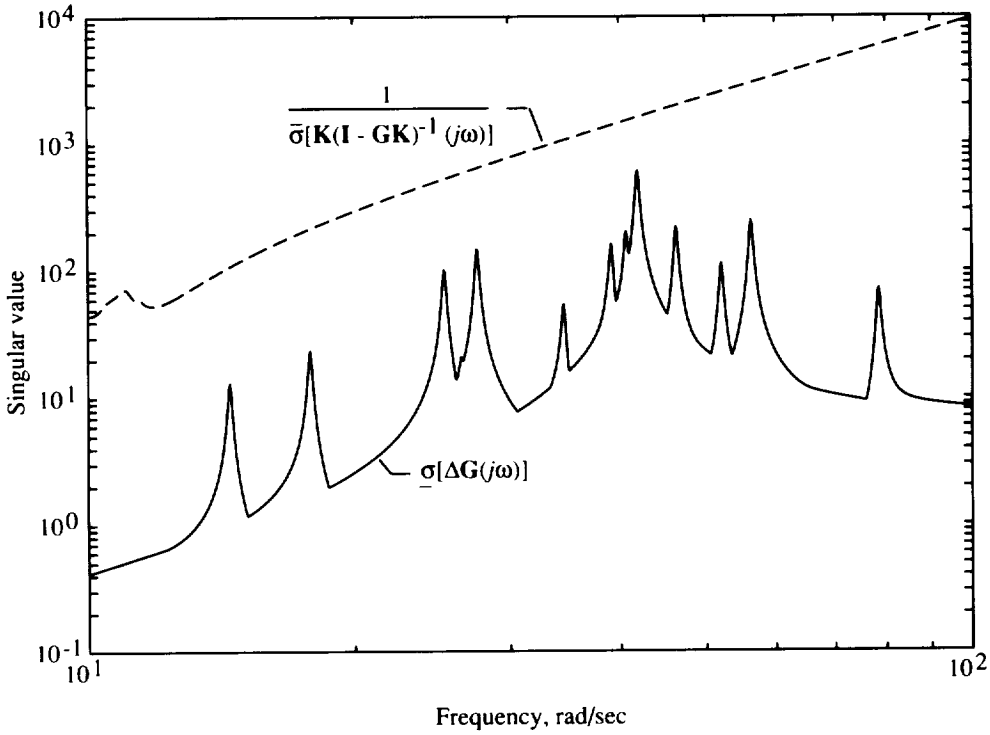

(a) Condition from inequality (41).

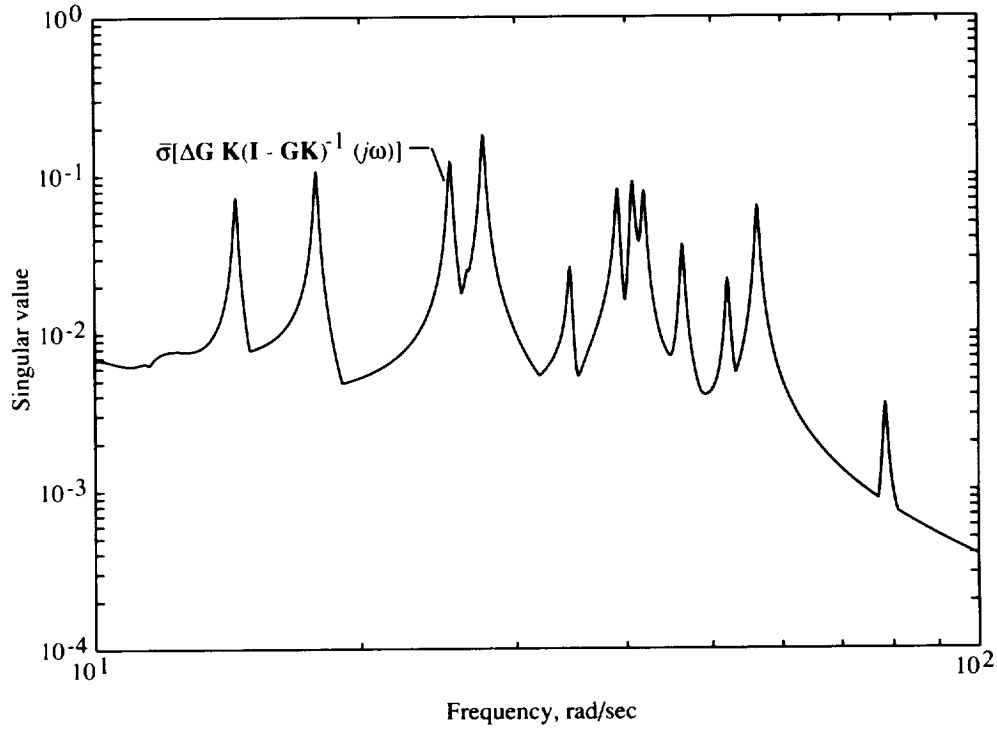

(b) Condition from inequality (40).

Figure 18. Robustness conditions for inequalities (40) and (41) for weighted suboptimal compensator ($\mathbf{K}(s)$) with $\epsilon_A = 0$ and $\mathbf{K}(s) = \frac{0.5}{(s + 0.1)}\mathbf{K}_A(s)$.

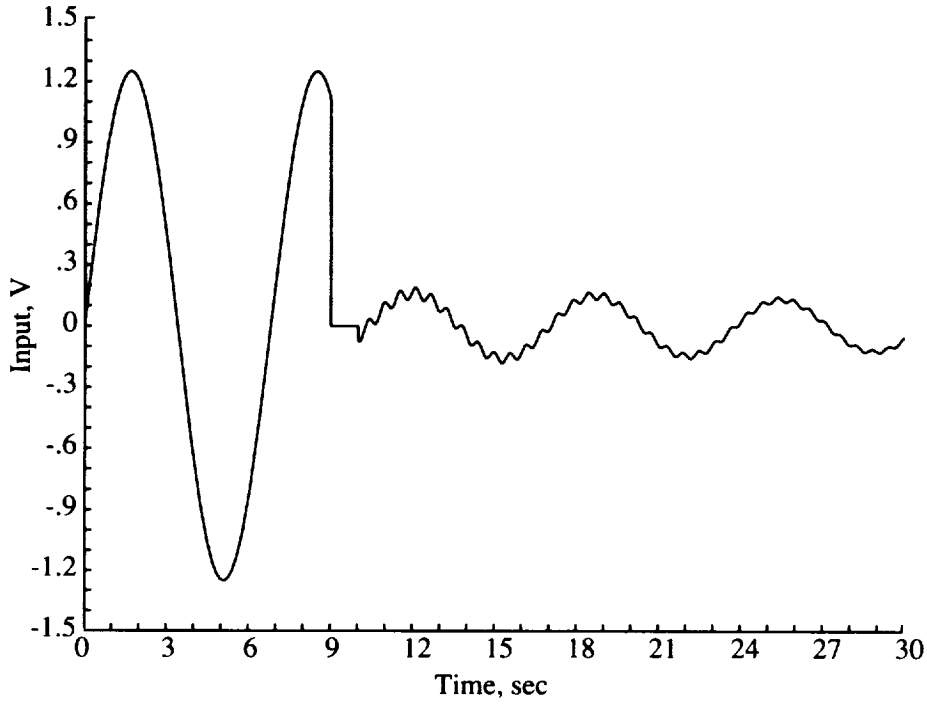

Figure 19. Input time history of actuator 7 for optimal compensator at $(k, i, a) = (0.1, 2, 0.5)$.

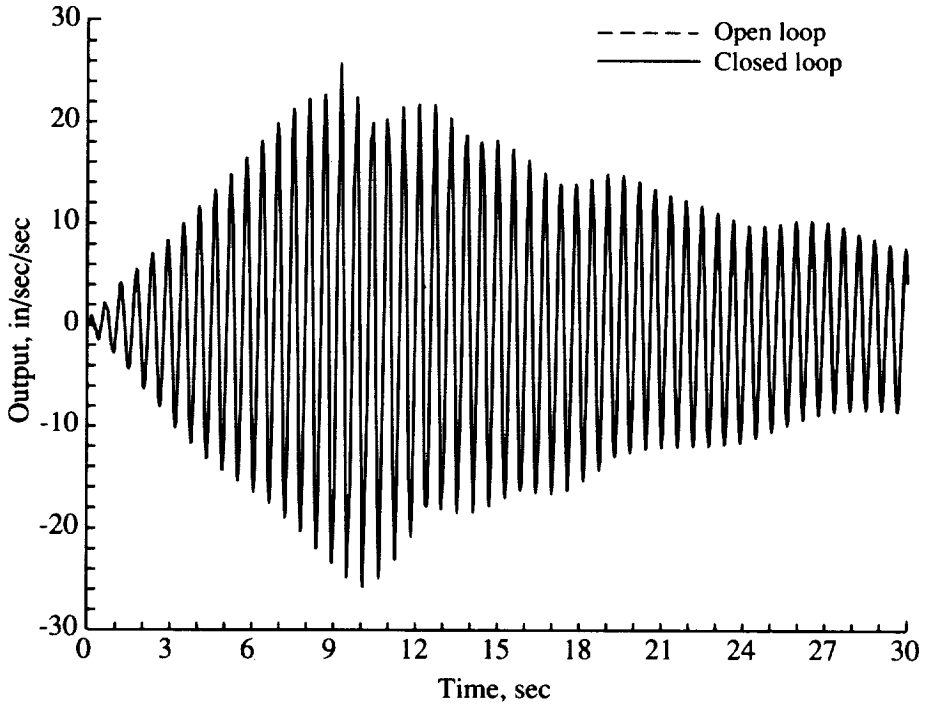

Figure 20. Output time history of accelerometer 7 for optimal compensator at $(k, i, a) = (0.1, 2, 0.5)$. In this figure the two curves coincide.

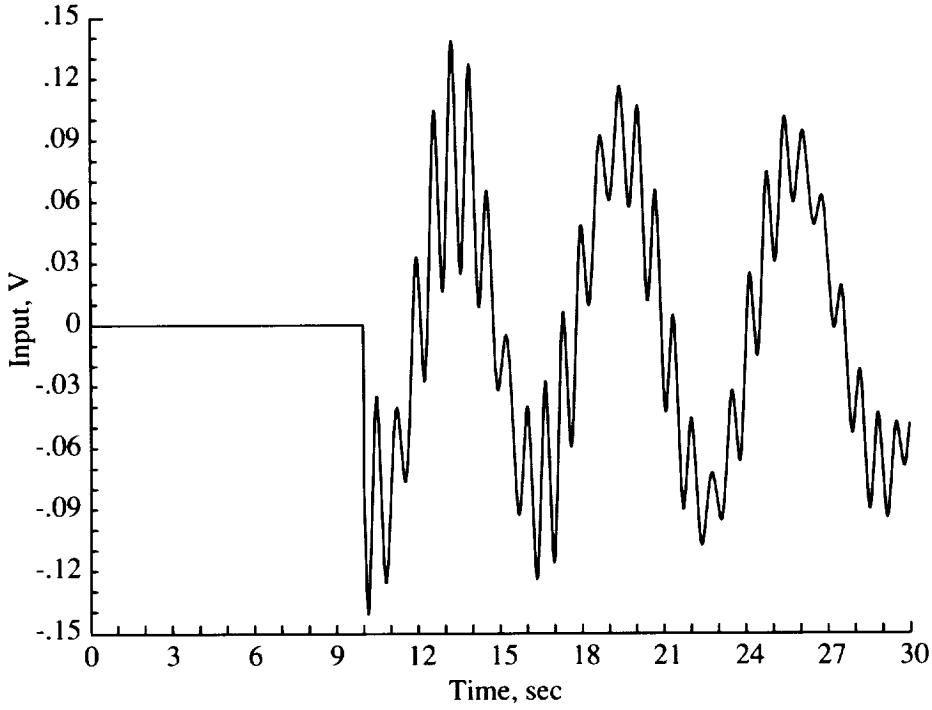

Figure 21. Input time history of actuator 8 for optimal compensator at $(k, i, a) = (0.1, 2, 0.5)$.

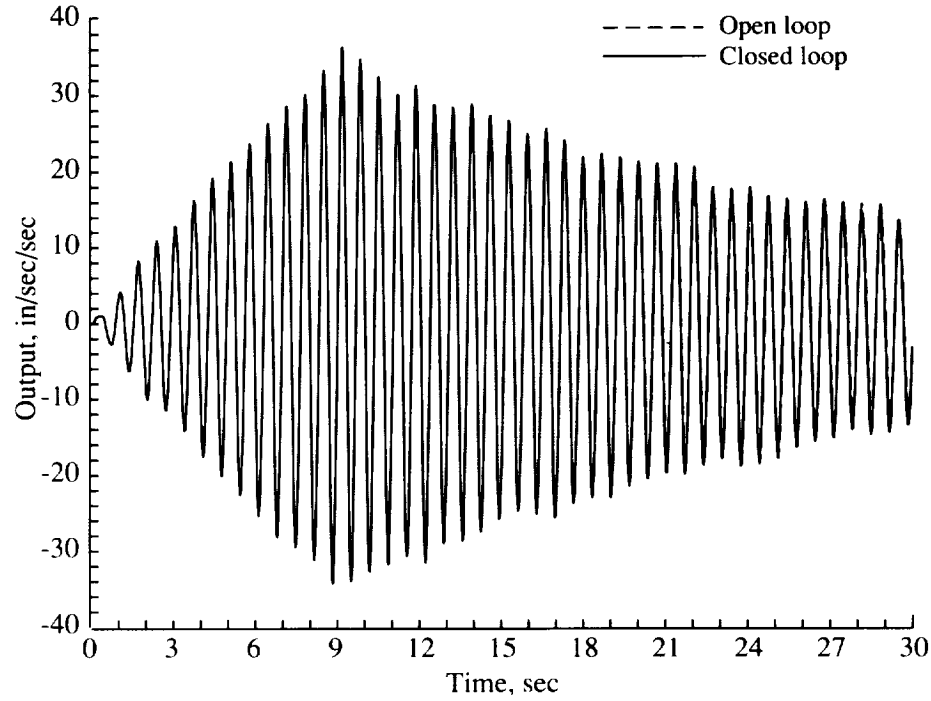

Figure 22. Output time history of accelerometer 8 for optimal compensator at $(k, i, a) = (0.1, 2, 0.5)$. In this figure the two curves coincide.

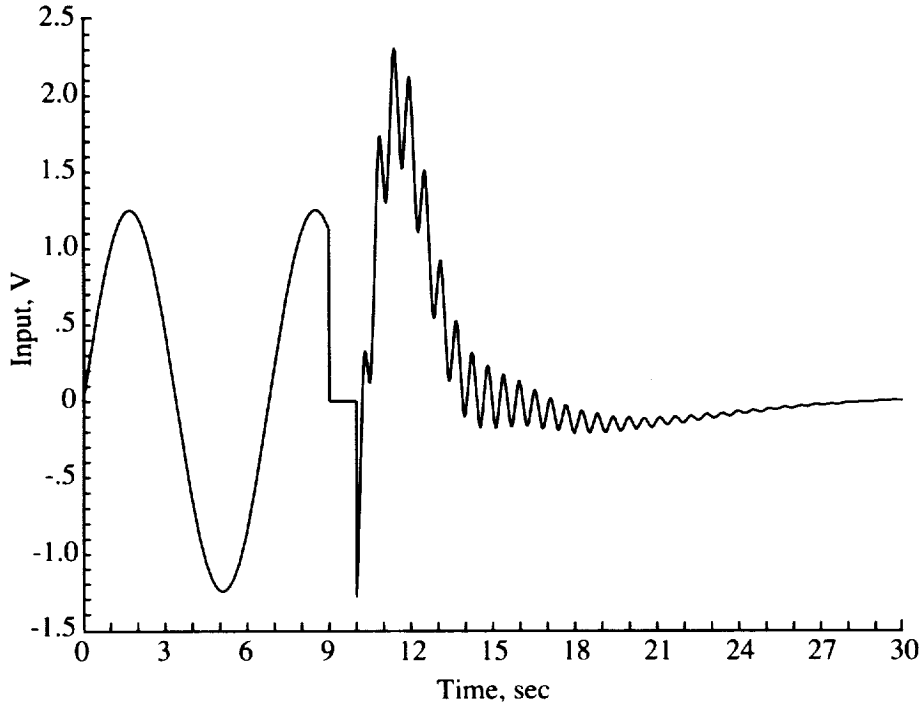

Figure 23. Input time history of actuator 7 for optimal compensator at $(k, i, a) = (2, 2, 0.5)$.

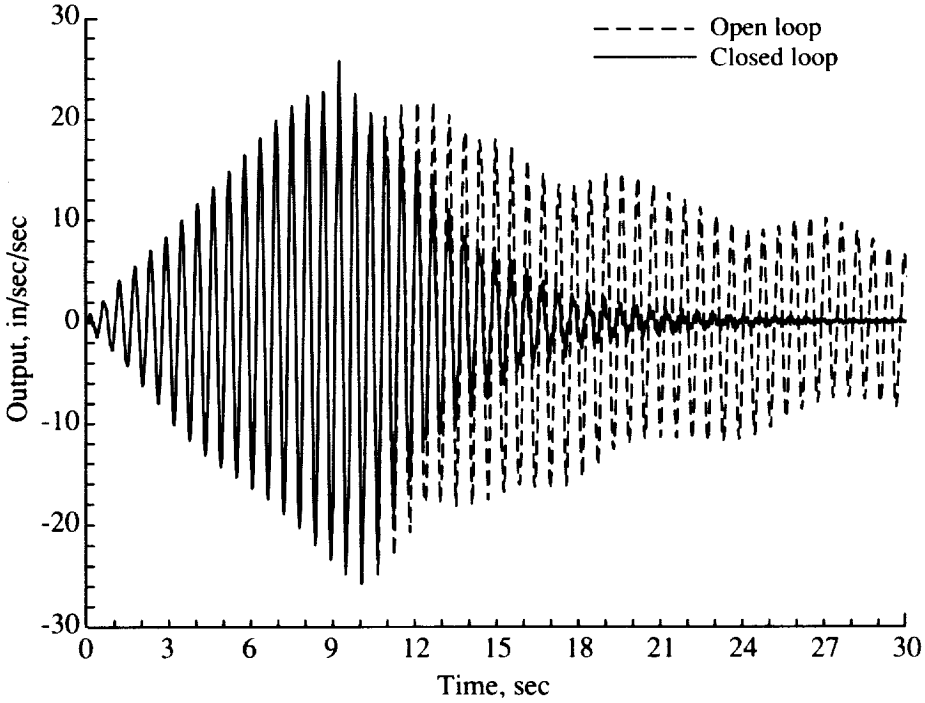

Figure 24. Output time history of accelerometer 7 for optimal compensator at $(k, i, a) = (2, 2, 0.5)$.

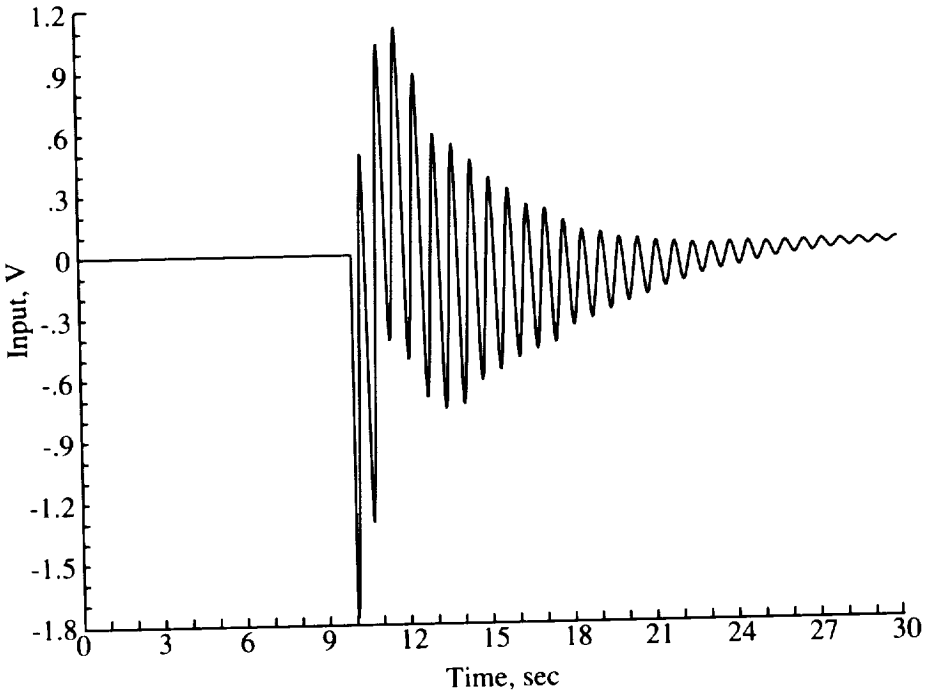

Figure 25. Input time history of actuator 8 for optimal compensator at $(k, i, a) = (2, 2, 0.5)$.

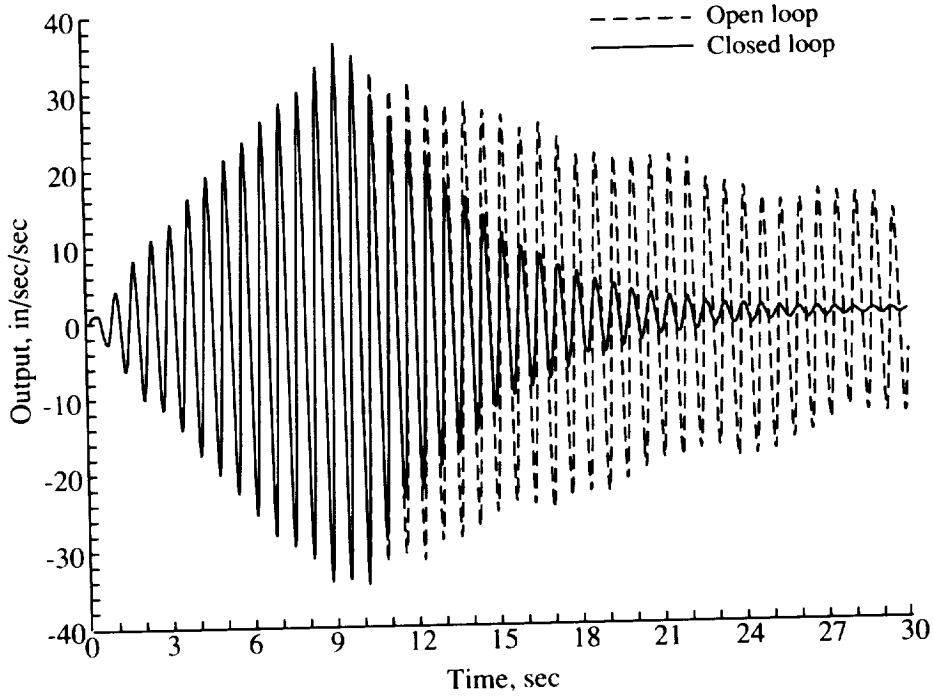

Figure 26. Output time history of accelerometer 8 for optimal compensator at $(k, i, a) = (2, 2, 0.5)$.

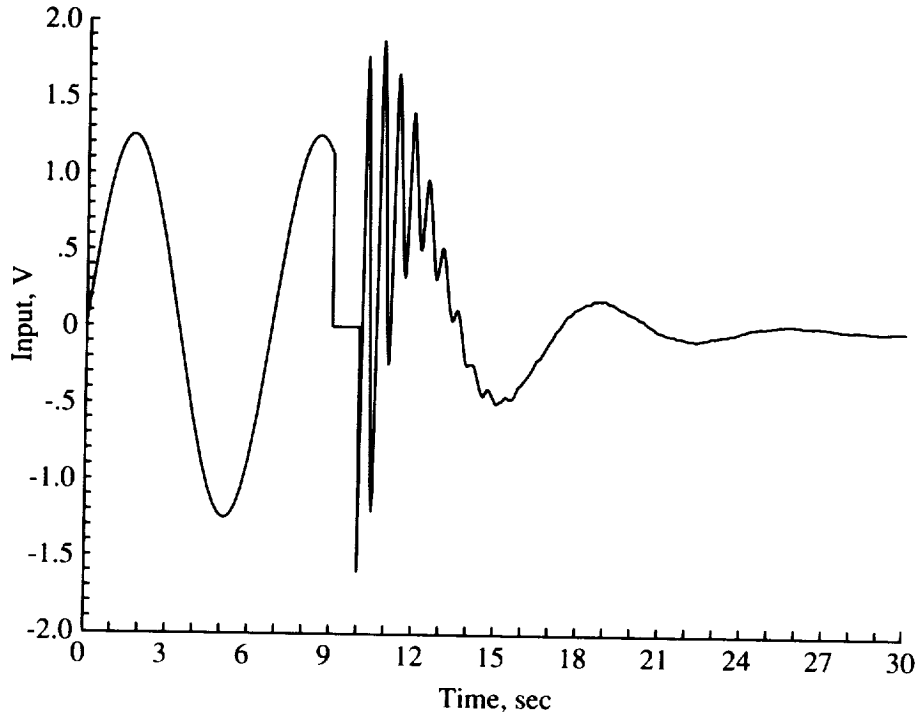

Figure 27. Input time history of actuator 7 for suboptimal compensator at $\epsilon_A = 0.9\epsilon_{A,\max}$ and $\epsilon_{A,\max} = 0.667$.

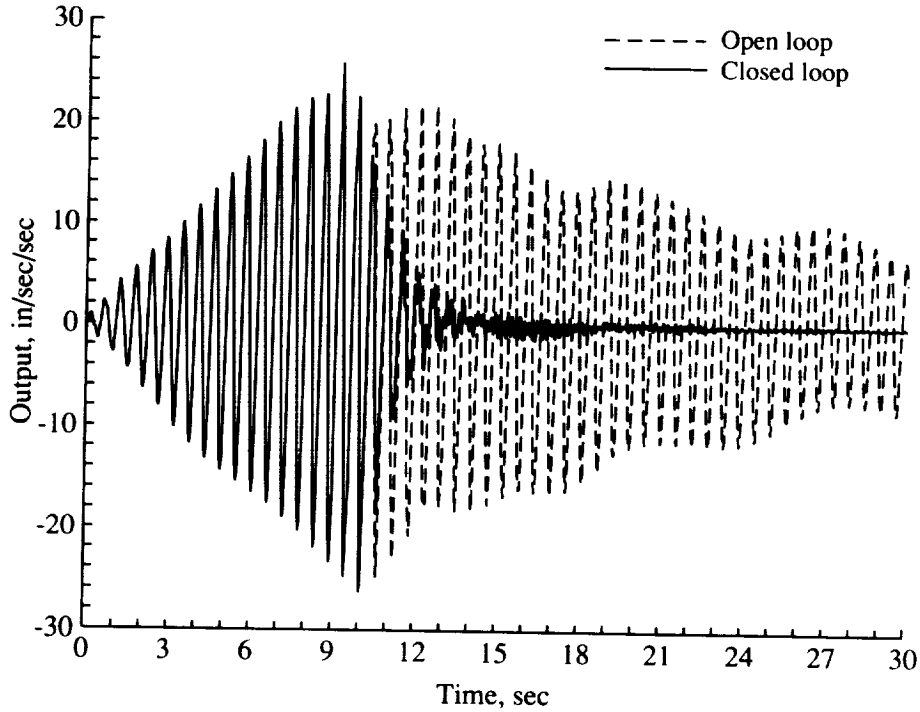

Figure 28. Output time history of suboptimal accelerometer 7 at $\epsilon_A = 0.9\epsilon_{A,\max}$ and $\epsilon_{A,\max} = 0.667$.

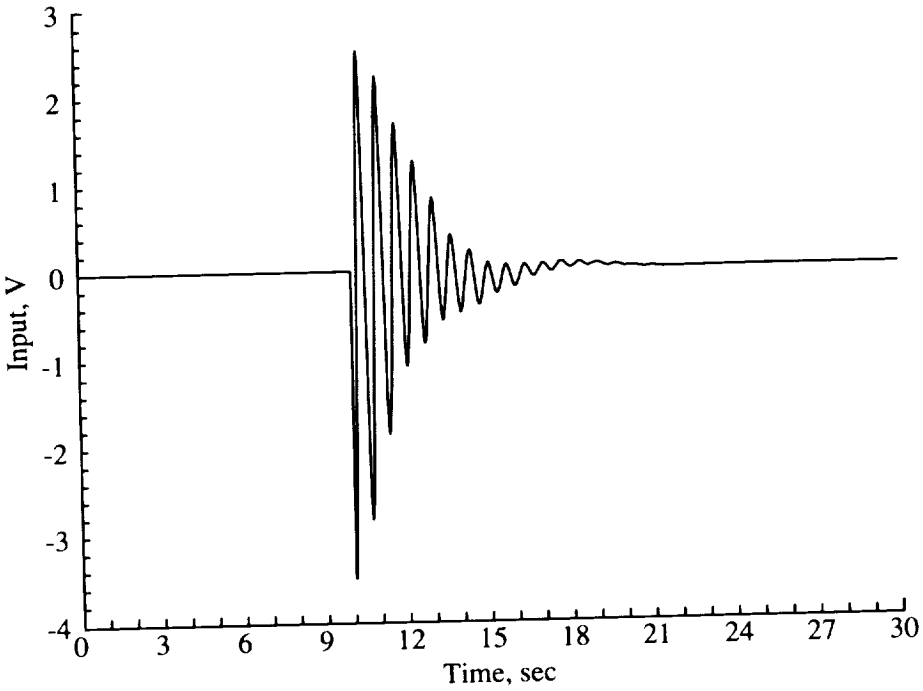

Figure 29. Input time history of actuator 8 for suboptimal compensator at $\epsilon_A = 0.9\epsilon_{A,\max}$ and $\epsilon_{A,\max} = 0.667$.

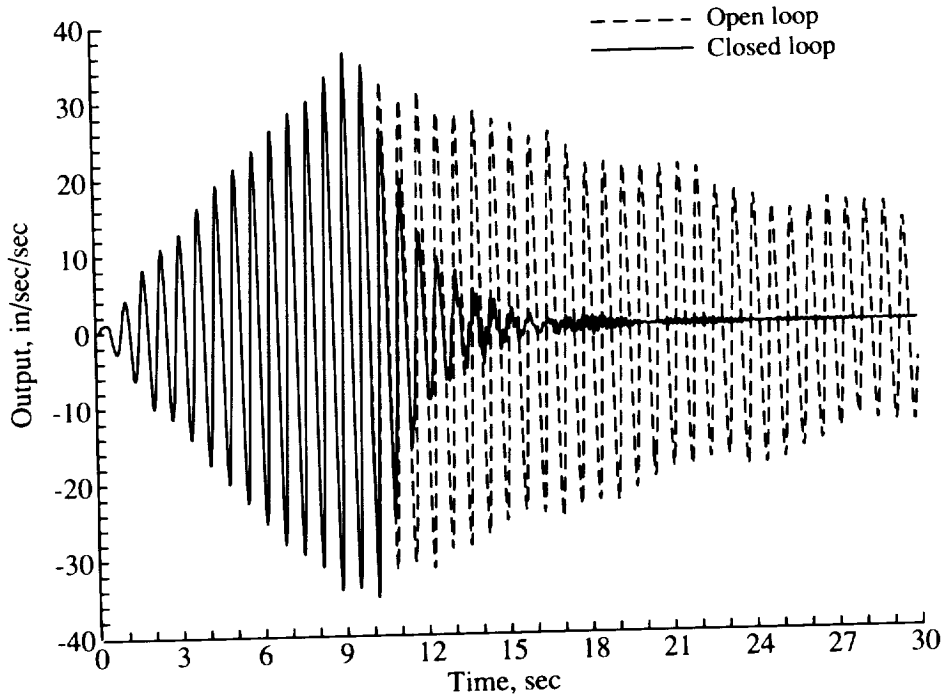

Figure 30. Output time history of suboptimal accelerometer 8 at $\epsilon_A = 0.9\epsilon_{A,\max}$ and $\epsilon_{A,\max} = 0.667$.

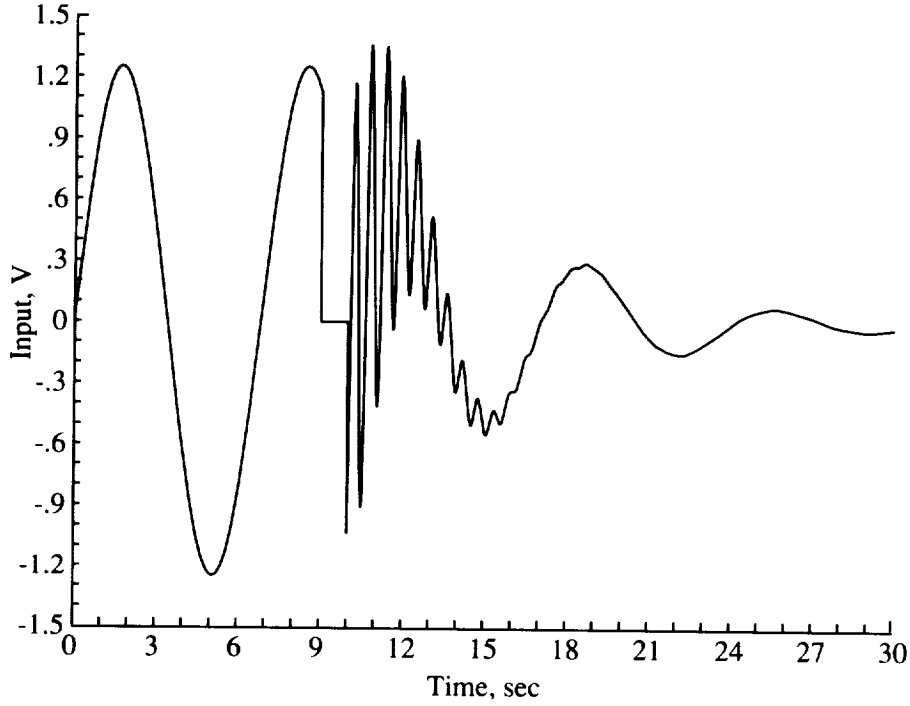

Figure 31. Input time history of actuator 7 for suboptimal compensator at $\epsilon_A = 0$.

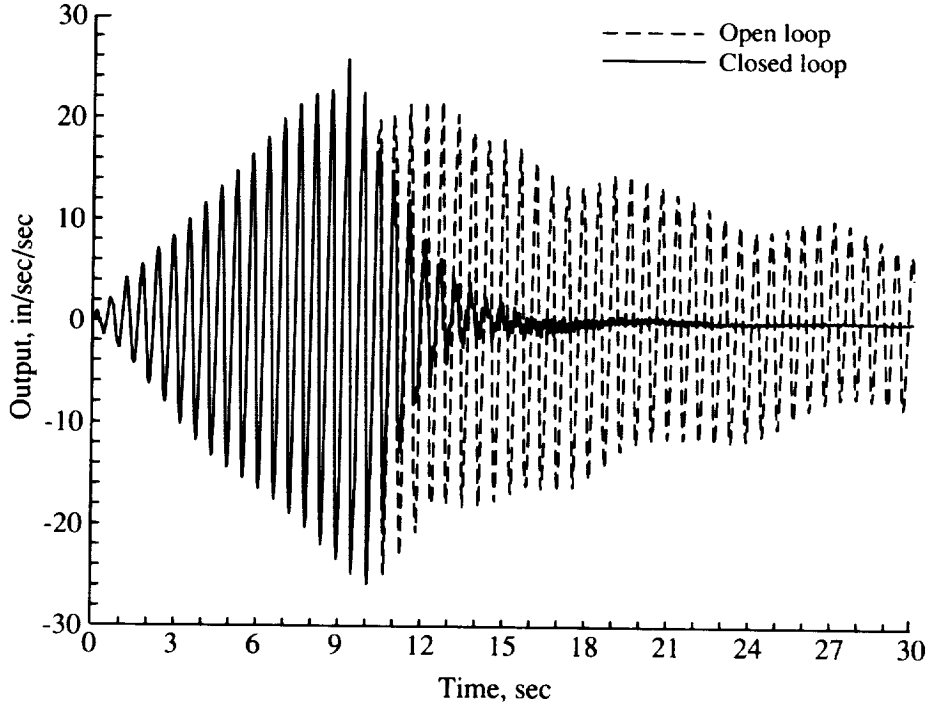

Figure 32. Output time history of suboptimal accelerometer 7 at $\epsilon_A = 0$.

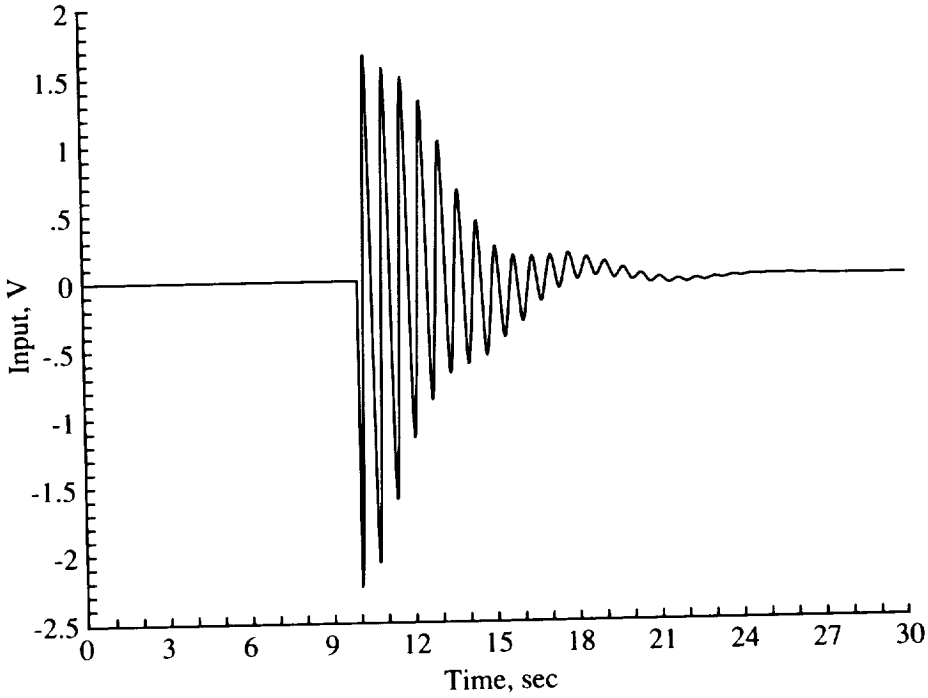

Figure 33. Input time history of actuator 8 for suboptimal compensator at $\epsilon_A = 0$.

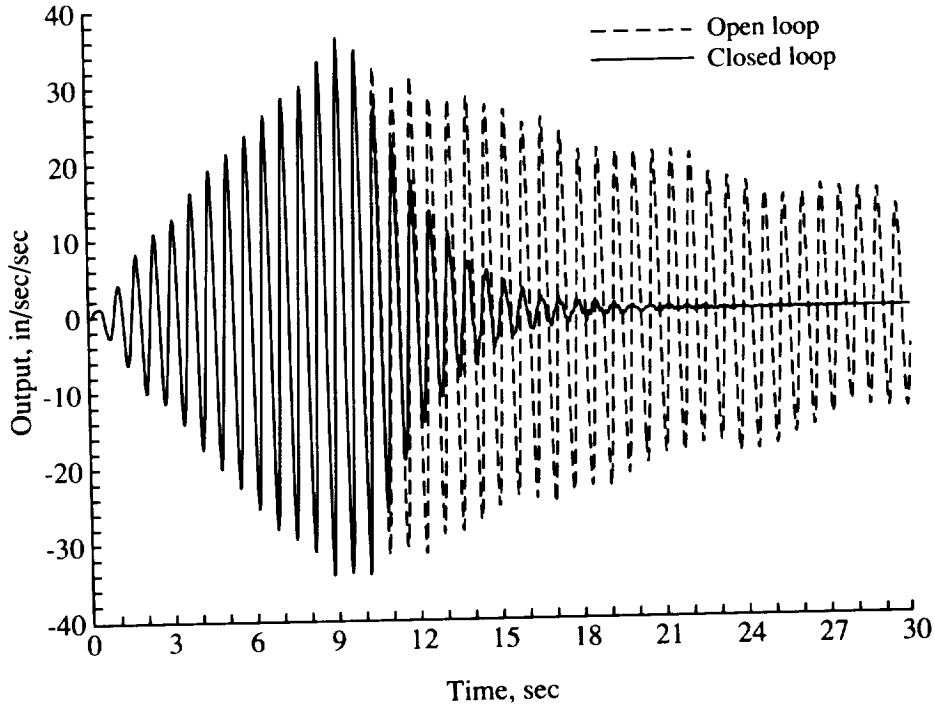

Figure 34. Output time history of suboptimal accelerometer 8 at $\epsilon_A = 0$.

*U.S. GOVERNMENT PRINTING OFFICE: 1993-728-150-60046

REPORT DOCUMENTATION PAGE

Form Approved
OMB No. 0704-0188

1. AGENCY USE ONLY *(Leave blank)*	2. REPORT DATE	3. REPORT TYPE AND DATES COVERED
	May 1993	Technical Paper

4. TITLE AND SUBTITLE
Robust Controller Design for Flexible Structures Using Normalized Coprime Factor Plant Descriptions

5. FUNDING NUMBERS
WU 585-03-11-05

6. AUTHOR(S)
Ernest S. Armstrong

7. PERFORMING ORGANIZATION NAME(S) AND ADDRESS(ES)
NASA Langley Research Center
Hampton, VA 23681-0001

8. PERFORMING ORGANIZATION REPORT NUMBER
L-17179

9. SPONSORING/MONITORING AGENCY NAME(S) AND ADDRESS(ES)
National Aeronautics and Space Administration
Washington, DC 20546-0001

10. SPONSORING/MONITORING AGENCY REPORT NUMBER
NASA TP-3325

11. SUPPLEMENTARY NOTES

12a. DISTRIBUTION/AVAILABILITY STATEMENT
Unclassified–Unlimited

Subject Category 18

12b. DISTRIBUTION CODE

13. ABSTRACT *(Maximum 200 words)*

Stabilization is a fundamental requirement in the design of feedback compensators for flexible structures. The search for the largest neighborhood around a given design plant for which a single controller produces closed-loop stability can be formulated as an H_∞ control problem. The use of normalized coprime factor plant descriptions, in which the plant perturbations are defined as additive modifications to the coprime factors, leads to a closed-form expression for the maximum neighborhood boundary allowing optimal and suboptimal H_∞ compensators to be computed directly without the usual γ iteration. This paper gives a summary of the theory on robust stabilization using normalized coprime factor plant descriptions, and it describes the application of the theory to the computation of robustly stable compensators for the phase 0 version of the Control-Structures Interaction (CSI) Evolutionary Model. Results from the application indicate that the suboptimal version of the theory has the potential of providing the basis for the computation of low-authority compensators that are robustly stable to expected variations in design model parameters and additive unmodeled dynamics.

14. SUBJECT TERMS
Feedback control; Robust stability; Coprime factorization; H_∞ control; Flexible structures

15. NUMBER OF PAGES
70

16. PRICE CODE
A04

17. SECURITY CLASSIFICATION OF REPORT	18. SECURITY CLASSIFICATION OF THIS PAGE	19. SECURITY CLASSIFICATION OF ABSTRACT	20. LIMITATION OF ABSTRACT
Unclassified	Unclassified		

NSN 7540-01-280-5500

Standard Form 298(Rev. 2-89)
Prescribed by ANSI Std. Z39-18
298-102

NASA-Langley, 1993

National Aeronautics and
Space Administration
Code JTT
Washington, D.C.
20546-0001

Official Business
Penalty for Private Use, $300

BULK RATE
POSTAGE & FEES PAID
NASA
Permit No. G-27

POSTMASTER: If Undeliverable (Section 158 Postal Manual) Do Not Return